Universität Rostock Traditio et Innovatio

HelmholtzZentrum münchen
Deutsches Forschungszentrum für Gesundheit und Umwelt

JOINT MASS SPECTROMETRY CENTRE

Investigation and development of analytical techniques for trace level detection of drugs, explosives and their precursors

Kumulative Dissertation

zur Erlangung des akademischen Grades

doctor rerum naturalium (Dr. rer. nat.)

der Mathematisch-Naturwissenschaftlichen Fakultät

der Universität Rostock

vorgelegt von

René Reiss

geb. am 05. August 1987 in Freiberg

Rostock, Oktober 2019

https://doi.org/10.18453/rosdok_id00002633

The presented work was prepared in the period from February 2015 to October 2019 at the chair of Analytical Chemistry in the working group Analytical and Technical Chemistry of the Institute of Chemistry of the University of Rostock. This dissertation was conducted within the framework of the Joined Mass Spectrometry Centre (JMSC) of the University of Rostock and the German Research Centre for Environmental Health Munich.

Einreichung der Dissertation: 14. Oktober 2019

Wissenschaftliches Kolloquium: 07. Januar 2020

1. Gutachter:
   Prof. Dr. Ralf Zimmermann, Lehrstuhl für Analytische Chemie, Abteilung Technische und Analytische Chemie, Institut für Chemie, Mathematisch-Naturwissenschaftliche Fakultät, Universität Rostock und Gruppenleiter Comprehensive Molecular Analytics, Helmholtz Zentrum München

2. Gutachter:
   Prof. Dr. Heiko Hayen, Lehrstuhl für Analytische Chemie, Institut für Anorganische und Analytische Chemie, Westfälische Wilhelms-Universität Münster

„Those who would give up essential Liberty, to purchase a little temporary Safety, deserve neither Liberty nor Safety“

Benjamin Franklin

Acknowledgements

Within the past years, I was able to participate in interesting and captivating tasks. In addition to the customary highs and lows of completing a doctoral thesis, I always enjoyed the scientific and technical work of my thesis and the warm and friendly work environment.

At the end of my PhD experience, I wish to thank everyone for their contribution to my work. Special thanks go to…

… Prof. Ralf Zimmermann for providing a highly interesting research topic and the necessary support that allowed me to conduct my own research.

… Dr. Sven Ehlert for the many helpful discussions and suggestions and the advices regarding my project work and PhD.

… Dr. Christopher Rüger, Jan Heide, Dr. Thorsten Streibel, Sophie Klingbeil and Christin Kühl, who helped me with various topics and endured my extensive discussions.

… Dr. Frank Hauser and Michael Pütz from the Bundeskriminalamt, for their friendly and versatile help and support at different stages of my work.

… all co-authors and the entire working group (both Rostock and Munich) for great teamwork, even over long distances and for the many contributions—sometimes funny, sometimes necessary, but always interesting.

... the entire SEMFreS team for providing insights into an interesting interdisciplinary project and fascinating experiments.

… my family, my parents-in-law and my friends Andreas, Klaus, Nadine and Christopher for great and cheerful times and helping me to regain my energy and motivation.

… the love of my life, my wife Franziska, for always being on my side, brightening up every day and always encouraging me to go further.

Erklärung gemäß §4 Absatz 1 Buchstaben g und h der Promotionsordnung der Mathematisch-Naturwissenschaftlichen Fakultät der Universität Rostock

Name: René Reiss **Anschrift:** In der Dreispitz 4A
65719 Hofheim am Taunus

Ich habe eine Dissertation zum Thema

Investigation and development of analytical techniques for trace level detection of drugs, explosives and their precursors

an der Mathematisch-Naturwissenschaftlichen Fakultät der Universität Rostock angefertigt. Dabei wurde ich von Herrn Prof. Dr. Ralf Zimmermann betreut.

Ich gebe folgende Erklärung ab:

1. Die Gelegenheit zum vorliegenden Promotionsvorhaben ist mir nicht kommerziell vermittelt worden. Insbesondere habe ich keine Organisation eingeschaltet, die gegen Entgelt Betreuerinnen/Betreuer für die Anfertigung von Dissertationen sucht oder die mir obliegenden Pflichten hinsichtlich der Prüfungsleistungen für mich ganz oder teilweise erledigt.

2. Ich versichere hiermit an Eides statt, dass ich die vorliegende Arbeit selbstständig angefertigt und ohne fremde Hilfe verfasst habe. Dazu habe ich keine außer den von mir angegebenen Hilfsmitteln und Quellen verwendet und die den benutzten Werken inhaltlich und wörtlich entnommenen Stellen habe ich als solche kenntlich gemacht.

Rostock, Oktober 2019 ……..

René Reiss

CONTRIBUTION TO THE MANUSCRIPTS FOR CUMULATIVE THESIS

The following manuscripts were created by René Reiss as first author and published in peer-reviewed journals. The contribution of René Reiss to each manuscript is given below.

Title: Ambient Pressure Laser Desorption—Chemical Ionization Mass Spectrometry for Fast and Reliable Detection of Explosives, Drugs, and Their Precursors

Authors: René Reiss, Sven Ehlert, Jan Heide, Michael Pütz, Thomas Forster and Ralf Zimmermann

Journal: Applied Sciences
Year: 2018

René Reiss redesigned the utilised systems, done the laboratory measurements, performed the data analysis and wrote the manuscript.

Title: Evaluation and application of gas chromatography - vacuum ultraviolet spectroscopy for drug- and explosive precursors and examination of non-negative matrix factorization for deconvolution

Authors: René Reiss, Beate Gruber, Sophie Klingbeil, Thomas Gröger, Sven Ehlert and Ralf Zimmermann

Journal: Spectrochimica Acta Part A: Molecular and Biomolecular Spectroscopy
Year: 2019

René Reiss designed the study, performed the sample preparation, processed the data, interpreted all results and wrote the manuscript.

Title: Comparison of three analytical methods for the on-site analysis of traces at clandestine drug laboratories

Authors: René Reiss‖, Frank Hauser‖, Sven Ehlert, Michael Pütz and Ralf Zimmermann

Journal: Science & Justice
Year: 2019

René Reiss contributed to the conception of the study and collection of samples, done IMS and APLD-MS measurements and wrote the manuscript.

‖These authors contributed equally to the manuscript.

Table of Contents

1. Zusammenfassung

Die Herstellung von Sprengstoffen und Drogen, deren Verkauf, die Umweltverschmutzung die durch Produktion oder durch unsachgemäße Entsorgung einhergeht, sowie die Unterstützung krimineller Milieus und nicht zu Letzt die Gefahr für Leib und Leben, stellen wesentliche Probleme und eine Bedrohung für unsere Gesellschaft dar. Beispielsweise starben alleine im Jahr 2015 weltweit über 450.000 Menschen durch den Konsum von illegalen Drogen. Hinzu kommt die chemische Vielfalt an natürlichen oder synthetischen Drogen und Sprengstoffen. Diese beruht auf den unterschiedlichen notwendigen Eigenschaften, die für eine militärische und zivile Nutzung zum Teil deutlich voneinander abweichen. Aus diesen genannten Gründen kommt der Untersuchung von Drogen, Sprengstoffen und deren Vorstufen im Bereich der Forensik eine besondere Bedeutung zu. Eine große Herausforderung der Analytischen Chemie in diesem komplexen Gebiet ist, leistungsfähige analytische Techniken für die Prüfung, Überwachung und Regulierung bereit zu stellen.

Die vorliegende Dissertation beschäftigt sich sowohl mit Techniken für die Untersuchung von Proben im Labor, als auch für die Analyse vor Ort. Dabei wird die Eignung der Kopplung von Gaschromatographie (GC) mit Vakuumultraviolett (VUV) Spektroskopie für Drogen- und Sprengstoffvorstufen überprüft und an realistischen Szenarien erprobt. Zudem wurde das Einsatzspektrum der Technik durch die Einführung einer datenbanklosen Dekonvulierung für koeluierende Spektren erweitert.

Im Bereich der Vorort-Analytik erfolgte für die Umgebungsdruck Laserdesorption (APLD), gekoppelt mit einem Massenspektrometer (APLD-MS), eine vollständige Überarbeitung und Optimierung. Zudem ergänzt eine selbstentwickelte Abrasterungseinheit die APLD um Bildgebungsfähigkeiten. Die APLD basiert auf der schockartigen Ablösung der Analyte von der Oberfläche, womit diese Technik besonders für schwerflüchtige Substanzen auf Oberflächen geeignet ist. Durch Designoptimierungen verbesserte sich die Nachweisgrenze um den Faktor 10 und die Ansprechzeiten verkürzten sich um den Faktor vier im Vergleich zum ursprünglichen Design. Des Weiteren wurden Drogen und Drogenvorstufen als mögliche Zielanalyte evaluiert und die praktische Anwendbarkeit für die Zielverbindungen durch Überprüfung realer Proben wie Asservate und Bombenrückstände getestet. Um zudem die allgemeinen Einsatzbereiche der APLD auszubauen, wurde ein Imaging-System für das Vermessen von Flächen bis 20x20 cm und schwerer Objekte bis zu zwei Kilogramm entwickelt.

Im Rahmen des BBK Projektes SEMFreS (Szenarien, Evaluierung und Messtechnik bei Freisetzung chemischer und explosionsgefährlicher Stoffe) erfolgte der Vergleich

verschiedener Techniken unterschiedlicher Komplexität. Als Grundlage dienen immunologische Schnelltests und Ionenmobilitätsspektrometer als bereits etablierte Techniken sowie die im Rahmen dieser Arbeit verbesserte APLD-Technik. Um praktisch verwendbare Ergebnisse zu erhalten, fanden für alle Techniken vergleichende Untersuchungen von Asservaten in einem ehemaligen illegalen 3,4-Methylendioxy-N-methylamphetamin (MDMA) Labor statt. Hierbei sind die Möglichkeiten und Grenzen dieser Vertreter verschiedener Technologiestufen aufgezeigt. Besonders bei komplexen Proben erwies sich die APLD-MS dabei als geeignetste der getesteten Methoden.

2. Abstract

Production, sale and pollution due to production and improper disposal, support of criminal milieus and endangerment of life are major issues in our society and can pose a threat to it. In 2015 alone, 450,000 people died worldwide due to drug misuse and illicit drugs. In addition to the chemical diversity of natural and synthetic drugs, explosives also exhibit great diversity. This diversity is based on different necessary compound properties that can strongly differ for military and civil use. For these reasons, the investigation of drugs, explosives and their precursors is a great concern in forensic science. Therefore, the primary challenge of analytical chemistry is to provide powerful analytical techniques for tasks such as examination, monitoring and regulation within this complex field of work.

The presented dissertation addresses techniques for investigating samples in the laboratory as well as for on-site investigations. Based on this, the potential of the coupling from gas chromatography (GC) and vacuum ultra violet (VUV) spectroscopy is investigated for laboratory measurements, focussing on drug and explosive precursors and a simulated case study. In addition, the scope of application was enhanced by introducing a deconvolution method for co-eluting peaks without need for a database.

In the field of on-site analysis, ambient pressure laser desorption (APLD) coupled to mass spectrometry (APLD-MS) was examined, optimised and extended by an imaging ability. The APLD is based on a shockwave-like ablation of analytes from a surfaces; it is therefore particularly suitable for low volatile substances on a surface. By optimising the design, the limit of detection (LOD) was improved by a factor of 10, and the delay time was reduced by a factor of four. Furthermore, drugs and drug precursors are investigated regarding whether they are suitable target compounds. To verify the practical relevance of these results, items of evidence and bomb residues were investigated. In addition, to extend the field of application, an imaging-setup was developed, allowing for surveying areas of up to 20x20 cm for objects of up to two kilogram in weight.

Within the SEMFreS project (“Szenarien, Evaluierung und Messtechnik bei Freisetzung chemischer und explosionsgefährlicher Stoffe”), organised by the Federal Office of Civil Protection and Disaster Assistance (BBK), the comparison of various different analytical techniques with various levels of complexity was performed. This comparison was based on immunoassay drug tests (IDT) and ion mobility spectrometry (IMS), as proven standards, in addition to the APLD that was improved within this dissertation. To gain information useful in practice, all techniques underwent comparative investigations of samples from a former clandestine 3,4-methylenedioxy-N-methamphetamine (MDMA) laboratory. Thereby, the possibilities and limits for representatives of different levels of technology are outlined. Thus, APLD proved to be the method of choice for complex samples.

3. Introduction and motivation

Drugs, explosives and their precursors are prominent target compounds in forensic science [1–6]. Their manifold usage in a wide variety of legal and, in particular, illegal activities requires efficient detection and analysis of these compound classes for forensic purposes.

On-site investigations can possess a high-risk potential, and laboratory investigations of samples can be challenging. One example of a high-risk scenario, a recently emerging method of methamphetamine synthesis in a single reaction vessel, is displayed in Figure 1 [7]. This method is gaining in popularity, especially for drug-addicted producers, as the synthesis requirements and educts are readily available, and the reaction control is supposedly simple [8]. The example displays a possible consequence for the incorrect choice of a reaction vessel. Therein, the choice of this bottle results in an explosion, with the possibility of secondary fires and injuries.

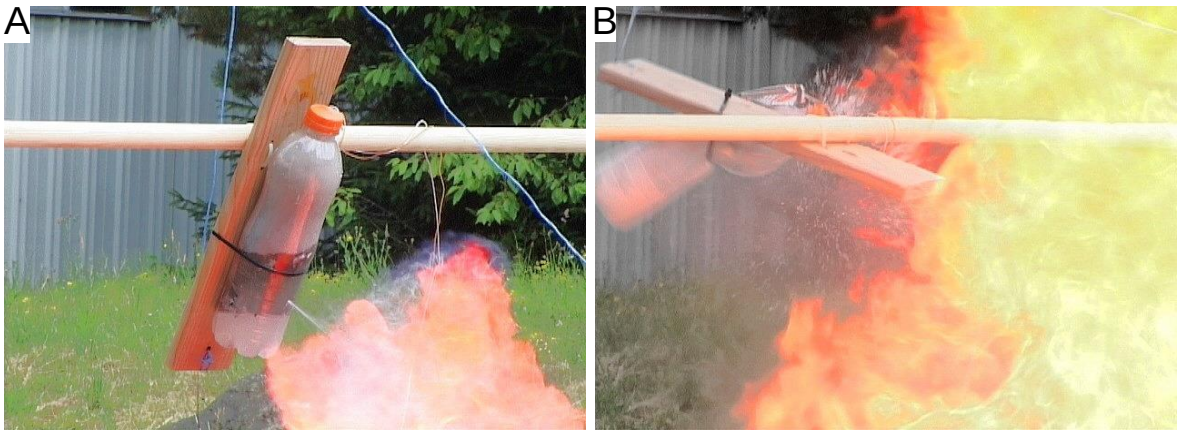

Figure 1: ‘shake and bake’ synthesis of methamphetamine. The reaction takes place inside a plastic bottle. A) Burning hydrogen, emitted through a hole in the reaction vessel, in which the hole is a consequence of hot elemental lithium touching the wall and melting it. B) Flashback of the flame inside the reaction vessel and subsequent hydrogen explosion. Modified from [7]. With kind permission by Dr. Schäper, State Criminal Police Office Bavaria.

Another example is the charge of a clandestine laboratory by law enforcement. Therefore, on-site investigators must be capable of obtaining a rapid overview of the risks and potential ongoing synthesis. The aforementioned methamphetamine synthesis requires repeated discharge of hydrogen to keep the pressure limit of the reaction vessel. Another potential risk could be toxic waste collections with unknown composition. Since on-site measurements are primarily limited to fundamental or rather unspecific information, subsequent laboratory measurements are necessary as well to obtain all necessary information or information that are valid for legal purposes.

This dissertation describes the development and evaluation of new analytical techniques for on-site analytics and the laboratory instrumentation of drugs, explosives and their precursors. Vacuum ultra violet spectroscopy, a recently improved technique that is now

sufficiently mature for operation as a detection system for GC [9], is investigated for the usage with forensic samples at laboratories subsequent to possible on-site investigations (publication 1).

This detector combines a robust system, similar to ultra violet (UV) detectors, with the ability to obtain compound-specific absorption spectra, a nearly universal compound detectability and the potential for simple quantification based on the Beer-Lamberts law. These advantages are evaluated for forensic target compounds and realistic forensic scenarios. In addition, a new spectra analysis method is suggested, allowing for a discovery-based deconvolution approach. Furthermore, possible solutions to the aforementioned threats are challenged. For this purpose, the redesign and optimisation of APLD was conducted (publication 2).

Ambient pressure laser desorption is a sensitive technique utilised for rapidly investigating suspicious surfaces. In addition to the instrumental development, APLD is compared with state-of-the-art on-site instrumentation. In this respect, laboratory standard experiments and real forensic samples from former clandestine laboratories were investigated (publication 3).

4. Drugs and explosives

Drugs and explosives can pose serious risks to first responders who must investigate suspicious samples or surfaces. In addition to the obvious risk of explosives, threads can arise from ongoing synthesis or toxic waste collections at clandestine laboratories. These secondary risks are valid for explosives and drugs, since some synthesis routes can include hazardous substances such as elemental lithium or pressurised hydrogen as mentioned in the introduction [7].

Figure 2: A) Overview of common illicit drugs and a cutting agent, f.l.t.r.: amphetamine, caffeine (cutting agent), psilocybin mushroom, heroin, cocaine, methamphetamine, opium, cannabis, shamanic psychoactive mixture and hashish. B) Overview of common explosives and other energetic compounds, f.l.t.r.: 2,4,6-trinitrotoluene (TNT), powdered propellant, gunpowder, pentaerythritol tetranitrate (PETN) DM12B1, PETN NSP 711, flash composition, SEMTEX H, ANFO and hexogen (RDX).

Examples of common illicit drugs and explosives are pictured in Figure 2. Therein nine illicit drugs in different application forms are presented (Figure 2 A). In addition, an overview of nine common explosives and energetic compounds is exhibited as well (Figure 2 B). Most plastic explosives are dyed and contain low amounts of 2,3-dimethyl-2,3-dinitrobutane (DMDNB) that were added due to legal restrictions. DMDNB has a relatively high vapour pressure and facilitates detection.

4.1 Drugs and drug precursors

Drug misuse is of major public concern. In 2015, approximately 168,000 people died worldwide due to drug disorders. Overall, drug usage resulted in about 450,000 deaths in

just this year [10]. These extended numbers of deaths are indirectly related to HIV and hepatitis C infections due to unsafe injection practices [10]. In addition to partial legislation, cannabis remained the main drug in 2016, based on the seized amount followed by cocaine, opium and methamphetamine [10]. In Europe, the most prevalent drug in 2016 based on the seized amount is cannabis, followed by cocaine, amphetamine, heroin and MDMA [11]. Between 1970 and 1990, drugs such as cannabis, amphetamine and heroin established themselves in the European market, followed by MDMA and cocaine in the years following [11]. Therefore, between 2011 and 2015, EU-based suppliers gained 46% of the total EU drug market revenue [11]. The drug seizures in the EU in 2016 are pictured in Figure 3 A. Based on the seizures, the extension of the European drug market can be estimated. Cannabis is the most relevant illicit drug, with 548 tonnes found at a total of 737,000 seizures. In sum, the classic synthetic drugs such as amphetamine, MDMA and methamphetamine and the half-synthetic drug heroin make up for 10.8 tonnes found at a total of 105,000 seizures. While these numbers are low, compared with cannabis and cocaine, the amount of MDMA is solely sufficient for the production of approximately 5.3 million tablets.

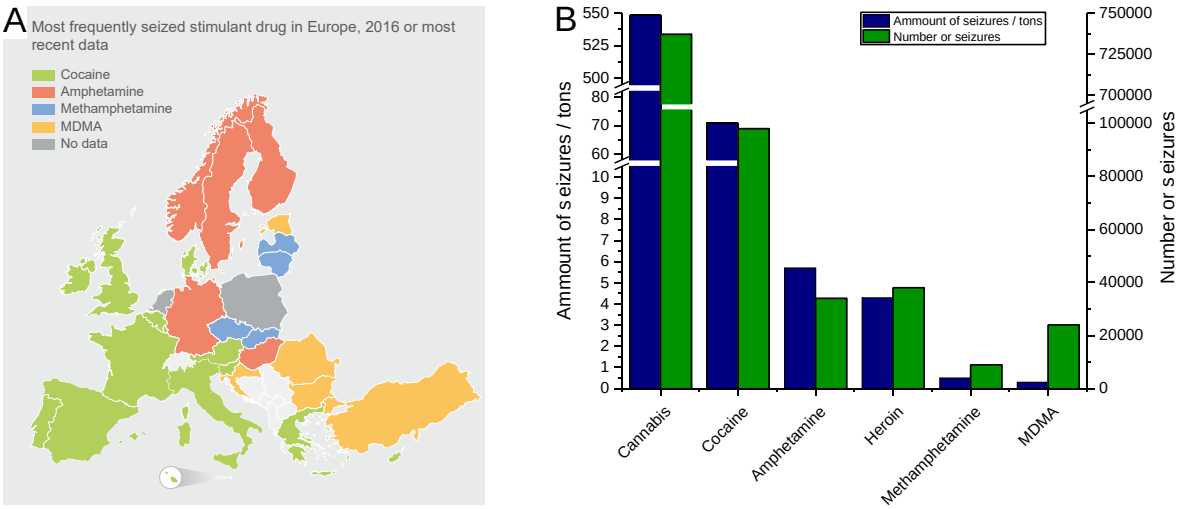

Figure 3: A) Overview of the most prominent illicit drug, based on seizures. Graphic adopted from [11]. B) Seized drugs in the EU. Most present drugs with the amount and the number of seizures in 2016. Data from [11].

The drugs most frequently seized in each country of the EU are illustrated on the right side of Figure 3 B, based on the seizure amount. Systematic differences can be seen among different countries. While South and Western Europe are dominated by cocaine, MDMA is prominent for Eastern Europe. For Middle and Northern Europe, amphetamine and methamphetamine are most frequently found. This divergence can be explained by the different import routes and production methods. Cocaine is mainly produced in South America and is consequently smuggled to Europe via sea routes in large ship containers. In contrast, the production of amphetamine and methamphetamine takes place in Europe,

primarily in Middle Europe, especially in the Netherlands and Belgium for amphetamine and the Czech Republic for methamphetamine. The Eastern prevalence for MDMA consumption cannot be directly correlated to the production locations and smuggling routes, since it is produces over many areas in Europe [12].

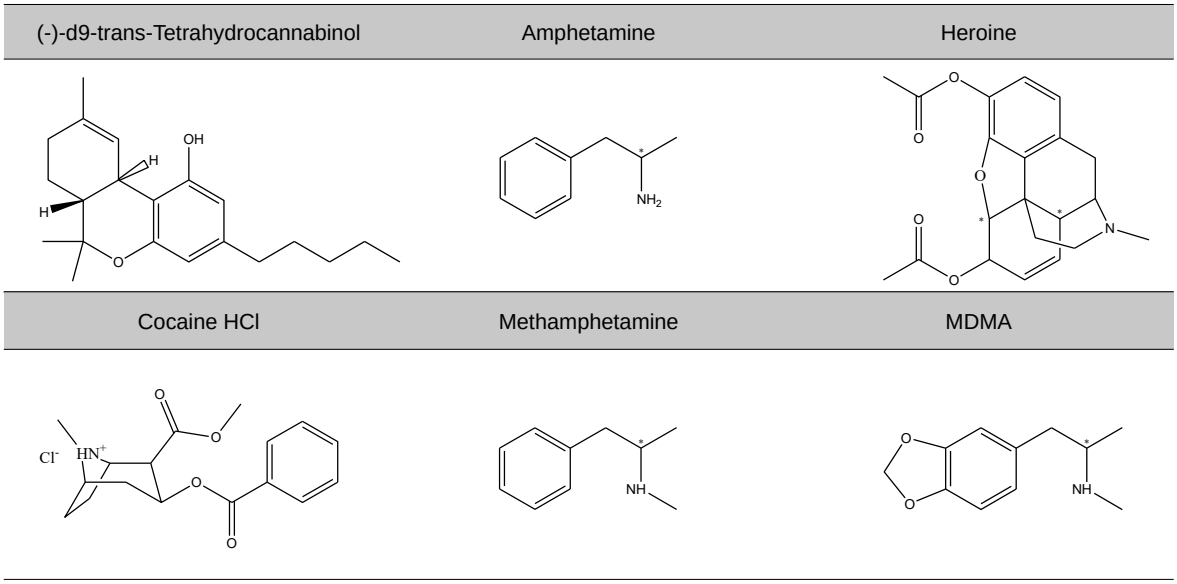

Figure 4: Chemical structures of the most prevalent drugs in the EU.

Due to the structural similarity of amphetamine, methamphetamine and MDMA, they are grouped as so-called amphetamine-type stimulants (ATS) [10]. An overview of the chemical structure of the most prevalent drugs in the EU is illustrated in Figure 4. The circumstance, that the production of ATS takes place within Europe, results in several additional problems, compared with drugs smuggled from foreign countries, such as cocaine. These issues are related to the synthesis of these compounds and can cause serious impacts on the environment and on law enforcement staff directly involved in the seizure. An important problem is related to the large amount of waste that is produced during the synthesis and purification. Assumptions presume that 20–30 kg of waste is generated in the production of one kilogram of amphetamine [12]. Illegally dumped waste materials, as well as the waste encountered at clandestine laboratories prior to dumping, is typically a complex unknown mixture and as such is a challenging analytical task. Other safety hazards that first responders can face are the production methods themselves. For example, a common synthesis route for amphetamine utilises a heterogeneous catalytic reduction with pressurised hydrogen [13]. For methamphetamine, elemental lithium is applied at the Birch reaction [13]. Both examples can cause serious damage if drug producers are careless. These risks are further increased if drug producers are consumers themselves or during law enforcement operations at clandestine laboratories. Figure 5 illustrates clandestine laboratories of different sizes and complexity.

Figure 5: Various examples of clandestine laboratories. A) Re-staged kitchen laboratory. B) Advanced clandestine MDMA laboratory. C) Examples of reflux cooled flasks in different sizes to produce of amphetamine.

Since ATS are structurally related substances, commonly applied synthesis methods for illicit production are similar as well. The method of choice is primarily based on the available precursors and equipment. The most common production method for amphetamine is the Leuckart method [13]. This method is usually performed in three steps, as displayed in Figure 6. The first step is a non-metal reduction; in this step, phenylacetone (BMK or benzyl methyl ketone) and formamide condensates to the N-formylamphetamine (NFA) under the elimination of formic acid. Afterwards, the NFA is hydrolysed to amphetamine using acid (e.g. hydrochloric acid). Then, the reaction mixture is alkaline adjusted, isolated and distilled. In addition, for further purification, the amphetamine base is precipitated, mostly as sulphate salt.

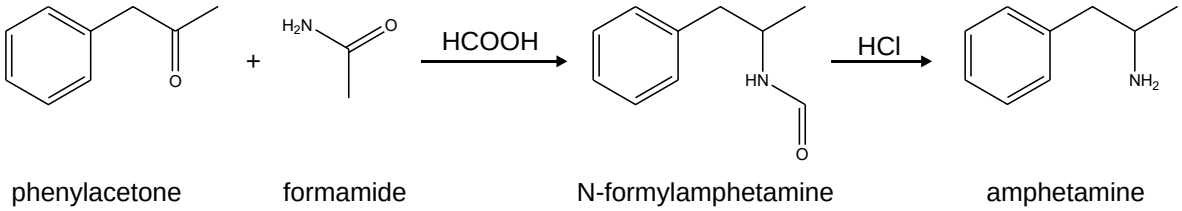

Figure 6: Leuckart reaction, typically utilised for the illicit production of amphetamine.

Common drug precursors are strictly monitored. Thus, illicit manufacturers attempt to avoid this observation by utilising uncontrolled substances or synthesising the precursors themselves from so-called pre-precursors. While increasingly more substances are monitored, the shift towards other compounds and pre-precursors is an ongoing procedure. For amphetamine, such a shift would be the usage of α-phenylacetoacetonitrile (APAAN) instead of BMK [14]. Precursors that are typically utilised for amphetamine, methamphetamine and MDMA are pictured in Figure 7.

APAAN	Phenylacetone	PMK	Safrole
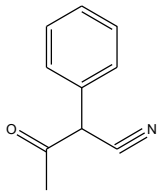	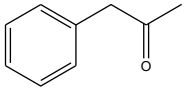	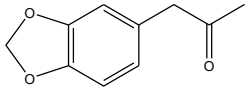	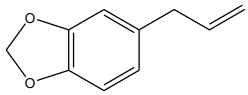

Figure 7: Chemical structures of drug precursors utilised to produce of amphetamine and MDMA.

4.2 Explosives and explosive precursors

Explosives are a class of chemical compounds used for various military and commercial applications. Depending on the intended application, different explosives with different characteristics are utilised. For military explosives, high performance outweighs parameters such as cost of production or environmental impact. For civil applications, such as the mining or demolition of buildings, safe handling and cost efficiency are more important. These versatile demands serve as a reason for today's large variety of explosives, totalling up to hundreds of different compounds [15]. Invented by Chinese alchemists in the ninth century [16], black powder remained the only relevant explosive until the discovery of nitro glycerin (NG) in 1847 by Ascanio Sobrero [17]. However, the breakthrough came with the invention of dynamite by Alfred Nobel, patented in 1867, by discovering a relatively safe way to handle NG via soaking it up in diatomaceous earth [18]. From thereon, the further development of explosives accelerated rapidly, resulting in multiple new compounds in the following years.

EGDN	2,4-DNT	2,6-DNT	RDX	TATP
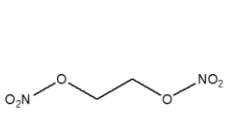	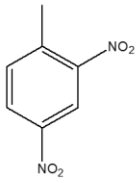	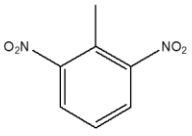	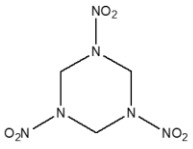	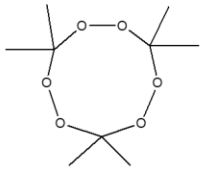
NG	**TNT**	**PA**	**Tetryl**	**PETN**
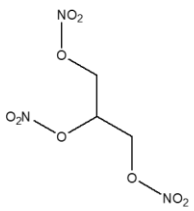	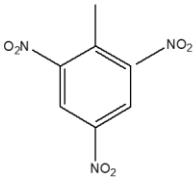	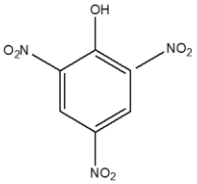	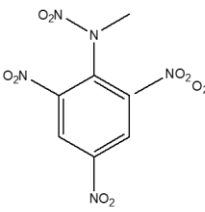	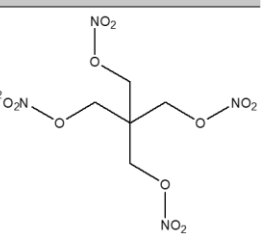

Figure 8: Chemical structures of various explosives (nitroglycol (EGDN), 2,4-dinitrotoluene (2,4-DNT), 2,6-dinitrotoluene (2,6-DNT), triacetone triperoxide (TATP), picric acid (PA), 2,4,6-trinitrophenyl-methylnitramine (Tetryl)).

The working principle of explosives is based on their energetic chemical structure and thus their reactivity. The chemical structures of various explosives are presented in Figure 8. They are frequently classified into organic and inorganic explosives. Organic explosives mostly include nitro or peroxide groups and their reactivity is based on low to critical thermodynamic stability or the abilities as a strong oxidizing agent, mostly containing nitro or peroxide groups. Examples include the aforementioned NG, TNT or TATP [19]. In contrast, inorganic explosives are salts that have a high content of oxygen in combination with combustion material, such as charcoal. Prevalent inorganic explosives include ammonia nitrate, black powder or flash powder [19]. Hexogen, known also as RDX (named after research department explosive or royal demolition explosive), is the most relevant high energetic explosive [15], which is due to the high energetic density and velocity of detonation. It belongs to the group of cyclic aliphatic compounds, classified as nitramides.

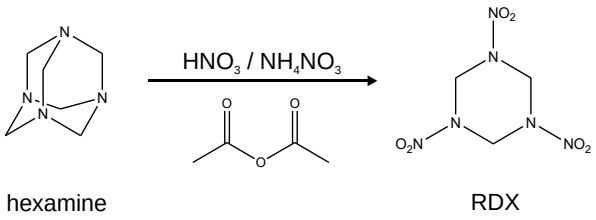

hexamine RDX

Figure 9: Possible synthesis path of RDX starting from hexamine.

The production is based on hexamine as educt, treated with fuming nitric acid under strict cooling (S-H procedure) or the addition of ammonia nitrate and subsequent heating [15]. This synthesis is given in Figure 9.

During the explosion, the chemical compound decomposes into small, mostly gaseous, molecules. Due to the intense heat of the explosion, vaporisable compounds, such as water, are evaporated. Examples of explosive reactions for the decomposition of TNT, equation (1), and ammonia nitrate, equation (2), as well as SEMTEX in Figure 10 are given below (the chemical reactions presume a start by initial ignition). Therein, one mole of pre-exploded TNT equals 10 moles of gaseous compounds, and one mole of ammonia nitrate equals 3.5 moles of gaseous explosion residues.

Organic explosive $$2\ C_7H_5N_3O_{6(s)} \rightarrow 3\ N_{2(g)} + 5\ H_2O_{(g)} + 12\ CO_{(g)} + 2\ C_{(s)} \quad (1)$$

Inorganic explosive $$2\ NH_4^+NO_{3(s)}^- \rightarrow 4\ H_2O_{(g)} + 2\ N_{2(g)} + O_{2(g)} \quad (2)$$

The explosion illustrated in Figure 10 was utilised to produce post-explosion sample surfaces during a measurement campaign at the Bundesanstalt für Materialforschung und -prüfung (BAM) for the SEMFreS project. For this particular explosion, 60 g of SEMTEX, a plastic explosive composed of PETN and RDX were selected and triggered.

Figure 10: Exemplary detonation of 60 g of SEMTEX, utilised to generate post-blast sample surfaces of this explosive.

Important physical parameters for characterising and comparing explosives are the speed of detonation, impact sensitivity and friction sensitivity. The term detonation indicates that the explosion-based shock wave inside the substance is faster than the speed of sound. As a result, the explosive material is compressed and thus heated up during the explosion, enhancing the reaction speed even further. In contrast, a sub-sonic reaction is called deflagration. The term impact sensitivity describes the energy that a hammer, with specific weight and from a specific height, must induce to trigger a detonation. Friction sensitivity is a measure that describes the necessary pressure applied to a surface to generate a reaction. Values for those critical parameters of conventional explosives are provided in Table 1. While the speed of detonation is of the same order of magnitude, the sensitivity values vary significantly. Impact and friction sensitivity can therefore explain the difficulties of handling NG and TATP.

Table 1: Values of explosives for the speed of detonation, impact sensitivity and friction sensitivity. Values obtained from [20].

Name	Speed of detonation / ms^{-1}	Impact sensitivity / J	Friction sensitivity / N
NG	7,850	0.55	360
TNT	7,224	19	350
RDX	8,882	7.5	148
TATP	6,322	0.3	0.1

In addition to the advantage of explosives, in legal applications, many such as TNT, RDX or PETN, are toxic to the environment or organisms [19]. This toxicological aspect, besides the safety issues, is another strong motivation for developing powerful analytic technologies that allow for on-site investigation of these substances in complex matrices. A known issue is the contamination of soil with TNT and RDX. Two parameters that influence the discharge of explosives into the environment are the vapour pressure and the solubility in water [21,22]. While the vapour pressure influences the distribution through the air, the water solubility influences the distribution through wash-out in the soil or ammunition dumpsites at the bottom of seas and oceans. Examples of both values are provided in Table 2. For

comparability, values for common environmental analysis targets are listed as well. The low vapour pressure of explosives complicates their detection with common approaches. An ablation technique that overcomes the problem of low vapour pressure of direct sampling, APLD, is described in more detail in Chapter 5.1.

Table 2: Vapour pressure and solubility in water of various explosives and common environmental analytes (dichlorodiphenyl-trichloroethane (p,p'-DDT)). All values, except those that are directly cited, are taken from the source mentioned in the caption.

Name	Molecular weight / g mol^{-1}	Vapour pressure / Pa (25°C) [23]	Solubility / mg l^{-1} (25°C) [19]
EGDN	152	64	5,600
2,4-DNT	182	0.3	280
2,6-DNT	182	1	208
RDX	222	3.5 E-19	60
TATP	222	130	4 [23]
NG	227	0.35	1,950
TNT	227	0.024	150
PA	229	0.068	12,400
Tetryl	287	3.8 E-8	80
PETN	316	5.7 E-5	2.1
Anthracence	178	9.1 E-4 [24]	0.045 [25]
p,p'-DDT	354	1.3 E-3 [26]	5.5 E-3 [27]
n-Hexadecane	226	0.19 [28]	9 E-4 [29]

5. Applied methods

To counter illegal drugs and enable the investigation of suspicious samples and surfaces, sensitive and versatile analytical techniques are required. Therefore, the following methods are utilised throughout this doctoral thesis.

5.1 Ambient pressure laser desorption

A breakthrough in the deployment of laser technology in analytical sciences was achieved through the invention of matrix-assisted laser desorption/ionisation (MALDI) [30,31]. More precisely, MALDI is both a laser desorption/ionisation (LDI) technique at once; thereby, a surface is irradiated with laser light. The surface is coated with a mixture of the analyte and a matrix. The matrix absorbs the incoming energy from the laser light, evaporates and simultaneously ionises the analyte. Afterwards, the released analyte ions are transferred into the mass analyser and are analysed. Since the invention of MALDI, multiple LDI techniques have been developed [32]. While other LDI techniques, such as surface-assisted laser desorption/ionisation (SALDI) [33], have been developed, the need for a specific surface still remains. This issue can be overcome by utilising a technique that separates desorption and ionisation processes, such as APLD.

Ambient pressure laser desorption is a sampling technique for low volatile substances from surfaces. Laser light can be transferred from the laser to the sample surface via a laser fibre [34,35]. The analyte is subsequently ablated from the sample surface and sucked into a transfer capillary. This transfer, coupled to the MS, is based on the pressure difference between the vacuum inside the MS and the surface at ambient pressure. Hence, no additional pumping is necessary. The same driving force is given for the hyphenation of APLD to ion mobility spectrometers, as these pump air inside. Analyte adsorption on the inside of the desorption head or the transfer capillary is avoided by heating both parts. The thermal desorption of substances from the surface by touching it with the desorption head is avoided by mounting a thin spacer of polytetrafluoroethylene (PTFE) at the top of the desorption head. A schematic drawing and detailed photographs from the desorption head are presented in Figure 11. Based on the laser radiation, APLD can be distinguished into continuous wave (CW) APLD and pulsed laser APLD. While continuous wave APLD is well suited for low volatile, non-thermolabile analytes, pulsed APLD is the method of choice for explosives and other thermolabile analytes. Through applying short pulses on the nanosecond scale, the thermal stress is minimised, and thus, thermal degradation is avoided. A shockwave-like ablation of substances from the surface is generated [36]. This leads to less thermal fragmentation and improved limits of detection. One advantage of APLD compared with other ambient sampling techniques, such as desorption electrospray

ionisation (DESI) [37] or low-temperature plasma torch (LTP) [38], is that it does not require any media, only electrical power. More importantly, the desorption and ionisation processes are separated. Due to the possibility of transferring analytes over a distance of a few meters, it is feasible to sample surfaces that are distant from the detector or at narrow places. In addition, this split allows for utilising multiple ionisation techniques and thereby increases the possible selectivity or detection limit for specific target compounds.

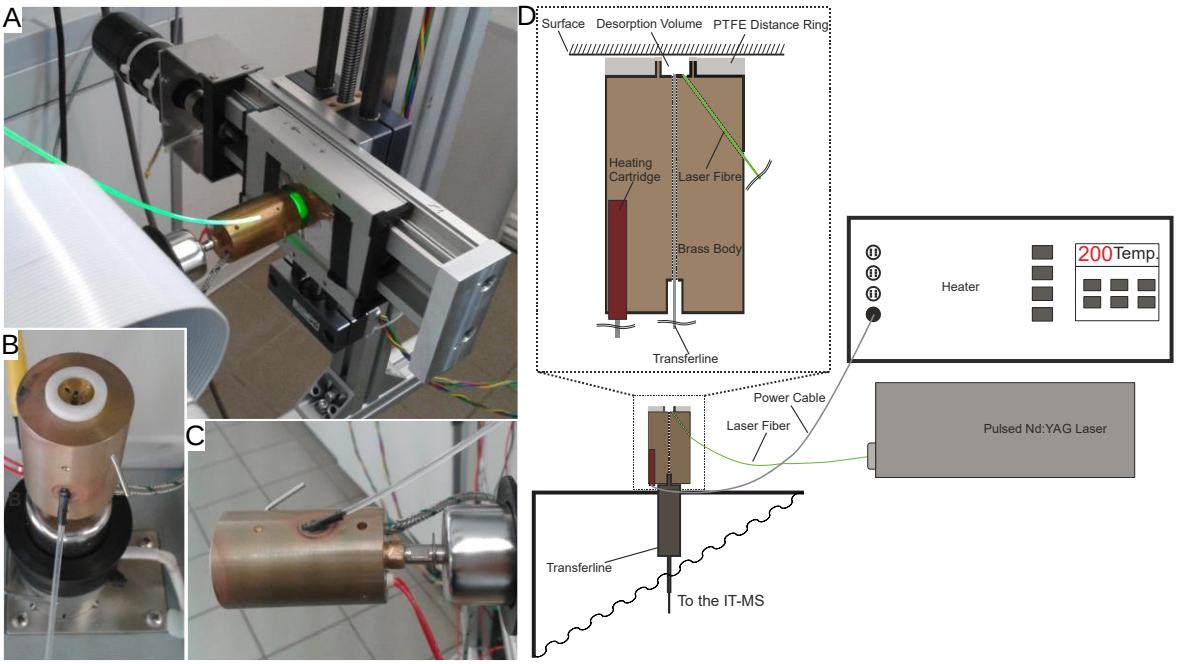

Figure 11: A) Laser desorption sampling for mass spectrometric analysis from a stainless steel surface with a self-build X-Y table; B) Deployed APLD head with a front view on desorption volume and PTFE ring; C) APLD head side view with attached laser fibre, heating cartridge and thermo-couple; D) Schematic drawing of the APLD-MS. The heating cartridge placed within the brass body ensures complete heating of the sampling head. A laser fibre transfers pulsed laser light, produced by the Nd:YAG laser, to the surface. The ablated analyte is subsequently transferred into the transferline and afterwards into the ion trap MS. There, it can be ionised via EI or CI ionisation and then be mass spectrometrically analysed.

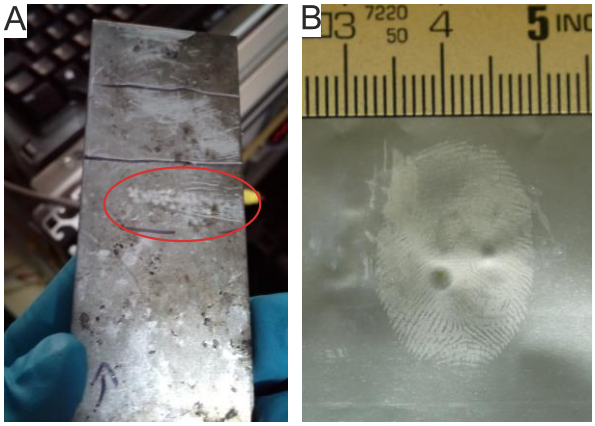

Figure 12: Samples of investigated APLD surfaces. A) Fingerprint on an aluminium surface after laser desorption. Desorption areas visible as a round spot in the middle of the fingerprint, marked with a red ellipse. B) Mark-sparing analysis of a cocaine-containing fingerprint with APLD.

Two examples of investigated surfaces are displayed in Figure 12. Therein, the residues of a post-blast surface and a fingerprint, containing cocaine, are investigated. The post-blast surface was generated during a controlled explosion, as presented in Figure 10. The white spots inside the red ellipse are a result of the APLD analysis. The possibility of mark-sparing surface analysis is demonstrated in the fingerprint analysis. Therein, only small areas of the fingerprint must be analysed, leaving most of the surface intact for further analysis (e.g. by dactyloscopy).

5.2 Mass spectrometry

Mass spectrometry is a common and well-established analytical technique in many laboratories. Since its invention, mass spectrometry has undergone multiple innovations and changes and has become a widespread technique applied in many different fields for numerous purposes [39]. Prominent examples of fields that benefit from the existence of MS include deoxyribonucleic acid (DNA) sequencing, medicinal chemistry, archaeology and even space exploration [40–43]. Common purposes are the detection, identification, structural elucidation or quantification of target compounds [44–47]. The basic concept of MS is to separate analytes, based on their mass-to-charge ratio with electric or magnetic fields or based on the time of flight.

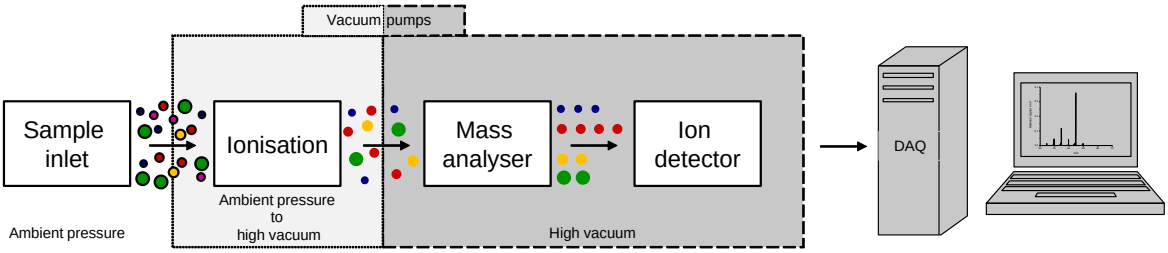

Figure 13: Schematic overview of the basic components of a mass spectrometer.

Figure 13 presents a graphical overview of the structure of a mass spectrometer. For all steps in this scheme, different techniques exist and are applied. The technique of choice strongly depends on the sample investigated and the information that should be obtained. The sample inlet is used to transfer the sample into the first vacuum stage of the MS. The hyphenation of MS to other systems such as GC or LC primarily occurs at this point. The mass spectrometric separation of species with different mass-to-charge ratios requires charge analytes. The analyte is consequently ionised in the following step. Common methods for ionisation include electron ionisation (EI) or chemical ionisation (CI), both described later in greater detail. In addition to vacuum ionisation techniques, combinations of sample inlet and ionisation also exist. These so-called ambient ionisation techniques ionise samples under elevated pressure. In such a case, the generated ions are guided through a capillary (metal/glass) while vacuum pumps reduce the amount of air or solvent. After the ions are formed, the mass analyser separates the formed ions by either time (time-of-flight MS) or interaction with electromagnetic fields. The latter case is subdivided into quadrupole mass filters, ion traps, sector field devices, orbitraps and Fourier transform ion cyclotron resonance analysers [32]. Unwanted interactions and collisions of the ions of interest are minimised by generating a strong vacuum that increases the mean free path. After the ions are separated based on their mass-to-charge ratios, a detection system is needed. The simplest commonly utilised detector is a Faraday cup. This device detects an electrical current directly based on the impact of the ions on a metal plate. More

sophisticated detectors multiply the incoming ions, such as an avalanche, to decrease the lowest number of ions that can be detected and thus increase the sensitivity. This avalanche is primarily generated by accelerating ions towards a surface that emits multiple electrons at ion impact. This multiplication can be performed several times to increase the electrical current even further. Examples of such detectors include channeltrons or microchannel plates. The received current is converted into a voltage signal that is amplified afterwards. After digitalising the analogue signal, it is available for computer-aided analysis.

5.3 Ionisation techniques

Mass spectrometric separation relies on charged analytes and thus on the ionisation of the sample material. Depending on the sample characteristics, a variety of techniques have been developed. Two well-known and commonly deployed techniques are electron ionisation and chemical ionisation. Both approaches are applied within the vacuum housing of the mass spectrometer and enable a reliable production of ions. The major difference is the degree of fragmentation (i.e. the so-called softness of ionisation).

5.3.1 Electron ionisation

Electron ionisation is one of the oldest and most prominent ionisation techniques in mass spectrometry [48]. EI uses electrons with an energy of approximately 70 eV to ionise gaseous molecules. The selection of an energy level fare greater than the ionisation energy of most molecules of 7–15 eV ensures a nearly universal ionisation behaviour. Furthermore, the highest ionisation cross-section plateau is given at this energy and thus maximises the ionisation efficiency [32]. The following properties of this ionisation technique are especially useful for the APLD-MS combination. A nearly universal ionisation behaviour, reproducible fragmentation, that is already of this method obtained knowledge and method robustness that allows for comparing obtained spectra with existing databases that already contain a wide range of different spectra. As the analytes must be evaporated, EI is mostly applied to less polar organic compounds with a molecular weight of less than 1000 g/mol. Figure 14 A displays a schematic drawing of an EI source. A resistant heated filament emits electrons; this filament is similar to those used in light bulbs and is made of a tungsten or rhenium alloy. The electrons emitted from the filament are accelerated towards the ion volume by an applied voltage of 70 V. The typical emission currents are in the range of 50 to 400 µA [32]. The neutral molecules are transferred into the ion volume via a perpendicular inlet. The electrons that enter the ion volume can ionise neutral molecules via collision and push electrons out of them, as explained in equation 3, where M stands for

the molecule and $M^{+\cdot}$for the molecular ion (radical cation).

$$M + e^- \rightarrow M^{+\cdot} + 2e^- \quad (3)$$

Afterwards, ions are accelerated and focussed towards the mass analyser through an electrical field applied at the lens system. The molecules retain some kinetic energy after an electron's impact. This internal energy can cause fragmentation of the ionised molecules, and the fragmentation pattern increases the complexity of the obtained mass spectra. While a more complex mass spectra results in issues for interpreting more complex samples, it is commonly a desired feature of EI for structural elucidation. The composition of the fragment spectra can be utilised to draw conclusions on the initial structure of the molecular ion. Functional groups, heteroatom, pi bonds and other sub-structures influence the electron distribution inside the molecule and determine the bond cleavage behaviour. Therefore, certain fragments deliver specific information about the molecule or a sub-structure based on the m/z difference between the molecular ion and the fragment. In addition, the m/z difference between two fragments can contain information about subsequent fragmentations. The molecular ion signals are not always observable, depending on the stability of the molecular ion. An EI spectra of 3-nitrotoluene can be seen in Figure 14 B. Therein typical aromatic fragments and the elimination of the nitro group are visible.

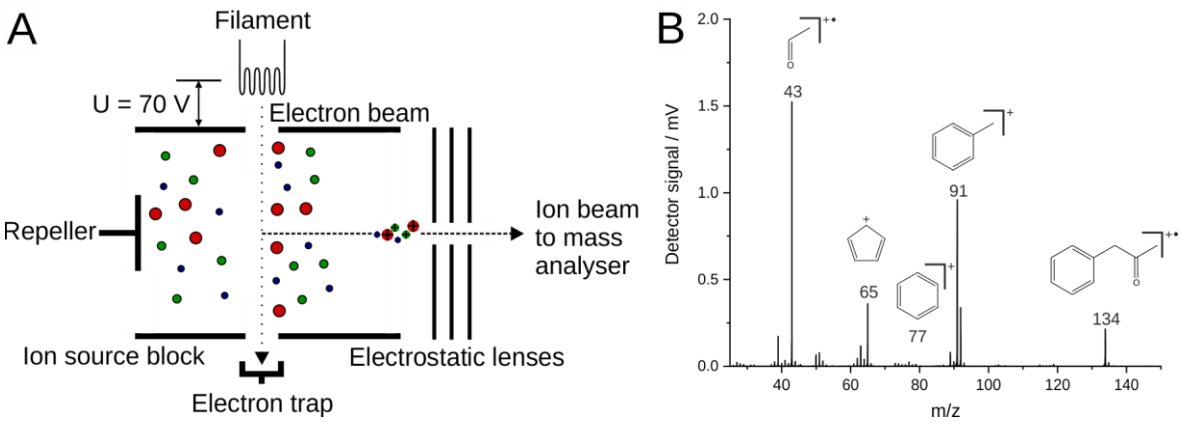

Figure 14: A) Schematic drawing of an electron ionisation source. Based on [32] B) Spectrum of BMK and characteristic fragments.

5.3.2 Chemical ionisation

In contrast to hard ionisation techniques, soft ionisation allows for retaining the molecular ion with a minimal degree of fragmentation. This behaviour is particularly valuable if the molecular mass signal should be determined or complex mixtures analysed. Chemical ionisation is the second oldest soft ionisation technique and was developed in the 1950s [49]. It was further optimised over several decades [50] and is still used today. Technically, CI is mostly identical to EI. The largest difference is an additional shielded volume with a reactant substance, as illustrated in Figure 15 A. This allows most CI sources to act as EI

sources by omitting the reactant substance. The coupling of APLD to an MS with CI ionisation benefits from three advantages; the potential for fast switching between EI and CI without prior set-up modifications, good limits of detection for strongly electronegative compounds such as explosives and the ability to obtain spectra with a minimal degree of fragmentation.

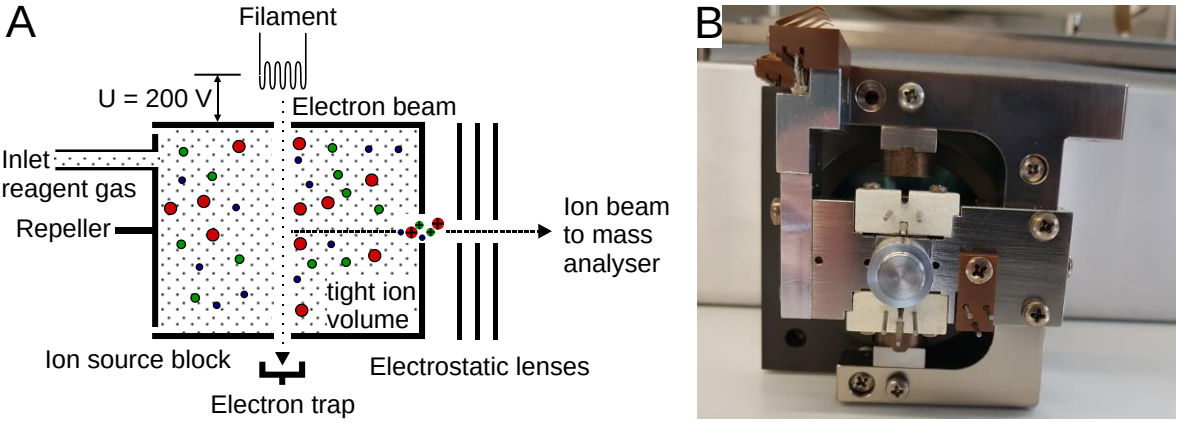

Figure 15: A) Schematic drawing of a chemical ionisation source. Based on [32]. B) Combined EI/CI Source of an Varian 240-MS.

The production of ions within the ion source is based on ion-molecule reactions. Thereby, bimolecular processes occur [32]. While ions are directly generated through collisions with high-energetic electrons in EI, these electrons first ionise a reactant substance in CI. Reactant substances are primarily gaseous, but liquids are applicable as well. The reactant substance must be vaporisable, and its ionisation energy must exceed the ionisation energy of the target analyte. Commonly applied reactant substances include methane, isobutene or ammonia, with methane being the most common. To prevent the analyte from being directly ionised by electrons, the pressure inside the ion volume is increased by a factor of 20–50 compared with an EI operation. This elevated pressure results in a 10^3 to 10^4 fold excess of reactant molecules compared with the analytes [32], limiting the direct reaction of the analyte to a low degree. To allow electrons to travel through the reactant gas, the kinetic energy of the electron is increased to approximately 200 eV, compared with 70 eV in EI. Inside the ion source, methane undergoes the following reactions [51]:

$$CH_4 + e^- \rightarrow CH_4^{+\cdot}, CH_3^+, CH_2^{+\cdot}, CH^+, C^{+\cdot}, H_2^{+\cdot}, H^+ \quad (4)$$

$$CH_4^{+\cdot} + CH_4 \rightarrow CH_5^+ + CH_3^{\cdot} \quad (5)$$

$$CH_3^+ + CH_4 \rightarrow C_2H_7^+ \rightarrow C_2H_5^+ + H_2 \quad (6)$$

$$CH_2^{+\cdot} + CH_4 \rightarrow C_2H_4^{+\cdot} + H_2 \quad (7)$$

$$CH_2^{+\cdot} + CH_4 \rightarrow C_2H_3^+ + H_2 + H^{\cdot} \quad (8)$$

$$C_2H_3^+ + CH_4 \rightarrow C_3H_5^+ + H_2 \quad (9)$$

$$C_2H_5^+ + CH_4 \rightarrow C_3H_7^+ + H_2 \quad (10)$$

Thereby, CH_5^+, $C_2H_5^+$ and $C_3H_5^+$ are the most dominant species and contribute most to the subsequent ionisation of the analyte. Their abundance strongly depends on the pressure inside the ion chamber. Thus, heavier methane-based species become more dominant with increasing pressure.

After the reactive methane species are generated, they can in turn generate two different types of analyte ions, either positively charged or negatively charged ions. While positive and negative analyte ions are produced simultaneously within the ion source, the method of choice depends on the chemical analyte properties, as the properties define the most common ion production path. Therefore, two different CI methods are acknowledged, positive chemical ionisation (PCI) and negative chemical ionisation (NCI), both named after the charge state of the produced analyte ions. Example spectra for positive and negative CI are presented in Figure 16. In general, four different ionisation methods are accountable for PCI [32,52]:

Proton transfer $$M + [BH]^+ \rightarrow [M + H]^+ + B \quad (11)$$

Electrophilic addition $$M + X^+ \rightarrow [M + X]^+ \quad (12)$$

Anion abstraction $$M + X^+ \rightarrow [M - A]^+ + AX \quad (13)$$

Charge exchange $$M + X^{+\cdot} \rightarrow M^{+\cdot} + X \quad (14)$$

Proton transfer mostly obtains protonated analytes. Electrophilic addition is the primary reason for analyte ions with a mass greater than the molecular mass. For methane, common adducts are $[M + H^+]^+$, $[M + C_2H_5^+]^+$ and $[M + C_3H_7^+]^+$. Through anion abstraction, the molecular mass appears lower. This reaction primarily takes place for hydride abstraction. While all the reaction pathways above deliver closed-shell ions, charge exchange transfers generate radical analyte ions.

Although NCI is limited to certain analyte types, it is especially useful for acidic analytes or analytes containing electronegative functional groups such as nitro groups [53]. Four different ionisation methods are accountable for NCI [54,55]:

Dissociation of acids $$M \rightarrow [M - H]^- + H^+ \quad (15)$$

Nucleophilic addition $$M + A^- \rightarrow [M + A]^- \quad (16)$$

Resonance capture $$M + e^- \rightarrow M^{\cdot -} \quad (17)$$

Ion-pair production $$M + e^- \rightarrow [M - B]^- + B^+ + e^- \quad (18)$$

In general, acidic analytes dissociate via proton loss. In addition, ions can be added through nucleophilic addition, similar to electrophilic addition for PCI. Furthermore, direct interactions with ions can occur, leading to ion-pair production or resonance capture.

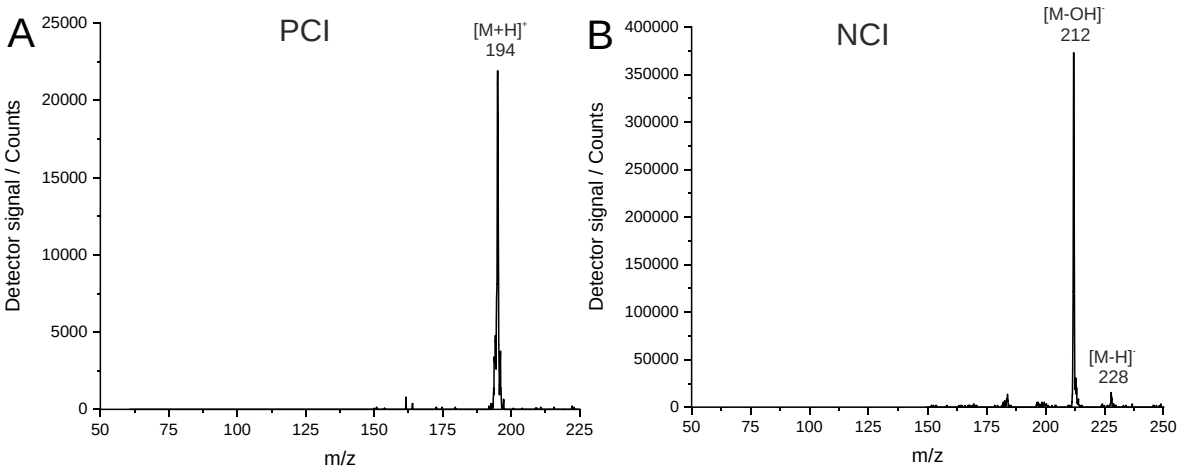

Figure 16: Examples for positive and negative CI spectra. A) Positive chemical ionisation spectrum of MDMA. B) Negative chemical ionisation spectrum of picric acid.

5.4 Mass analyser–ion trap mass spectrometry

In the 1950s, Wolfgang Paul developed a new type of mass analyser, the Paul trap [56]. This mass analyser allowed for storing and separating ions through resonance stimulation in a radiofrequency (RF) controlled quadrupole field. In 1989, Paul and his colleague Dehmelt were honoured with the Nobel Prize in Physics for this invention. The general working principle of a quadrupole ion trap (QIT) is as follows: generated ions are guided into the QIT, and there, the ions are stored and accumulated by applying an RF potential. After the ions are accumulated, they are sent to the detector by adjusting the frequency of the RF potential, separated by their mass-to-charge ratio. In addition, specific ions can be rejected by applying an additional direct current (DC) potential at the endcap electrodes.

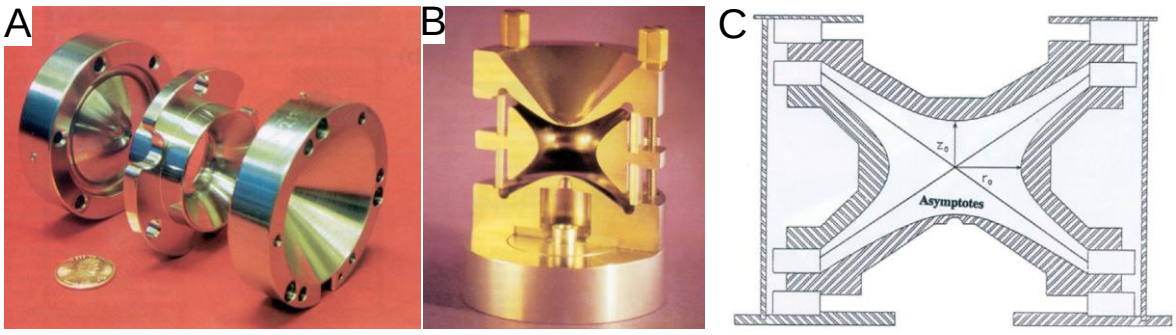

Figure 17: Quadrupol ion trap. A) Cross section of a QIT. B) The three electrodes, two endcaps and ring electrode. C) Shematic drawing of an ideal QIT. The geometric shape of the trap is fully described by z_0 and r_0. Copied from [57]. With kind permission by © John Wiley & Sons, Inc.

Figure 17 illustrates the structure of such a QIT. It consists of three electrodes, two endcaps and a ring electrode, as pictured in Figure 17 A. The hyperbolic shape of the electrodes allows for generating a quadrupole field if a RF potential is applied. If these three electrodes are put together, a QIT as depicted in Figure 17 B can be achieved. Figure 17 C displays a drawing of the ideal ion trap geometry. Such an ideal ion trap can be described by the following equation:

$$r_0^2 = 2z_0^2 \tag{19}$$

With this equation, the geometry of the QIT from Figure 17 C can be obtained. In this case, r_0 is the distance of the ring electrode from the trap centre, and z_0 is the distance from the endcap electrode to the trap centre. A vivid explanation of the forces that ions experience in a QIT, while an RF potential is applied, is drawn in Figure 18 A. This mechanical analogue of a three-dimensional potential field inside the QIT is utilised to enhance the comprehensibility. In this model, the ions inside a QIT are symbolised by a ball that sits on a saddle. If the saddle is static, the ball would roll down on one side. In a QIT, the ions would follow the lowest energetic level and collide with a wall. To prevent the ball from falling, the saddle rotates around the centre. Due to this rotation, the position of the lowest energy changes. If this rotation is fast enough, the ball cannot fall because, by the time the ball begins to move down on one side, this side already become a higher level based on the ball's inertia or speed of the ions. Since the ball and especially real ions have a certain energy and speed, specific trajectories are obtained. Figure 18 B illustrates an example of such trajectories within a QIT via microphotography. The white lines originate from a single charged particle of aluminium dust. To allow additional ions to be stored and to increase the resolution of the ion trap, a damping gas is added to absorb parts of the potential energy from the ions. A common damping gas is helium, as it is lightweight and inert. Due to this damping gas, the kinetic energy of the ions can be decreased from 10 eV to approximately 0.1 eV [57,58].

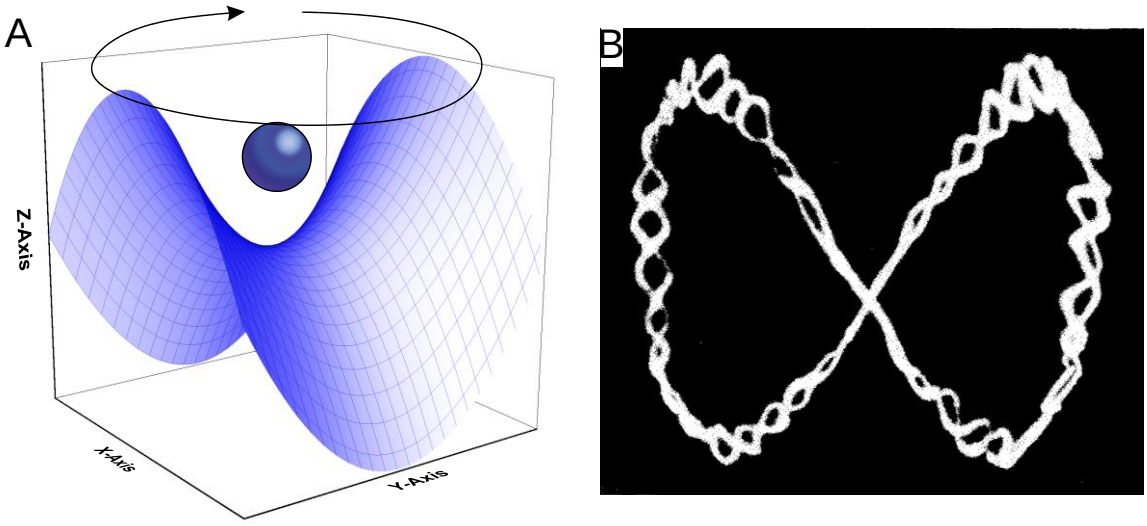

Figure 18: A) Mechanical saddle model to explain the stability of ion trajectories inside a QIT with an applied RF field. B) Microphotograph of a single charged particle of aluminium dust inside an RF field of a QIT. Part B copied from [59]. With kind permission by © AIP Publishing LLC.

The trajectories depend on the mass-to-charge ratio of the trapped ions based on a given endcap electrode voltage. This can be used to selectively eject ions from the trap and measure them at the detector. The frequency of the applied potential is therefore changed, which leads to a change in stable trajectories. When the frequency increases, increasingly more ions are ejected based on their increasing mass-to-charge ratio. This type of operation is known as scanning MS. In addition to the RF potential, a DC potential can be added. This DC potential allows for ejecting unwanted m/z and isolating specific m/z-ratios or m/z-ranges. The later application of another DC potential allows for selectively stimulating the isolated masses. A sufficiently strong stimulation allows for fragmenting the isolated ions inside the trap via collision-induced dissociation (CID). These generated fragments can be captured again by an applied RF potential and are available for further investigation. The procedure of fragmenting ions and analysing the resulting fragments is known as MS/MS or tandem mass spectrometry. In the case of multiple fragmentation circles, one speaks of MS^n. The advantage of MS^n is the ability to obtain more in-depth insights into the structure of the fragmented analyte. In proteome analysis, this technique is commonly applied to investigate peptide structures [60]. The number of ions that can be stored inside an ion trap is limited due to space charge effects among the ions and ion packages. Hence, an optimal ion filling exists. Underfilling and overfilling would cause lower detector signals or distorted spectra. A short pre-measurement determines the collection time that ensures optimal filling (so-called automatic gain control). Thus, varying analyte concentrations can be compensated efficiently.

5.5 Gas chromatography coupled to vacuum ultraviolet spectroscopy

Gas chromatography is a separation technique for gaseous or volatile/semi-volatile analytes. The separation principle is based on the adsorption and distribution of analytes between a mobile and stationary phase. Inert gases, such as nitrogen or helium, are preferred as a mobile phase, as they offer the best performance for non-inflammable and affordable gases. Stationary phases are usually polysiloxane-coated glass capillaries. Due to capillary lengths of several dozen meters and, thus, high absolute number of theoretical plates, the separation efficiency is high compared with other chromatographic techniques [61]. These capabilities make GC a frequently applied technique if complex or high-matrix-loaded samples of drugs, drug precursors and explosive precursors must be investigated. In addition, such target compounds can be challenging to analyse, due to their continually expanding number and wide variety of compound structures. To gain the best GC performance, selective and sensitive detector techniques are necessary. Commonly applied detectors for forensic samples are the flame ionisation detector (FID) [62] and the mass spectrometric detectors [63]. For FID, the impossibility of identifying analytes or gaining specific information about them is the most substantial drawback, and MS (e.g. with electron ionisation) is nearly universal and provides analyte-specific information, but common drawbacks include the need for a more sophisticated quantification approach and more complex instrumentation. A recently improved technique that comes of age is vacuum ultraviolet absorption spectroscopy. This overcomes the mentioned drawbacks, by combining the selectivity of a spectral detection system and the robustness of an absorption-based spectroscopic technique. Regarding other spectroscopic techniques, the applicability of Beer-Lambert's law allows for a straightforward and robust quantification. While the development of this technique dates back to 1987 [64], recent interests are based on instrumental improvements, that allowed a simpler and more flexible deployment [9,65,66].

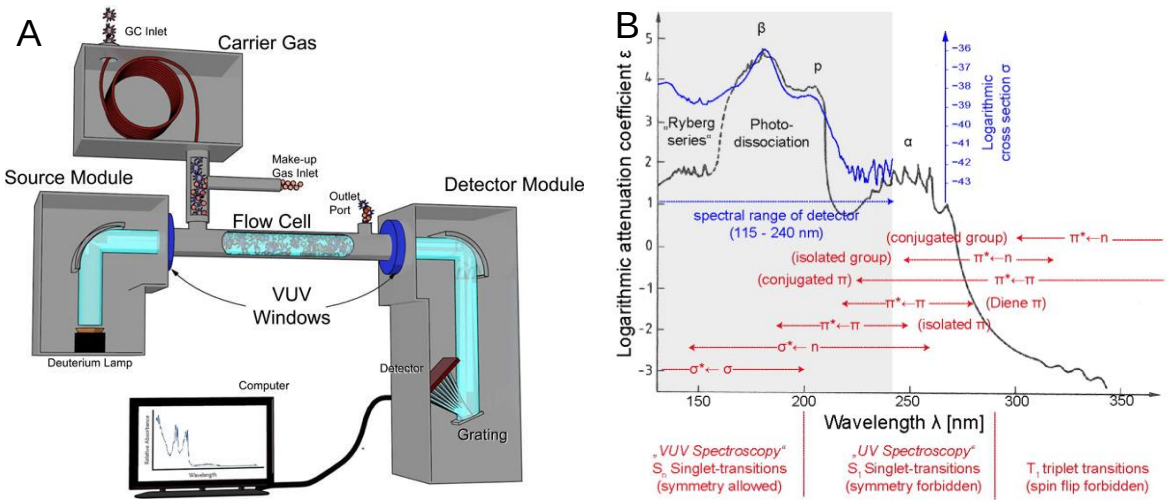

Figure 19: A) Schematic overview of a GC-VUV system, copied from [67]. B) Gasphase absorption spectra of benzene, with electronic transitions (red) and empiric VUV spectra (blue). Copied from [67]. With kind permission by © John Wiley & Sons, Inc.

A schematic drawing of a GC system coupled to a VUV detector (GC-VUV) is observable in Figure 19 A. The flow from the GC separation into the detection flow cell is illustrated. In the flow cell, the analyte absorbs light emitted from a deuterium lamp. The change in light intensity (absorption) is analysed at the detector for all observed wavelengths simultaneously. The acquisition speed can be adjusted by regulating the dwell time within the flow cell via a make-up gas stream. While the basic set-up is similar to a classic UV detector, the combination of enclosure and deuterium lamp allows for investigating wavelengths in the range of 115–240 nm. This allows for a nearly universal detection behaviour, since almost every chemical substance absorbs light at wavelengths below 185 nm and exhibits a high sensitivity as the absorption coefficient is higher, compared with wavelengths applied at UV spectroscopy [68]. In Figure 19 B, an absorption spectrum of benzene and the corresponding transition states are explained, allowing for the generation of substance-specific absorption spectra.

5.6 Immunoassay drug tests

Immunoassay drug tests (IDT) are a well-established method for detecting target compounds [69]. They are frequently applied in laboratories and driver's controls and can even be used by untrained personnel at workplaces [70]. The availability of compound class specific test kits and their wide distribution among security forces contributed to their role as a basic technique for conducted method comparisons. Immunoassay drug tests enable a quick, easy-to-use and affordable analysis for specific target compounds. A commonly applied type of immunoassay for drug testing is a lateral flow assay [71]. The basic principle of an immunoassay is explained based on a lateral flow assay, as presented in Figure 20. Therein, schemes of the antibody, the analyte and the labelled antibody are given. The analyte and a tracer labelled antibody are transported by capillary forces from the sampling

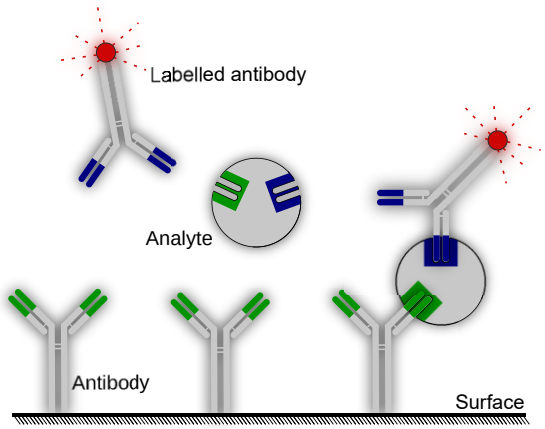

Figure 20: Basic principle of an enzyme immunoassay (EIA). Three steps are drawn: the coated antibody on the left, the approaching analyte and labelled antibody in the middle and the bonded antibody on the right.

surface to the test area. Common tracers are gold nanoparticles for a red colour [72], radioactive species or fluorescence exhibiting dyes [73,74]. At the test area, another antibody is bonded to the surface, typically an organic polymer. The antibody is specific for a certain analyte and can bind the analyte, and thus the labelled antibody, at its surface. All non-bounded antibodies migrate further to the end of the test, leaving only analyte-bonded antibodies on the surface. By investigating the signal intensity of the retained antibody tracers, it is possible to draw conclusions regarding the presence of the investigated analyte.

Real-world results for an immunoassay drug test are presented in Figure 21. The white strip on the left side of the assembly soaks up water. Afterwards, this water solubilises the marked antibodies and moves further due to capillary effect. On its way, it passes and solubilises the investigated sample. Further behind, the mixture flows through the immobilised antibodies. Therefore, if present, the analyte bonds the immobilised antibody and labelled antibody to the analyte. This results in a red-coloured bar. The excessively labelled antibody moves further on to a second part of coated antibodies. In contrast with the first antibodies, these are specifically made to directly bond the excessively labelled antibody. This second reaction results in the second red control mark.

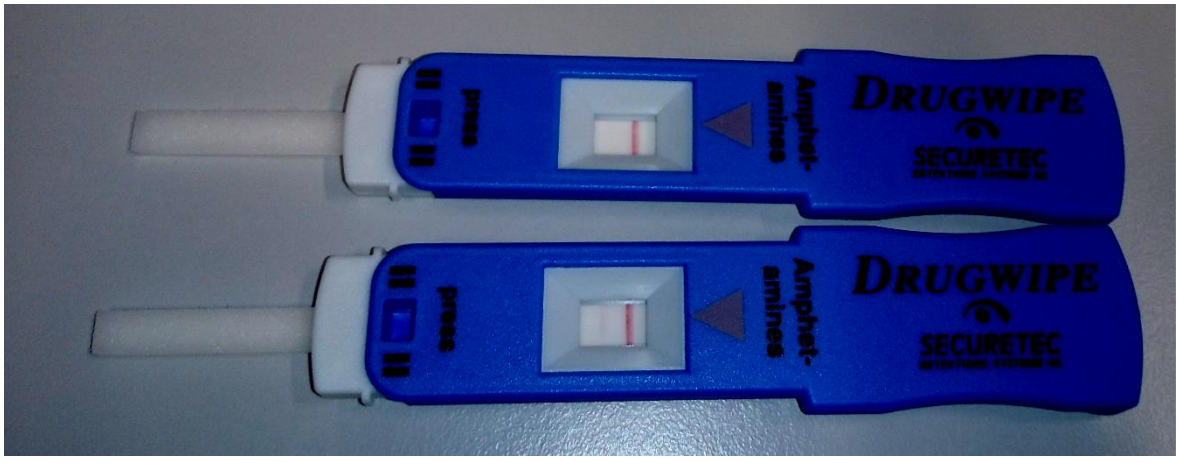

Figure 21: Immunoassay drug tests for amphetamine. Upper test, blind test with no amphetamine and thus only one red mark. Lower test, near LOD with approximately two nanograms of amphetamine. One strong and one weak red mark are visible. A second weak red mark proves the presence of amphetamine.

The upper IDT reveals a blind test with no amphetamine present in the sample. In contrast, the lower IDT was tested with two nanograms of amphetamine absolute, the corresponding

limit of detection (LOD), and revealed two red marks. As the mark for positive results is only slightly visible, the LOD of this immunoassay is nearly reached.

5.7 Ion mobility spectrometry

Ion mobility spectrometry (IMS) is a versatile analytical technique well known in the field of forensic science and is applied at most airports today [75–77]. It has become the most successful and widely utilised technique for detecting explosives [78]. The primary benefits are a compact and lightweight instrumental set-up and relatively low acquisition and maintenance costs compared with other analytical techniques. The combination of these benefits with the wide distribution leads to its involvement at the conducted method comparisons. Ion mobility spectrometry is based on the shape and size of an ion. Thus, isomers can be differentiated [79]. One disadvantage of most IMS is a low separation power (peak capacity, resolution), potentially leading to issues in identifying target compounds in complex matrices and causing false detection alerts [80,81]. The development of IMS began in the 1950s and utilised a drift cell with low electric field strength to investigate ion mobility and ion reactions in the gas phase [82]. In addition to novel IMS developments such as travelling wave IMS [83], field asymmetric IMS [84] or trapped IMS [85], drift tube systems are still commonly used, particularly for handheld systems. If applied at ambient pressure, drift tube IMS does not need vacuum pumps, which further decreases the weight and costs. Additional weight reductions and an increase in robustness can be obtained by utilising a radioactive ion source such as Ni^{63}. The working principle of a drift tube IMS with Ni^{63} ionisation is illustrated in Figure 22.

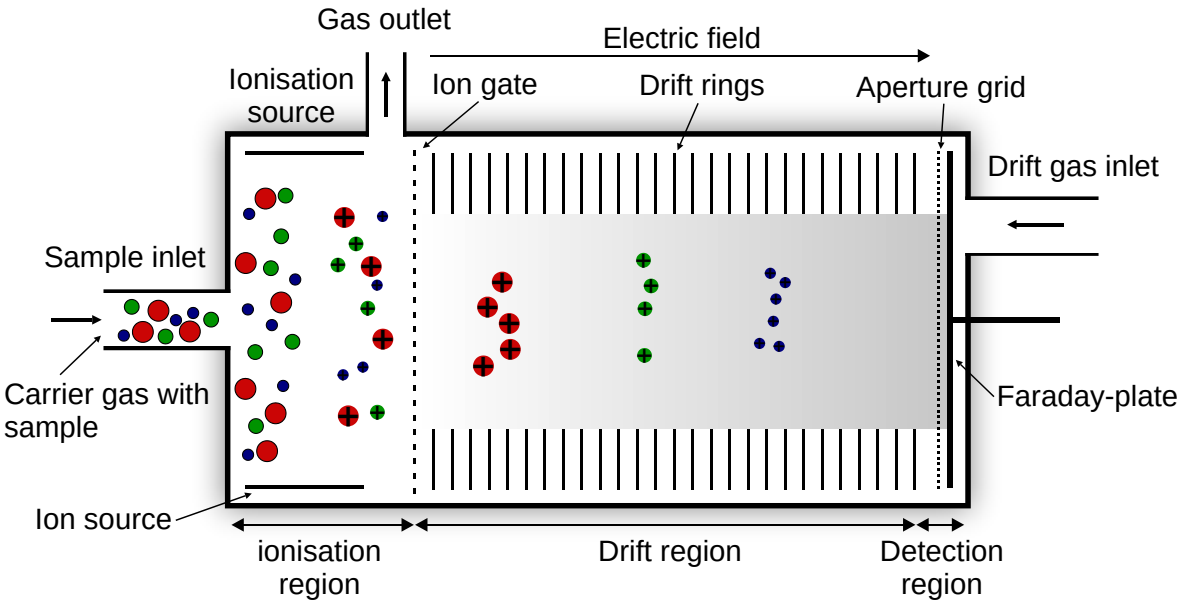

Figure 22: Schematic overview for the working procedure of a drift tube ion mobility spectrometer (drawn for the detection of positive ions).

At the gas outlet, a pump continuously transports air out of the instrument, which induces a stream of air from the sample inlet into the device. The incoming air sample passes through the ionisation region, where the compounds are ionised by a radioactive atmospheric-pressure chemical ionisation. The generated ions are diverted towards the drift region due to an applied electric field. By switching a second electric field on and off at the ion gate, the ions are pulsed and begin moving at the beginning of the drift region at the same time. The drift region itself is the main part of the IMS and separates the ions based on their charge, mass and collision cross section. This is achieved by applying a continuously rising electrical field at the drift ring, towards the detector. At the same time, clean drift gas travels the opposite direction in the drift region, from the detector to the gas outlet. Therefore, the ions are accelerated by the electric field but are simultaneously slowed down due to collisions with drift gas molecules. The electric field and collisions cause a separation of the analytes by size and shape and allow for the time-dependent detection. A simple, yet common detector is a Faraday cup, similar to that described for MS. Afterwards, the detected currents are amplified and stored in a computer system to be prepared for analysis.

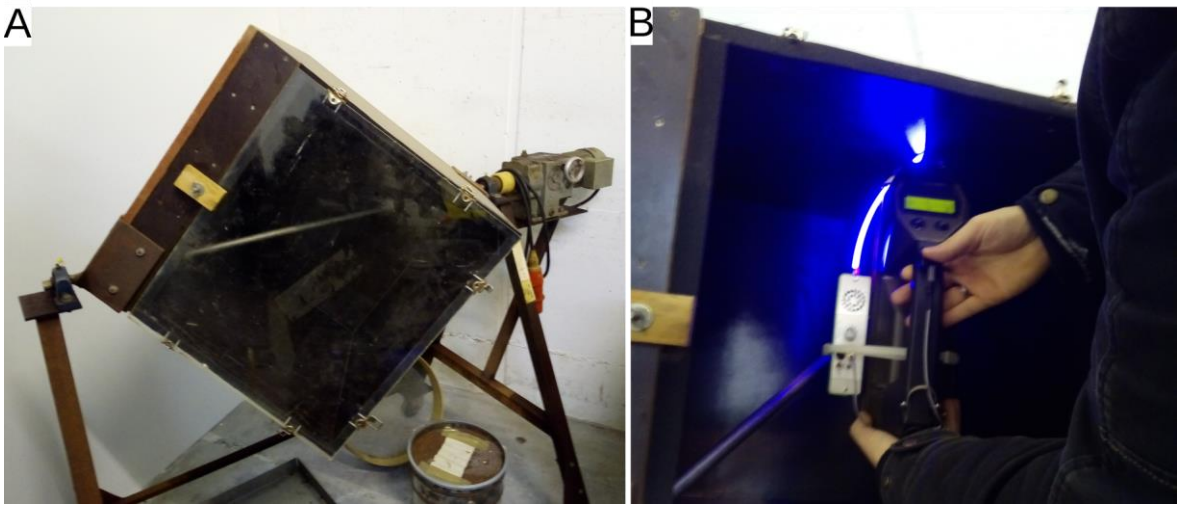

Figure 23: Application examples of a handheld IMS, coupled to APLD. A) Homemade mixer for blending herbal mixtures with new psychoactive substances. B) Surface sampling of the inside of the mixer to monitor for target compounds.

An example of a handheld drift tube IMS is pictured in Figure 23. Therein, the IMS is combined with a lightweight, battery-operated APLD system. This combination results in a highly mobile, lightweight and small measurement device. In the example, the inner surface of a mixer for herbal blends is investigated. This mixer was confiscated and previously utilised to coat herbal mixtures with new psychoactive substances.

6. Results and discussion

The subsequent sections divide the published results regarding their field of application. Therefore, the investigated techniques are separated into laboratory and on-site techniques. Publication 1 examines and extends GC-VUV for laboratory usage. Publication 2 concerns enhancing the APLD performance, and Publication 3 compares the application of APLD-MS with other techniques for on-site investigations.

6.1 Evaluation and application of GC-VUV

In the field of forensic science, VUV has been utilised up to now to investigate new designer stimulants and cannabinoids [86,87] and to identify thermal decomposition products of nitrate ester explosives [88]. While these publications extend the range of applications for VUV for forensic target compounds, they represent only some relevant fields. To add new fields and enhance the knowledge about the capabilities of VUV, drug and explosive precursors in Publication 1 are investigated with GC-VUV. Therefore, 19 drug and explosive precursors and simulated smuggling of drug precursors in gasoline cans were examined.

The LOD determination for all investigated compounds revealed an LOD between 0.7 ng and 3.3 ng of the total amount of substance. Compared with common detection techniques [9] such as GC coupled flame ionisation detectors (GC-FID), GC-VUV exhibits a 10 times-higher LOD utilising a signal-to-noise ratio of S/N > 3. While no correlations could be observed, regarding the number of sigma bonds, heteroatoms or pi bonds, a lower LOD was obtained for the investigated analytes with an aromatic structure present.

To review the ability to differentiate isomeric compounds, exemplary results for nitroaromatic compounds of varying complexity are drawn in Figure 24. Part A exhibits the behaviour for 2-/3-/4-nitrophenol. The main absorption band at 175 nm reveals a hypsochromic shift for an increasing distance between the phenol and nitro functional groups. The second absorption band at higher wavelengths also shifts hypsochrom resulting in one broad absorption band for 4-nitrophenol. These differences allow for differentiating between the isomers. Figure 24 B demonstrates the isomeric differentiability for three DNT isomers.

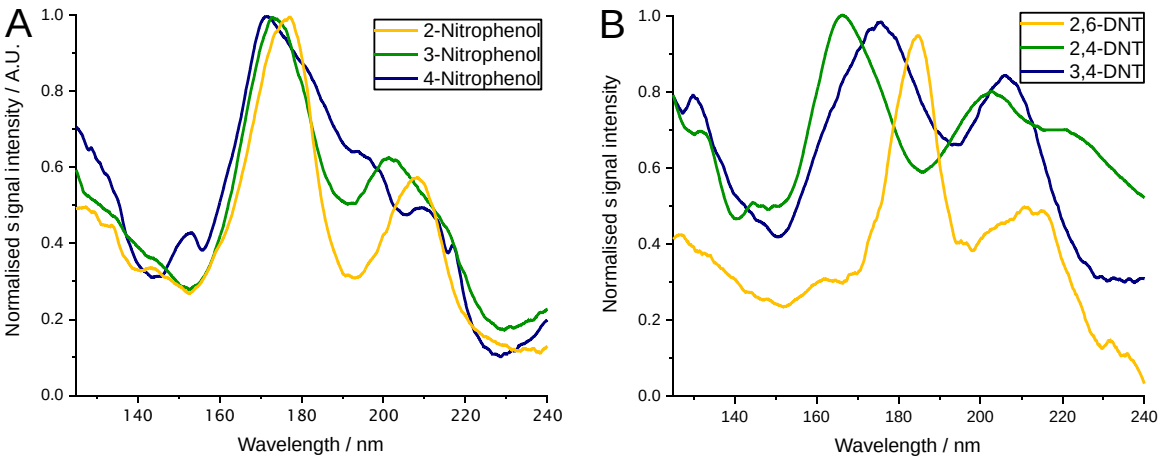

Figure 24: A) Normalised absorption spectra of three nitrophenols. B) Normalised absorption spectra of three dinitrotoluene isomers.

Another investigated topic was the issue of co-eluting peaks frequently encountered with chromatographic separations of complex mixtures. To solve this, either multiple measurements using different chromatographic approaches or the deconvolution of the co-eluting peaks can be utilised. For VUV absorption spectroscopy, a supervised method based on a linear combination of spectra has been established [9]. However, all co-eluting compounds must be known, and retention indices and spectra must be deposited in a spectral library. Therefore, the need for a pre-determined library is one of the largest drawbacks of VUV deconvolution. To extend the abilities of VUV detectors and overcome the mentioned limitations, non-negative matrix factorisation (NMF) was introduced for VUV spectroscopy. It does not require pre-determined retention indices and a spectral library, which allows for deconvoluting unknown substances, as in non-targeted studies. While NMF in general is a well-known mathematical technique and has been adopted to techniques, such as GC-MS and high-performance liquid chromatography coupled to MS (HPLC-MS) [89,90], no investigations have previously been conducted with respect to a successful application to VUV absorption spectroscopy. In Figure 25 A, the deconvolution of the co-eluting cyclandelate and safrole is demonstrated. In addition to Figure 25 A, Figure 25 B introduces an example with a four-times-reduced signal intensity for the deconvolution of 3-nitrophenol and 2,6-DNT. In both examples, the deviation between the area of a deconvoluted peak and its nominal area is compared. While spectral-based deconvolution reveals an overall area error of 0.4%, NMF yielded a result with a 5.0% error (Figure 25 A). While the signal intensity of B is only one fourth that of A, the overall error increases slightly but remains in the dimension for both methods. Thereby, higher and more differentiated errors align with the noisier NMF spectra. Therefore, it could be assumed that the basic deconvolution error is at the same level for both methods, and the measured deviations are random errors.

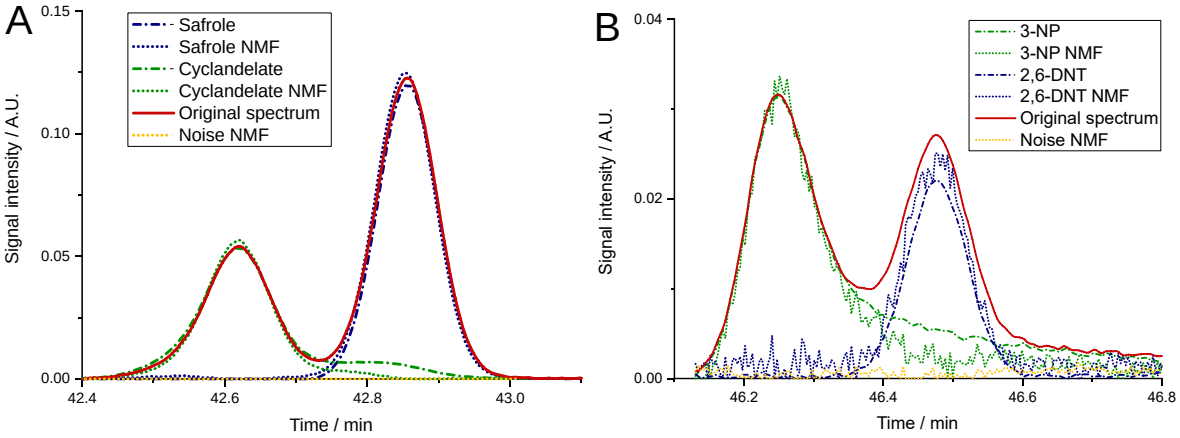

Figure 25: A) Deconvolution of cyclandelate and safrole via spectral deconvolution (dot-dashed line) and NMF (dotted line) from a deconvolution sample. B) Deconvolution of 3-nitrophenol and 2,6-DNT via spectral deconvolution (dot-dashed line) and NMF (dotted line) from the same measurement as A).

A more complex deconvolution describes the detection of 1‰ BMK in a gasoline matrix using GC-VUV. This scenario was selected because the smuggling of drug precursors in gasoline is a known forensic scenario [91]. The total-intensity GC-VUV chromatogram of the analysed sample exhibits a co-elution of BMK with 1,2-diethylbenzene from the gasoline. In this case, the quantification and identification of BMK is challenging, especially because both peak maxima appear simultaneously. Deconvolution of these compounds is performed, at first via spectral deconvolution and second by NMF. For spectral deconvolution, the area of the non-spiked 1,2-diethylbenzene and the deconvoluted area of the spiked sample results in a deviation of approximately 7%. Given that the area of 1,2-diethylbenzene is small compared with the BMK signal (about 4% area), it is highly probable that this deviation can be tolerated for many cases. While NMF is capable of separating an approximately 1:1 separation, the attempt of deconvoluting BMK-spiked gasoline reveals no useful information due to the non-applicability of the requisite boundary conditions. In this case, both deconvoluted peaks reveal no separable maxima and therefore NMF delivers no physically reasonable results.

After the mentioned examples revealed promising, yet limited results for the NMF deconvolution, systematic testing was performed. This was done by investigating the repeatability, allowed peak ratio and maximum peak overlap of co-eluting compounds. Furthermore, the obtained values were compared with spectral deconvolution. A graphical overview of these parameters for two co-eluting peaks, with different peak area ratios and peak overlaps, is provided in Figure 26. Figure 26 A illustrates the repeatability of every investigated combination by measuring the maximum standard deviation, based on the thousandfold calculation of the NMF. As a result, the relative maximum standard deviation for most peaks with an area overlap of up to 33% is less than 5%. In addition, the peak area ratio has only little effect on the deviation, while a peak overlap greater than 33% results in increased deviations. This increase achieves its maximum at 10.9% with almost complete

overlap and would allow separating nearly fully overlapping peaks for all peak ratios. For comparison, spectral deconvolution is reported to separate mixed components with a peak area ratio of up to 99:1 [92]. In Figure 26 B, the deconvoluted peaks are summed up and are compared afterwards with the original spectra. As a result, the relative difference of both areas was plotted. Figure 26 B reveals different maximum standard deviations, especially for a highly overlapping peak area. This is most likely due to the hard colour cut applied for improved interpretability. For peaks with an area overlap of up to 33%, the error is less than 10% and with a maximum error of 13.8%, all peaks can be separated. These results indicate that NMF can separate all investigated combinations of peak ratios and peak overlaps and can reproduce the initial data with minor challenges. In general, the obtained results reveal that VUV spectroscopy is a promising detector technique for investigating forensic scenarios.

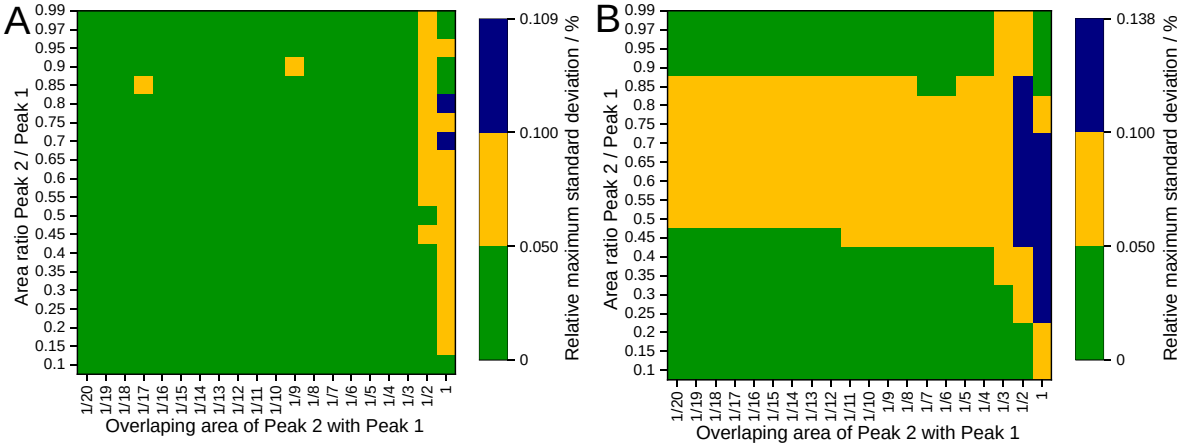

Figure 26: Systematic measurement of reproducibility and compliance of NMF deconvolution for different deconvolution issues of two peaks. Therefore, the results are expressed by a coloured pixel for every investigated combination of the area ratio between peak 1 and peak 2 and the area overlap of peak 2 with peak 1. The colour coding is arbitrary and should reflect relevant levels. These levels are green for relative deviations of up to 5%, yellow for relative deviations between 5% and 10% and orange for greater than over 10% relative deviation. The measured deconvolutions range from an area ratio between peak 1 and peak 2 from one to ten with only slight overlap to practically equal peaks with a high area overlap. Part B illustrates the reproducibility, by measuring the maximum standard deviation of 1,000 measurements for every investigated combination. In part C, the deconvoluted peaks are summed up again and are then compared with the original spectra, and the resulting relative difference of both areas was plotted.

6.2 Improvements of the APLD-MS

The aim of Publication 2 was to extend the capabilities and limits of the APLD technique. The original APLD ion trap MS (IT-MS) unit was investigated only for the desorption of explosives and exhibits issues with high desorption delays [34]. To overcome these issues, Publication 2 describes the improvements of the APLD set-up to reduce the desorption delay and expands the field of application to drugs and drug precursors. In addition, real-case samples demonstrate the actual performance, and newly constructed equipment allow for performing the imaging of suspicious surfaces.

For the set-up improvements, various parameters, such as the temperature of sampling, desorption area or desorption head material, were modified and optimised. Furthermore, the diameter of the laser fibre was increased, leading to a higher surface desorption area. The resulting improvements are pictured in Figure 27, for the desorption of Tetryl. Therein, the major decrease of the full width at half maximum (FWHM) is presented. As the original desorption system utilised a longer transferline, the operator can now choose between faster analytical results (novel APLD) or greater flexibility at surface sampling (original APLD). In addition, these improvements of the FWHM lead to a general improvement of the LOD, for Tetryl from 30 ng for the original APLD-MS down to 2 ng for the novel one. To obtain a more general overview, this comparison was performed for five different explosives that have been previously measured before.

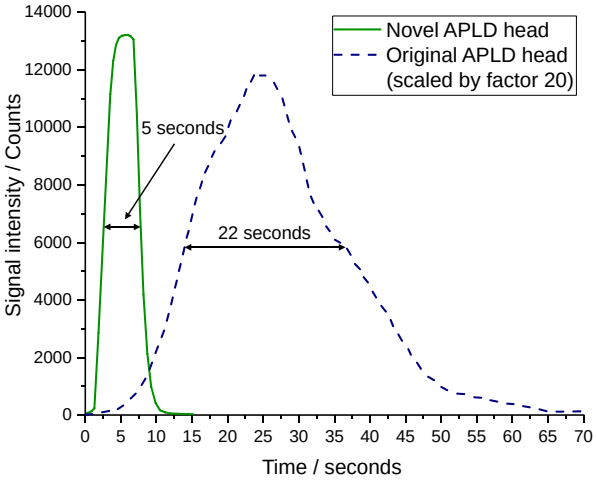

Figure 27: Comparison of smoothed desorption from spots with about 1.5 µg Tetryl. Measured at negative CI mode and fragment m/z 241. The novel system with a short transferline and heated APLD head is drawn as a solid line, the original measurement system with a long transferline is drawn as a dashed line. Compared is the FWHM.

The drugs and drug precursors compound class extension successfully proved the applicability of the APLD for non-thermo labile but also low volatile compounds. Therefore, eight compounds of different volatility and molecular masse were measured. The achieved LODs for the tested compounds are in the same range compared with measured explosives (e.g. 17 ng for cocaine hydrochloride and 10 ng for methamphetamine).

To demonstrate the practical usability of the APLD, two real-world scenarios were investigated. The first attempted to obtain information from post-blast residues regarding the utilised explosive. The second investigated the possibilities of measuring substance-specific signals on a complex matrix, consisting of an herbal mixture. To summarise the results, Figure 28 A and B describe the investigation of post-blast residues of a Second World War bomb. Evidence for the presence of TNT residues was found on all investigated shrapnel. In addition, the obtained substance-specific fragments support this assumption. The scenario in Figure 28 C and D was selected because it concerns an intensifying issue regarding the added compound class of drugs. The talk is of new psychoactive substances, more specifically, 5F-Cumyl-PINACA on an herbal blend and on the corresponding storage bag. In addition, to demonstrate the flexibility of the APLD in combination with MS, these investigations were conducted with the same set-up as for the TNT detection but with EI ionisation.

The results reveal the positive detection of 5F-Cumyl-PINACA on the herbal mixture itself and on the inside of the bag. While the signal intensity for the inside of the bag is about only half as high as the direct desorption signals, both exhibit the same compound related fragment pattern.

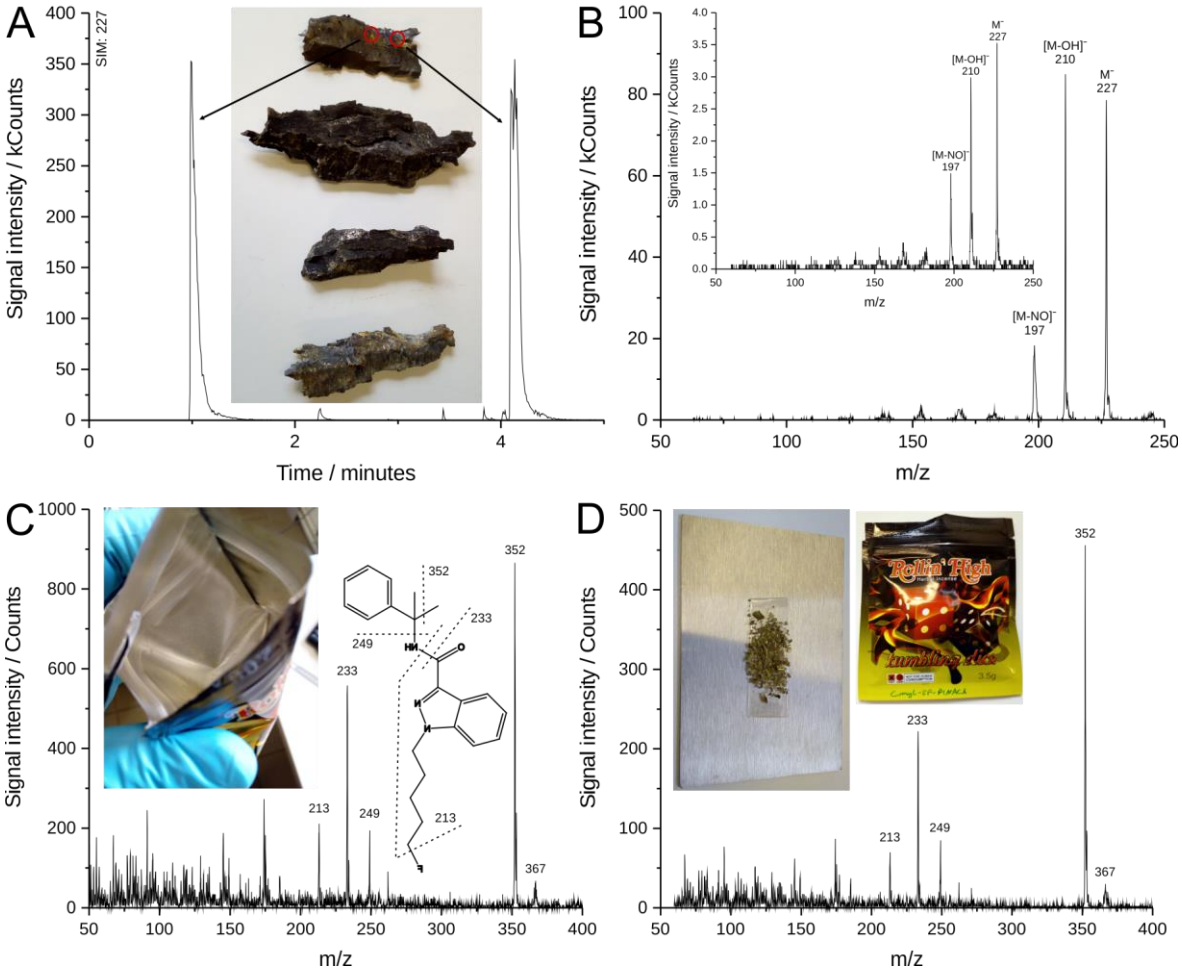

Figure 28: A) and B) Detection of TNT from the surface of shrapnel recovered from a defused bomb of the Second World War. Measurement was performed in negative CI Mode. A) The exemplary findings, marked with red circles, correspond to the single-ion traces in the mass profile in which the TNT signal at *m/z* 227 is plotted. B) The full-size mass spectrum reveals the first peak to be at approximately 1 min. The panel on the left displays the spectrum of a 10 ng TNT standard sample, measured under the same conditions. C) And D) APLD EI-mass spectra of the herbal blend material. Direct laser desorption exhibits intense signals at higher *m/z*, tentatively assigned to 5F-Cumyl-PINACA from an herbal blend sold as 'Rollin'High'. This new psychoactive substance was detected directly from the herbal blend and from residues remaining on the emptied bag. C) Displays a mass spectrum achieved by desorbing the inner side of the bag and D) presents a direct measurement of the herbal blend.

Based on the theoretical possibility, to perform ongoing APLD measurement for several hours, a set-up to systematically map surfaces was developed. Such measurements were made possible based on the improved FWHM for the novel APLD head, resulting in drastically reduced time consumption.

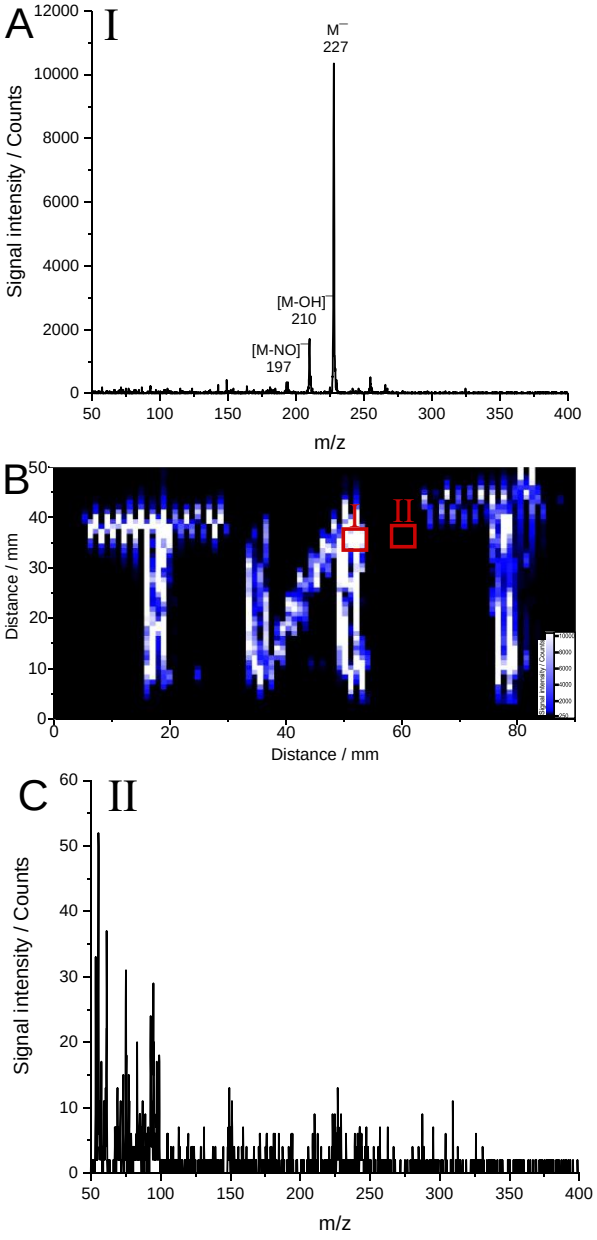

Figure 29: APLD mapping capabilities demonstrated in a TNT example generated with CI negative detection mode. If the position of the X-Y table and the signal intensity are combined at any point on the surface, the drawn image can be achieved. The image B) displays a prepared stainless-steel surface labelled with the word TNT. The total amount of substance applied for this image was approximately 20 µg. The colour changes from black (no TNT detected) to white (high amounts of TNT detected). Therefore, spectrum A) reveals the basis for a 'white area' and C) indicates a 'black' area.

The developed system enables the APLD-MS to scan flat surfaces on objects up to an imaging size of 20 cm by 20 cm with sub-millimetre lateral resolution and an object weight of 2 kg. One example of such an image is provided in Figure 29. Therein, a surface was coated with trails of TNT containing methanol, describing the word 'TNT'. The subsequent imaging of this surface revealed the previously written word TNT and thus demonstrated the capabilities of this combination. Two spectra of different spots were added, confirming the nearly complete absence of TNT residues on blank spots. This example demonstrates the ability to obtain consistent signals and perform long-term measurements. Therefore, based on this imaging set-up, the field of application for APLD is extended further. Arriving at the overall result that new compound classes were investigated, the LOD and the FWHM were improved, and demonstrations were performed for laboratory measurements and realistic forensic issues.

6.3 Method comparison of possible on-site analytical techniques

Quick and reliable analytical results are crucial for first responders to make adequate decisions. Multiple analytical techniques are currently available that claim to provide these analytical results. Therefore, it can be challenging to understand whether a certain technology is suitable for a certain issue. To provide support regarding this issue, the aim of Publication 3 is to compare currently applied methods and potential future methods, for

the case of trace analysis of surfaces, during on-site investigations. For this comparison, the techniques IDT, IMS and APLD-MS are selected, representing different approaches for the on-site analysis of target compounds. Immunoassay drug tests are inexpensive and can be handled properly after a short briefing. Ion mobility spectrometry is capable of analysing multiple target compounds and is more cost effective if many samples are analysed. Ambient mass spectrometry is capable of analysing a wide variety of target compounds, even simultaneously.

The comparison begins by determining the LOD for different compounds with similar methods and standards. Therefore, 10 compounds are investigated. The obtained LODs are in the same range for IDT and IMS, ranging from two nanograms of amphetamine for both techniques to two nanograms of MDMA for IDT and five nanograms for IMS. The LODs for APLD-MS are approximately 10 times higher compared with the two other techniques, with 20 ng for amphetamine and 21 ng for MDMA. The detectable compound classes differ as well, resulting in four compounds by IMDs and eight by IMS, and all were detected by APLD-MS. To consolidate the comparison, all techniques are discussed in detail. Thereby, major parameters, such as the complexity of the analytical technique, user requirements and selectivity, among others, are discussed as well. Additionally, APLD-MS is compared with direct analysis in real time [93], DESI [94], dielectric barrier discharge ionisation [95], easy ambient sonic spray ionisation (EASI) [96], IR desorption [97] and LTP [98]. This is performed, because APLD-MS is one of multiple direct sampling techniques that could theoretically be utilised for such investigations. To enhance the comprehensibility and clarify the technological differences, seven key parameters were defined.

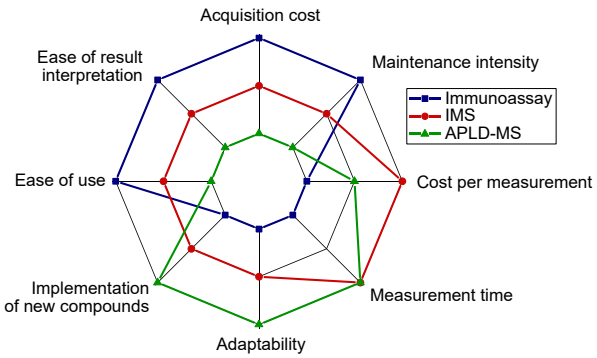

Figure 30: Visualisation of key parameters for the comparison of all three methods. Plus indicated positive or better, zero indicates neutral or in between and minus indicates negative or worse with respect to the other techniques.

The impacts of the investigated techniques on each parameter are presented in Figure 30. The figure exhibits that each technique has its strengths and weaknesses and that there is not a single technique suitable for all applications. If only few samples should be analysed for amphetamine, methamphetamine or MDMA, IDTs could be the method of choice. In the case that routine measurements are needed, and the target compounds are limited to known compounds of drug production, using IMS could be advantageous. Assuming that complex samples must be investigated, APLD-MS or another ambient MS technique can demonstrate its strengths. To test the investigated techniques under real conditions, practical measurements were performed at a former

clandestine MDMA laboratory. Parts of the clandestine laboratory are observable in Figure 31 A. Three different samples were acquired and analysed. In addition to two spots from an actively used Büchner funnel and drying closet, one sample was obtained from the wall behind the equipment. This sample is particularly interesting because the laboratory was equipped with professional equipment, allowing for a less MDMA-contaminating workflow during production, compared with amateur productions. The results provided in Figure 31 B for IDT, Figure 31 C for IMS and Figure 31 D for APLD-MS. While the obtained signal intensity and thus the MDMA concentration differ strongly between the sample spots, all techniques were capable of detecting MDMA at all spots from across the clandestine laboratory.

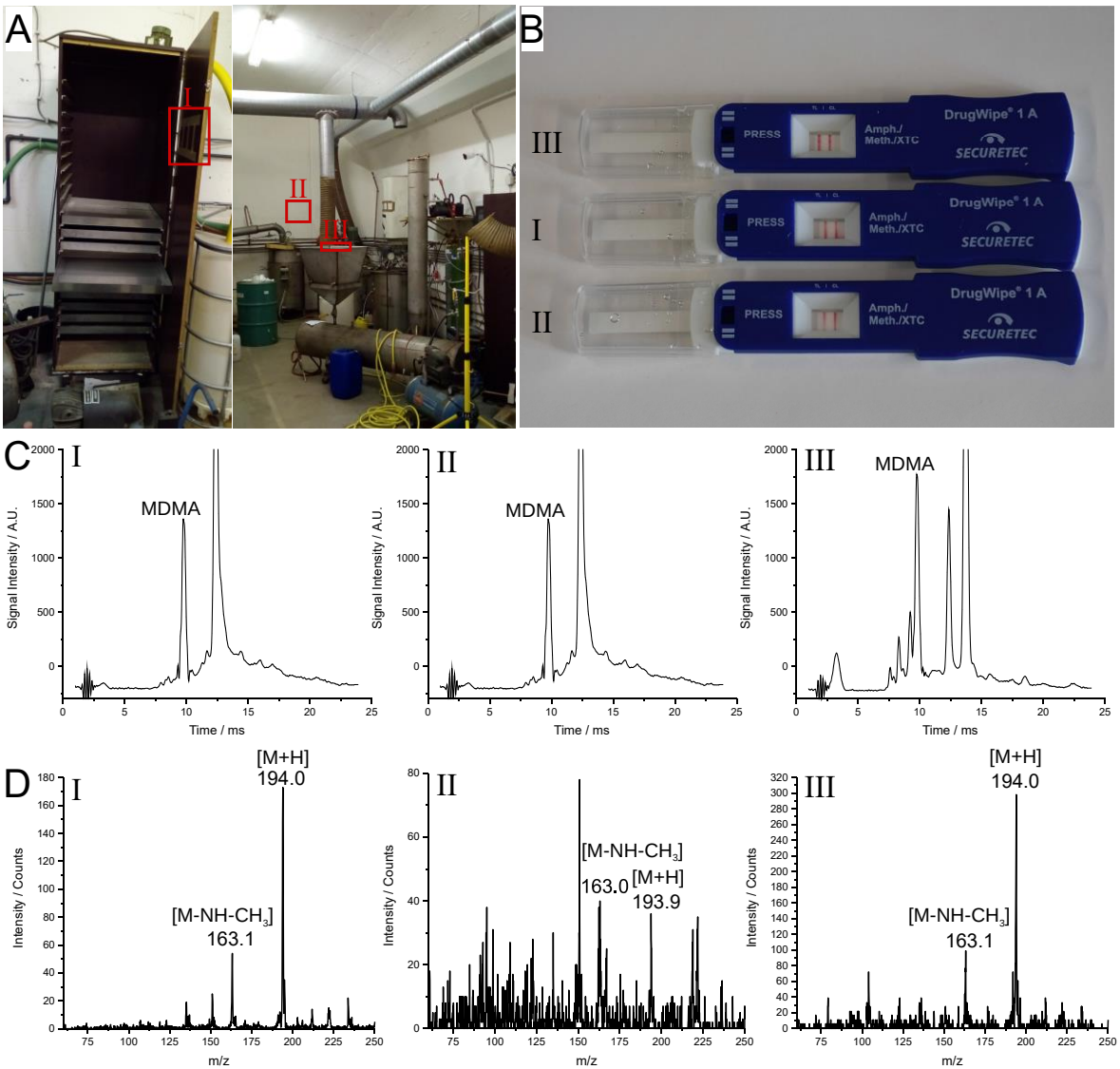

Figure 31: A) Sampling spots at a former clandestine MDMA laboratory in Germany. The sampled areas are (from left to right) drying closet, wall and Büchner funnel, all marked with red rectangles. B) Positive immunoassay drug tests of the sample areas indicated at A). The results are (from top to bottom) Büchner funnel, drying closet and wall. C) IMS measurements of the three sampling sports. The signal at approximately 9.8 ms is related to MDMA. IMS plasmagrams are in the following order (from left to right): drying closet, wall and Büchner funnel. D) Positive chemical ionisation mass spectra of the three sampling spots. Spectra are in the following order (from left to right): drying closet, wall and Büchner funnel.

Samples from the contaminated glassware are analysed for amphetamine and the intermediate NFA, in addition to the precursors APAAN and BMK. The amphetamine was synthesised in a four-step reaction via the Leuckart method [14,99,100]. Therefore, samples belong to the aqueous wastes from Leuckart step 1, Leuckart step 2 and a steam distillation. All techniques achieved the detection of amphetamine. Ion mobility spectrometry and APLD-MS were capable of detecting the intermediate NFA, and only APLD managed to detect the drug precursor BMK.

In conclusion, all techniques obtained quality results for within their limitations. Therefore, the preferred technique depends on the analytical capabilities necessary for a certain issue. More analytical flexibility and explanatory power correlate to more sophisticated techniques. Therefore, the choice of which technique to select, should be based on the needed complexity of the analytical results on site.

7. Summary and outlook

The present dissertation investigates drugs, explosives and their precursors with different analytical techniques and performs improvements, extensions and evaluations for these techniques, among others, for real-world scenarios. This is done for laboratory and on-site analytical techniques. Thereby, laboratory and on-site analytical techniques are complimentary, as both address different fields of application for the same target. At both areas, powerful analytical techniques are required, to complete given tasks. In addition, continuous improvements are necessary to keep pace with the rising complexity of samples. These originate from an ongoing competition between further regulation and the bypassing of these regulations in addition to the invention and production of new compounds.

For laboratory investigations, a recently introduced GC detector, based on vacuum ultraviolet spectroscopy, was evaluated for its suitability for drug and explosive precursors. In general, GC-VUV combines the ease and robustness of a UV detector and identification possibilities similar to IR or Raman spectroscopy. The investigations revealed, that isomeric compound separation and identification is easily achievable and that provided deconvolution capabilities are applicable for real-world cases. Furthermore, a new analysis tool was introduced, allowing for the deconvolution of coeluting peaks without need for spectral-based databases. Especially for highly complex mixtures, the introduced deconvolution tool is a valuable extension, as it allows for peak separation without prior measurement of pure substance spectra, thus enhancing the deconvolution capabilities even further.

For on-site investigations, APLD proofed itself as a suitable tool for investigating surfaces with low-volatile substances, particularly in combination with a lance probe in remote places. The simple/robust design and the sole need for electricity are advantages compared with other surface-analysing techniques, such as DESI or EASI. The extensive testing under real-world conditions leads to multiple design improvements, which in turn resulted in an up to 15 times improved LOD and response time reduction of the system by a factor of four. In addition, the investigations of drugs and drug precursors extended the scope of this method. Furthermore, the implementation of an imaging system for large and heavy surfaces allowed for covering additional areas of application and enhancing the value of this technique. The enhanced APLD was then compared with different state-of-the-art technologies for on-site investigations. The results identified different capability shortfalls of current techniques for surface analysis and the advantage of the enhanced APLD, especially for complex samples.

8. References

[1] M.J. West, M.J. Went, Detection of drugs of abuse by Raman spectroscopy, Drug Test. Anal. 3 (2011) 532–538. https://doi.org/10.1002/dta.217.

[2] E. Gerace, F. Seganti, C. Luciano, T. Lombardo, D. Di Corcia, H. Teifel, M. Vincenti, A. Salomone, On-site identification of psychoactive drugs by portable Raman spectroscopy during drug-checking service in electronic music events, Drug Alcohol Rev. 38 (2019) 50–56. https://doi.org/10.1111/dar.12887.

[3] C. Bermúdez, C. Cabezas, S. Mata, M. Berdakin, J.M. Tejedor, J.L. Alonso, Analysis of illicit drugs by direct ablation of solid samples, Eur. J. Mass Spectrom. (Chichester, Eng) 21 (2015) 775–781. https://doi.org/10.1255/ejms.1399.

[4] J. Andrasko, L. Lagesson-Andrasko, J. Dahlén, B.-H. Jonsson, Analysis of Explosives by GC-UV, J. Forensic Sci. 62 (2017) 1022–1027. https://doi.org/10.1111/1556-4029.13364.

[5] D.R. Justes, N. Talaty, I. Cotte-Rodriguez, R.G. Cooks, Detection of explosives on skin using ambient ionization mass spectrometry, Chem. Commun. (Camb.) (2007) 2142–2144. https://doi.org/10.1039/b703655h.

[6] S. Park, J. Lee, S.G. Cho, E.M. Goh, S. Lee, S.-S. Koh, J. Kim, Mass Spectrometric Analysis of Eight Common Chemical Explosives Using Ion Trap Mass Spectrometer, Bulletin of the Korean Chemical Society 34 (2013) 3659–3664. https://doi.org/10.5012/bkcs.2013.34.12.3659.

[7] J. Schäper, M. Wende, “Shake and bake” synthesis of methamphetamine – An experimental study, Toxichem Krimtech 39 (2015) 220–223.

[8] S. Vidal, D. Décary-Hétu, Shake and Bake: Exploring Drug Producers’ Adaptability to Legal Restrictions Through Online Methamphetamine Recipes, Journal of Drug Issues 48 (2018) 269–284. https://doi.org/10.1177/0022042617751685.

[9] K.A. Schug, I. Sawicki, D.D. Carlton, H. Fan, H.M. McNair, J.P. Nimmo, P. Kroll, J. Smuts, P. Walsh, D. Harrison, Vacuum ultraviolet detector for gas chromatography, Anal. Chem. 86 (2014) 8329–8335. https://doi.org/10.1021/ac5018343.

[10] United Nations Office on Drugs and Crime, World Drug Report 2018, United Nations, Vienna, 2018.

[11] European Monitoring Centre for Drugs and Drug Addiction and Europol, European Drug Report 2018. Trends and Developments, Publications Office of the European Union,

Luxembourg, 2018.

[12] European Monitoring Centre for Drugs and Drug Addiction and Europol, EU Drug Markets Report 2016. In-depth Analysis, Publications Office of the European Union, Luxembourg, 2016.

[13] United Nations Office on Drugs and Crime, RECOMMENDED METHODS FOR THE IDENTIFICATION AND ANALYSIS OF AMPHETAMINE, METHAMPHETAMINE AND THEIR RING-SUBSTITUTED ANALOGUES IN SEIZED MATERIALS, United Nations, Vienna, 2006.

[14] F.M. Hauser, T. Rößler, J.W. Hulshof, D. Weigel, R. Zimmermann, M. Pütz, Identification of specific markers for amphetamine synthesised from the pre-precursor APAAN following the Leuckart route and retrospective search for APAAN markers in profiling databases from Germany and the Netherlands, Drug Test. Anal. 10 (2018) 671–680. https://doi.org/10.1002/dta.2296.

[15] J. Köhler, Explosivstoffe, 10th ed., Wiley - VCH, Weinheim, 2008.

[16] E. Gray, H. Marsh, M. McLaren, A short history of gunpowder and the role of charcoal in its manufacture, J Mater Sci 17 (1982) 3385–3400. https://doi.org/10.1007/BF00752183.

[17] A. Sobrero, Sur plusieurs composés détonants produits avec l’acide nitrique et le sucre, la dextrine, la lactine, la mannite et la glycerine, Comptes Rendus Hebdomadaires des Séances L’Académie des Sciences 24 (1847) 247–248.

[18] S. Meyers, E.S. Shanley, Industrial explosives - a brief history of their development and use, Journal of Hazardous Materials 23 (1990) 183–201. https://doi.org/10.1016/0304-3894(90)85027-Z.

[19] D.H. Rosenblatt, E.P. Burrows, W.R. Mitchell, D.L. Parmer, Organic Explosives and Related Compounds, in: O. Hutzinger, F. Brochhagen, E.P. Burrows, H. Fiedler, J. Konietzko, W.R. Mitchell, K. Mross, W. Mücke, D.L. Parmer, D.H. Rosenblatt (Eds.), Anthropogenic Compounds, Springer Berlin Heidelberg, Berlin, Heidelberg (1991) 195–234.

[20] T.M. Klapötke, Energetic Materials Encyclopedia, De Gruyter, Berlin, Boston, 2018.

[21] M. Simini, R.S. Wentsel, R.T. Checkai, C.T. Phillips, N.A. Chester, M.A. Major, Evaluation of soil toxicity at joliet army ammunition plant, Environ Toxicol Chem 14 (1995) 623–630. https://doi.org/10.1002/etc.5620140410.

[22] N. Okusu, H. Hall, A. Orndorff, R. Bens, M. Schweighauser, Milan Army Ammunition Plant remedial investigation report: Volume 1. Final report 89-91 (1991).

[23] V.M. Boddu, C. Costales-Nieves, R. Damavarapu, D.S. Viswanath, M.K. Shukla, Physical Properties of Select Explosive Components for Assessing Their Fate and Transport in the Environment, in: M.K. Shukla, V.M. Boddu, J.A. Steevens, R. Damavarapu, J. Leszczynski (Eds.), Energetic Materials, Springer International Publishing, Cham (2017) pp. 343–371.

[24] T. Mahnel, V. Štejfa, M. Maryška, M. Fulem, K. Růžička, Reconciled thermophysical data for anthracene, The Journal of Chemical Thermodynamics 129 (2019) 61–72. https://doi.org/10.1016/j.jct.2018.08.034.

[25] J.W. Readman, R.F.C. Mantoura, M.M. Rhead, L. Brown, Aquatic distribution and heterotrophic degradation of Polycyclic Aromatic Hydrocarbons (PAH) in the Tamar Estuary, Estuarine, Coastal and Shelf Science 14 (1982) 369–389. https://doi.org/10.1016/S0272-7714(82)80009-7.

[26] H.A.J. Govers, E. Ruts, F.W.M. van der Wielen, A.G. van Haelst, Determination of Vapour Pressure and Related Thermodynamic Properties of Polycyclic Aromatic Compounds, Polycyclic Aromatic Compounds 9 (1996) 75–83. https://doi.org/10.1080/10406639608031204.

[27] H. Ma, F.Y. Cui, Z.W. Zhao, Z.Q. Liu, D.M. Liu, Water Solubility Enhancement of DDT by Humic Acid and Extracellular Organic Matter of Aquatic Algae, AMR 518-523 (2012) 565–568. https://doi.org/10.4028/www.scientific.net/AMR.518-523.565.

[28] M.B. King, H. Al-Najjar, A method for correlating and extending vapour pressure data to lower temperatures using thermal data: Vapour pressure equations for some n-alkanes at temperatures below the normal boiling point, Chemical Engineering Science 29 (1974) 1003–1011. https://doi.org/10.1016/0009-2509(74)80092-8.

[29] C.L. Yaws, Water solubility and Henry's law constant, Waste Management 13 (1993) 538–539. https://doi.org/10.1016/0956-053X(93)90137-L.

[30] N.C. Fenner, N.R. Daly, Laser Used for Mass Analysis, Rev. Sci. Instrum. 37 (1966) 1068–1070. https://doi.org/10.1063/1.1720410.

[31] F.J. Vastola, A.J. Pirone, Ionization of organic solids by laser irradiation, Adv. mass spectrom 4 (1968) 107–111.

[32] J.H. Gross, Mass Spectrometry: A Textbook, 2nd ed., Springer-Verlag Berlin Heidelberg, Berlin, Heidelberg, 2011.

[33] F. Rowell, J. Seviour, A.Y. Lim, C.G. Elumbaring-Salazar, J. Loke, J. Ma, Detection of nitro-organic and peroxide explosives in latent fingermarks by DART- and SALDI-TOF-mass spectrometry, Forensic Science International 221 (2012) 84–91. https://doi.org/10.1016/j.forsciint.2012.04.007.

[34] S. Ehlert, J. Hölzer, J. Rittgen, M. Pütz, R. Schulte-Ladbeck, R. Zimmermann, Rapid on-site detection of explosives on surfaces by ambient pressure laser desorption and direct inlet single photon ionization or chemical ionization mass spectrometry, Anal Bioanal Chem 405 (2013) 6979–6993. https://doi.org/10.1007/s00216-013-6839-8.

[35] S. Ehlert, A. Walte, R. Zimmermann, Ambient pressure laser desorption and laser-induced acoustic desorption ion mobility spectrometry detection of explosives, Anal. Chem. 85 (2013) 11047–11053. https://doi.org/10.1021/ac402704c.

[36] L. Li, D.M. Lubman, Pulsed laser desorption method for volatilizing thermally labile molecules for supersonic jet spectroscopy, Rev. Sci. Instrum. 59 (1988) 557. https://doi.org/10.1063/1.1139832.

[37] N. Stojanovska, M. Tahtouh, T. Kelly, A. Beavis, S. Fu, Qualitative analysis of seized cocaine samples using desorption electrospray ionization- mass spectrometry (DESI-MS), Drug Test. Anal. 7 (2015) 393–400. https://doi.org/10.1002/dta.1684.

[38] W. Chen, K. Hou, L. Hua, X. Xiong, H. Li, Water-assisted low temperature plasma ionization source for sensitive detection of explosives, RSC Adv. 4 (2014) 14791. https://doi.org/10.1039/c4ra00683f.

[39] D.H. Chace, Measuring Mass: From Positive Rays to Proteins. Michael A Grayson, ed. Philadelphia, PA: Chemical Heritage Press (2002) 160, Clinical Chemistry 49 (2003) 342. https://doi.org/10.1373/49.2.342/-a.

[40] E.S. Lander, L.M. Linton, B. Birren, C. Nusbaum, M.C. Zody, J. Baldwin, K. Devon, K. Dewar, M. Doyle, W. FitzHugh, R. Funke, D. Gage, K. Harris, A. Heaford, J. Howland, L. Kann, J. Lehoczky, R. LeVine, P. McEwan, K. McKernan, J. Meldrim, J.P. Mesirov, C. Miranda, W. Morris, J. Naylor, C. Raymond, M. Rosetti, R. Santos, A. Sheridan, C. Sougnez, Y. Stange-Thomann, N. Stojanovic, A. Subramanian, D. Wyman, J. Rogers, J. Sulston, R. Ainscough, S. Beck, D. Bentley, J. Burton, C. Clee, N. Carter, A. Coulson, R. Deadman, P. Deloukas, A. Dunham, I. Dunham, R. Durbin, L. French, D. Grafham, S. Gregory, T. Hubbard, S. Humphray, A. Hunt, M. Jones, C. Lloyd, A. McMurray, L. Matthews, S. Mercer, S. Milne, J.C. Mullikin, A. Mungall, R. Plumb, M. Ross, R. Shownkeen, S. Sims, R.H. Waterston, R.K. Wilson, L.W. Hillier, J.D. McPherson, M.A. Marra, E.R. Mardis, L.A. Fulton, A.T. Chinwalla, K.H. Pepin, W.R. Gish, S.L. Chissoe, M.C. Wendl, K.D. Delehaunty, T.L. Miner, A. Delehaunty, J.B. Kramer, L.L. Cook, R.S. Fulton, D.L. Johnson, P.J. Minx, S.W.

Clifton, T. Hawkins, E. Branscomb, P. Predki, P. Richardson, S. Wenning, T. Slezak, N. Doggett, J.F. Cheng, A. Olsen, S. Lucas, C. Elkin, E. Uberbacher, M. Frazier, R.A. Gibbs, D.M. Muzny, S.E. Scherer, J.B. Bouck, E.J. Sodergren, K.C. Worley, C.M. Rives, J.H. Gorrell, M.L. Metzker, S.L. Naylor, R.S. Kucherlapati, D.L. Nelson, G.M. Weinstock, Y. Sakaki, A. Fujiyama, M. Hattori, T. Yada, A. Toyoda, T. Itoh, C. Kawagoe, H. Watanabe, Y. Totoki, T. Taylor, J. Weissenbach, R. Heilig, W. Saurin, F. Artiguenave, P. Brottier, T. Bruls, E. Pelletier, C. Robert, P. Wincker, D.R. Smith, L. Doucette-Stamm, M. Rubenfield, K. Weinstock, H.M. Lee, J. Dubois, A. Rosenthal, M. Platzer, G. Nyakatura, S. Taudien, A. Rump, H. Yang, J. Yu, J. Wang, G. Huang, J. Gu, L. Hood, L. Rowen, A. Madan, S. Qin, R.W. Davis, N.A. Federspiel, A.P. Abola, M.J. Proctor, R.M. Myers, J. Schmutz, M. Dickson, J. Grimwood, D.R. Cox, M.V. Olson, R. Kaul, N. Shimizu, K. Kawasaki, S. Minoshima, G.A. Evans, M. Athanasiou, R. Schultz, B.A. Roe, F. Chen, H. Pan, J. Ramser, H. Lehrach, R. Reinhardt, W.R. McCombie, M. de La Bastide, N. Dedhia, H. Blöcker, K. Hornischer, G. Nordsiek, R. Agarwala, L. Aravind, J.A. Bailey, A. Bateman, S. Batzoglou, E. Birney, P. Bork, D.G. Brown, C.B. Burge, L. Cerutti, H.C. Chen, D. Church, M. Clamp, R.R. Copley, T. Doerks, S.R. Eddy, E.E. Eichler, T.S. Furey, J. Galagan, J.G. Gilbert, C. Harmon, Y. Hayashizaki, D. Haussler, H. Hermjakob, K. Hokamp, W. Jang, L.S. Johnson, T.A. Jones, S. Kasif, A. Kaspryzk, S. Kennedy, W.J. Kent, P. Kitts, E.V. Koonin, I. Korf, D. Kulp, D. Lancet, T.M. Lowe, A. McLysaght, T. Mikkelsen, J.V. Moran, N. Mulder, V.J. Pollara, C.P. Ponting, G. Schuler, J. Schultz, G. Slater, A.F. Smit, E. Stupka, J. Szustakowki, D. Thierry-Mieg, J. Thierry-Mieg, L. Wagner, J. Wallis, R. Wheeler, A. Williams, Y.I. Wolf, K.H. Wolfe, S.P. Yang, R.F. Yeh, F. Collins, M.S. Guyer, J. Peterson, A. Felsenfeld, K.A. Wetterstrand, A. Patrinos, M.J. Morgan, P. de Jong, J.J. Catanese, K. Osoegawa, H. Shizuya, S. Choi, Y.J. Chen, Initial sequencing and analysis of the human genome, Nature 409 (2001) 860–921. https://doi.org/10.1038/35057062.

[41] D.G. Savage, J. Lindenbaum, S.P. Stabler, R.H. Allen, Sensitivity of serum methylmalonic acid and total homocysteine determinations for diagnosing cobalamin and folate deficiencies, The American Journal of Medicine 96 (1994) 239–246. https://doi.org/10.1016/0002-9343(94)90149-X.

[42] R.G. Fairbanks, R.A. Mortlock, T.-C. Chiu, L. Cao, A. Kaplan, T.P. Guilderson, T.W. Fairbanks, A.L. Bloom, P.M. Grootes, M.-J. Nadeau, Radiocarbon calibration curve spanning 0 to 50,000 years BP based on paired 230Th/234U/238U and 14C dates on pristine corals, Quaternary Science Reviews 24 (2005) 1781–1796. https://doi.org/10.1016/j.quascirev.2005.04.007.

[43] J.H. Hoffman, R.C. Chaney, H. Hammack, Phoenix Mars Mission--the thermal evolved gas analyzer, J Am Soc Mass Spectrom 19 (2008) 1377–1383. https://doi.org/10.1016/j.jasms.2008.07.015.

[44] H. Gu, S. Yang, J. Li, B. Hu, H. Chen, L. Zhang, Q. Fei, Geometry-independent neutral desorption device for the sensitive EESI-MS detection of explosives on various surfaces, Analyst 135 (2010) 779. https://doi.org/10.1039/b921579d.

[45] J. Yinon, J.E. McClellan, R.A. Yost, C. Lifshitz, Electrospray ionization tandem mass spectrometry collision-induced dissociation study of explosives in an ion trap mass spectrometer, Rapid Commun. Mass Spectrom. 11 (1997) 1961–1970. https://doi.org/10.1002/(SICI)1097-0231(199712)11:18<1961:AID-RCM99>3.0.CO;2-K.

[46] M. Astratov, A. Preiß, K. Levsen, G. Wünsch, Identification of pollutants in ammunition hazardous waste sites by thermospray HPLC/MS, International Journal of Mass Spectrometry and Ion Processes 167-168 (1997) 481–502. https://doi.org/10.1016/S0168-1176(97)00089-X.

[47] P.-K. So, T.-T. Ng, H. Wang, B. Hu, Z.-P. Yao, Rapid detection and quantitation of ketamine and norketamine in urine and oral fluid by wooden-tip electrospray ionization mass spectrometry, Analyst 138 (2013) 2239–2243. https://doi.org/10.1039/c3an36641c.

[48] F.H. Field, J.L. Franklin, Electron impact phenomena and the properties of gaseous ions, Academic Press, 1957. https://doi.org/10.1021/ed035p320.2

[49] V.L. Tal'roze, A.K. Ljubimova, Secondary processes in the ion source of a mass spectrometer- reprinted from report of the Soviet Academy of Sciences, Volume LXXXVI, n5 (1952), J. Mass Spectrom. 33 (1998) 502–504.

[50] B. Munson, Development of chemical ionization mass spectrometry, International Journal of Mass Spectrometry 1 (2000) 243–251. https://doi.org/10.1016/S1387-3806(00)00301-8

[51] W.J. Richter, H. Schwarz, Chemical Ionization—A Mass-Spectrometric Analytical Procedure of Rapidly Increasing Importance, Angew. Chem. Int. Ed. Engl. 17 (1978) 424–439. https://doi.org/10.1002/anie.197804241.

[52] D.F. Hunt, J.F. Ryan, Cheical ionization mass spectrometry studies. I. Identification of alcohols, Tetrahedron Letters 12 (1971) 4535–4538. https://doi.org/10.1016/S0040-4039(01)97523-9.

[53] R.W. Giese, Detection of DNA adducts by electron capture mass spectrometry, Chem. Res. Toxicol. 10 (1997) 255–270. https://doi.org/10.1021/tx9601263.

[54] J.G. Dillard, Negative ion mass spectrometry, Chemical Reviews 73 (1973) 589–643.

[55] J.A. Larameé, B.C. Arbogast, M.L. Deinzer, Electron capture negative ion chemical ionization mass spectrometry of 1,2,3,4-tetrachlorodibenzo-p-dioxin, Anal. Chem. 58 (1986) 2907–2912. https://doi.org/10.1021/ac00127a004.

[56] W. Paul, H. Steinwedel, Notizen: Ein neues Massenspektrometer ohne Magnetfeld, Zeitschrift für Naturforschung A 8 (1953). https://doi.org/10.1515/zna-1953-0710.

[57] March, R., E., An Introduction to Quadrupole Ion Trap Mass Spectrometry, J Mass Spectrom 32 (1997) 351–369. https://doi.org/10.1002/(SICI)1096-9888(199704)32:4<351::AID-JMS512>3.0.CO;2-Y

[58] W. Paul, Elektromagnetische Käfige für geladene und neutrale Teilchen, Phys. Bl. 46 (1990) 227–236. https://doi.org/10.1002/phbl.19900460708.

[59] R.F. Wuerker, H. Shelton, R.V. Langmuir, Electrodynamic Containment of Charged Particles, Journal of Applied Physics 30 (1959) 342–349. https://doi.org/10.1063/1.1735165.

[60] R. Aebersold, M. Mann, Mass spectrometry-based proteomics, Nature 422 (2003) 198–207. https://doi.org/10.1038/nature01511.

[61] H.-J. Hübschmann, Handbook of GC/MS: Fundamentals and applications, Wiley-VCH, Weinheim, 2015.

[62] N. RAIKOS, K. CHRISTOPOULOU, G. THEODORIDIS, H. TSOUKALI, D. PSAROULIS, Determination of amphetamines in human urine by headspace solid-phase microextraction and gas chromatography, Journal of Chromatography B 789 (2003) 59–63. https://doi.org/10.1016/S1570-0232(03)00047-3.

[63] B. Fodor, I. Molnár-Perl, The role of derivatization techniques in the analysis of plant cannabinoids by gas chromatography mass spectrometry, TrAC Trends in Analytical Chemistry 95 (2017) 149–158. https://doi.org/10.1016/j.trac.2017.07.022.

[64] B.S. Middleditch, N.-J. Sung, A. Zlatkis, G. Settembre, Trace analysis of volatile polar organics by direct aqueous injection gas chromatography, Chromatographia 23 (1987) 273–278. https://doi.org/10.1007/BF02311779.

[65] I.G.M. Anthony, M.R. Brantley, C.A. Gaw, A.R. Floyd, T. Solouki, Vacuum Ultraviolet Spectroscopy and Mass Spectrometry: A Tandem Detection Approach for Improved Identification of Gas Chromatography-Eluting Compounds, Anal. Chem. 90 (2018) 4878–4885. https://doi.org/10.1021/acs.analchem.8b00531.

[66] I.G.M. Anthony, M.R. Brantley, A.R. Floyd, C.A. Gaw, T. Solouki, Improving Accuracy and Confidence of Chemical Identification by Gas Chromatography/Vacuum Ultraviolet Spectroscopy-Mass Spectrometry: Parallel Gas Chromatography, Vacuum Ultraviolet, and Mass Spectrometry Library Searches, Anal. Chem. 90 (2018) 12307–12313. https://doi.org/10.1021/acs.analchem.8b04028.

[67] T. Gröger, B. Gruber, D. Harrison, M. Saraji-Bozorgzad, M. Mthembu, A. Sutherland, R. Zimmermann, A Vacuum Ultraviolet Absorption Array Spectrometer as a Selective Detector for Comprehensive Two-Dimensional Gas Chromatography: Concept and First Results, Anal. Chem. 88 (2016) 3031–3039. https://doi.org/10.1021/acs.analchem.5b02472.

[68] L.M.L. Nollet, Chromatographic analysis of the environment, CRC/Taylor & Franciss, Boca Raton, 2006.

[69] C.P.-y. Chan, Y.-c. Cheung, R. Renneberg, M. Seydack, New trends in immunoassays, Adv. Biochem. Eng. Biotechnol. 109 (2008) 123–154. https://doi.org/10.1007/10_2007_075.

[70] N. de Giovanni, N. Fucci, The Current Status of Sweat Testing For Drugs of Abuse: A Review, Current Medicinal Chemistry 20 (2013) 545–561. https://doi.org/10.2174/092986713804910139.

[71] L. Wilson, A. Jehanli, C. Hand, G. Cooper, R. Smith, Evaluation of a rapid oral fluid point-of-care test for MDMA, J. Anal. Toxicol. 31 (2007) 98–104. https://doi.org/10.1093/jat/31.2.98.

[72] D. Quesada-González, A. Merkoçi, Nanoparticle-based lateral flow biosensors, Biosens. Bioelectron. 73 (2015) 47–63. https://doi.org/10.1016/j.bios.2015.05.050.

[73] R.M. Lequin, Enzyme immunoassay (EIA)/enzyme-linked immunosorbent assay (ELISA), Clinical Chemistry 51 (2005) 2415–2418. https://doi.org/10.1373/clinchem.2005.051532.

[74] D. Wild, Immunoassay for Beginners, in: The Immunoassay Handbook, Elsevier (2013) 7–10.

[75] S. Armenta, S. Garrigues, M. de La Guardia, J. Brassier, M. Alcalà, M. Blanco, C. Perez-Alfonso, N. Galipienso, Detection and characterization of emerging psychoactive substances by ion mobility spectrometry, Drug Test. Anal. 7 (2015) 280–289. https://doi.org/10.1002/dta.1678.

[76] E. Sisco, J. Verkouteren, J. Staymates, J. Lawrence, Rapid detection of fentanyl, fentanyl analogues, and opioids for on-site or laboratory based drug seizure screening using thermal desorption DART-MS and ion mobility spectrometry, Forensic Chem. 4 (2017) 108–115. https://doi.org/10.1016/j.forc.2017.04.001.

[77] H. Lai, I. Corbin, J.R. Almirall, Headspace sampling and detection of cocaine, MDMA, and marijuana via volatile markers in the presence of potential interferences by solid phase microextraction-ion mobility spectrometry (SPME-IMS), Anal. Bioanal. Chem. 392 (2008) 105–113. https://doi.org/10.1007/s00216-008-2229-z.

[78] R. Ewing, A critical review of ion mobility spectrometry for the detection of explosives and explosive related compounds, Talanta 54 (2001) 515–529. https://doi.org/10.1016/S0039-9140(00)00565-8.

[79] Z. Karpas, R.M. Stimac, Z. Rappoport, Differentiating between large isomers and derivation of structural information by ion mobility spectrometry / mass spectrometry techniques, International Journal of Mass Spectrometry and Ion Processes 83 (1988) 163–175. https://doi.org/10.1016/0168-1176(88)80093-4.

[80] C.L. Crawford, H.H. Hill, Evaluation of false positive responses by mass spectrometry and ion mobility spectrometry for the detection of trace explosives in complex samples, Analytica Chimica Acta 795 (2013) 36–43. https://doi.org/10.1016/j.aca.2013.07.070.

[81] L.A. Viehland, Minimizing false positives in ion mobility spectrometry by changing the field or pressure, Int. J. Ion Mobil. Spec. 18 (2015) 171–175. https://doi.org/10.1007/s12127-015-0181-0.

[82] A.B. Kanu, P. Dwivedi, M. Tam, L. Matz, H.H. Hill, Ion mobility-mass spectrometry, J. Mass Spectrom. 43 (2008) 1–22. https://doi.org/10.1002/jms.1383.

[83] K. Giles, S.D. Pringle, K.R. Worthington, D. Little, J.L. Wildgoose, R.H. Bateman, Applications of a travelling wave-based radio-frequency-only stacked ring ion guide, Rapid Commun. Mass Spectrom. 18 (2004) 2401–2414. https://doi.org/10.1002/rcm.1641.

[84] R. Guevremont, R.W. Purves, Atmospheric pressure ion focusing in a high-field asymmetric waveform ion mobility spectrometer, Rev. Sci. Instrum. 70 (1999) 1370–1383. https://doi.org/10.1063/1.1149599.

[85] K. Michelmann, J.A. Silveira, M.E. Ridgeway, M.A. Park, Fundamentals of trapped ion mobility spectrometry, J Am Soc Mass Spectrom 26 (2015) 14–24. https://doi.org/10.1007/s13361-014-0999-4.

[86] L. Skultety, P. Frycak, C. Qiu, J. Smuts, L. Shear-Laude, K. Lemr, J.X. Mao, P. Kroll, K.A. Schug, A. Szewczak, C. Vaught, I. Lurie, V. Havlicek, Resolution of isomeric new designer stimulants using gas chromatography - Vacuum ultraviolet spectroscopy and theoretical computations, Analytica Chimica Acta 971 (2017) 55–67. https://doi.org/10.1016/j.aca.2017.03.023.

[87] A. Leghissa, J. Smuts, C. Qiu, Z.L. Hildenbrand, K.A. Schug, Detection of cannabinoids and cannabinoid metabolites using gas chromatography with vacuum ultraviolet spectroscopy, Sep Sci plus 1 (2018) 37–42. https://doi.org/10.1002/sscp.201700005.

[88] C.A. Cruse, J.V. Goodpaster, Generating highly specific spectra and identifying thermal decomposition products via Gas Chromatography / Vacuum Ultraviolet Spectroscopy (GC/VUV): Application to nitrate ester explosives, Talanta 195 (2019) 580–586. https://doi.org/10.1016/j.talanta.2018.11.060.

[89] T. Ieda, S. Hashimoto, T. Isobe, T. Kunisue, S. Tanabe, Evaluation of a data-processing method for target and non-target screening using comprehensive two-dimensional gas chromatography coupled with high-resolution time-of-flight mass spectrometry for environmental samples, Talanta 194 (2019) 461–468. https://doi.org/10.1016/j.talanta.2018.10.050.

[90] J. Rapin, A. Souloumiac, J. Bobin, A. Larue, C. Junot, M. Ouethrani, J.-L. Starck, Application of non-negative matrix factorization to LC/MS data, Signal Processing 123 (2016) 75–83. https://doi.org/10.1016/j.sigpro.2015.12.014.

[91] Europol, LARGEST EVER EUROPEAN HAUL OF AMPHETAMINE PRECURSOR BMK SEIZED, 2015. https://www.europol.europa.eu/newsroom/news/largest-ever-european-haul-of-amphetamine- (accessed 8 June 2018).

[92] J. Schenk, J.X. Mao, J. Smuts, P. Walsh, P. Kroll, K.A. Schug, Analysis and deconvolution of dimethylnaphthalene isomers using gas chromatography vacuum ultraviolet spectroscopy and theoretical computations, Analytica Chimica Acta 945 (2016) 1–8. https://doi.org/10.1016/j.aca.2016.09.021.

[93] E. Sisco, T.P. Forbes, M.E. Staymates, G. Gillen, Rapid Analysis of Trace Drugs and Metabolites Using a Thermal Desorption DART-MS Configuration, Anal. Methods 8 (2016) 6494–6499. https://doi.org/10.1039/C6AY01851C.

[94] N. Stojanovska, T. Kelly, M. Tahtouh, A. Beavis, S. Fu, Analysis of amphetamine-type substances and piperazine analogues using desorption electrospray ionisation mass

spectrometry, Rapid Commun. Mass Spectrom. 28 (2014) 731–740. https://doi.org/10.1002/rcm.6832.

[95] K. Hiraoka, S. Ninomiya, L.C. Chen, T. Iwama, M.K. Mandal, H. Suzuki, O. Ariyada, H. Furuya, K. Takekawa, Development of double cylindrical dielectric barrier discharge ion source, Analyst 136 (2011) 1210–1215. https://doi.org/10.1039/c0an00621a.

[96] B.D. Sabino, M.L. Sodré, E.A. Alves, H.F. Rozenbaum, F.O.M. Alonso, D.N. Correa, M.N. Eberlin, W. Romão, Analysis of street Ecstasy tablets by thin layer chromatography coupled to easy ambient sonic-spray ionization mass spectrometry, Brazilian Journal of Analytical Chemistry 1 (2011) 222–227.

[97] T.P. Forbes, M. Staymates, E. Sisco, Broad spectrum infrared thermal desorption of wipe-based explosive and narcotic samples for trace mass spectrometric detection, Analyst 142 (2017) 3002–3010. https://doi.org/10.1039/c7an00721c.

[98] J.K. Dalgleish, M. Wleklinski, J.T. Shelley, C.C. Mulligan, Z. Ouyang, R. Graham Cooks, Arrays of low-temperature plasma probes for ambient ionization mass spectrometry, Rapid Commun. Mass Spectrom. 27 (2013) 135–142. https://doi.org/10.1002/rcm.6435.

[99] F.S. Crossley, M.L. Moore, STUDIES ON THE LEUCKART REACTION, J. Org. Chem. 09 (1944) 529–536. https://doi.org/10.1021/jo01188a006.

[100] J.D. Power, M.G. Barry, K.R. Scott, P.V. Kavanagh, An unusual presentation of a customs importation seizure containing amphetamine, possibly synthesized by the APAAN-P2P-Leuckart route, Forensic Science International 234 (2014) e10-3. https://doi.org/10.1016/j.forsciint.2013.10.003.

9. Appendix

9.1 List of abbreviations

APAAN	α-Phenylacetoacetonitrile
APLD	Ambient pressure laser desorption
APLD-MS	Ambient pressure laser desorption coupled to mass spectrometry
ATS	Amphetamine-type stimulants
BAM	Bundesanstalt für Materialforschung und -prüfung
BMK	Phenylacetone or benzyl methyl ketone
CI	Chemical ionisation
CID	Collision-induced dissociation
CW	Continuous wave
DC	Direct current
DESI	Desorption electrospray ionisation
DMDNB	2,3-dimethyl-2,3-dinitrobutane
DNA	Deoxyribonucleic acid
DNT	Dinitrotoluene
EASI	Easy ambient sonic spray ionisation
EI	Electron ionisation
FID	Flame ionisation detector
FWHM	Full width at half maximum
GC	Gas chromatography
GC-FID	Gas chromatography coupled to flame ionisation detectors
GC-MS	Gas chromatography coupled to mass spectrometry
GC-VUV	Gas chromatography coupled to vacuum ultraviolet spectroscopy
HPLC-MS	High-performance liquid chromatography coupled to mass spectrometry
IDT	Immunoassay drug tests
IMS	Ion mobility spectrometry
IT-MS	Ion trap mass spectrometry
LDI	Laser desorption/ionisation
LOD	Limit of detection
LTP	Low-temperature plasma torch

MALDI	Matrix-assisted laser desorption/ionisation
MDMA	3,4-Methylenedioxy-N-methamphetamine
MS	Mass spectrometry
NCI	Negative chemical ionisation
NFA	N-Formylamphetamine
NG	Nitroglycerin
NMF	Non-negative matrix factorisation
p,p'-DDT	Dichlorodiphenyltrichloroethane
PA	Picric acid
PCI	Positive chemical ionisation
PETN	Pentaerythritol tetranitrate
PTFE	Polytetrafluoroethylene
QIT	Quadrupole ion trap
RDX	Hexogen, research department explosive or royal demolition explosive
RF	Radiofrequency
SALDI	Surface-assisted laser desorption/ionisation
SEMFreS	Szenarien, Evaluierung und Messtechnik bei Freisetzung chemischer und explosionsgefährlicher Stoffe
TATP	Triacetone triperoxide
TNT	Trinitrotoluene
UV	Ultra violet
VUV	Vacuum ultra violet

9.2 List of figures

9.3 Scientific publications

9.3.1 Publication 1

Evaluation and application of gas chromatography - vacuum ultraviolet spectroscopy for drug- and explosive precursors and examination of non-negative matrix factorization for deconvolution

Published by

René Reiss, Beate Gruber, Sophie Klingbeil, Thomas Gröger, Sven Ehlert and Ralf Zimmermann

Spectrochimica Acta Part A: Molecular and Biomolecular Spectroscopy
Year 2019, Volume 219, Page 129-134

DOI: 10.1016/j.saa.2019.04.032

Spectrochimica Acta Part A: Molecular and Biomolecular Spectroscopy 219 (2019) 129–134

Contents lists available at ScienceDirect

Spectrochimica Acta Part A: Molecular and Biomolecular Spectroscopy

journal homepage: www.elsevier.com/locate/saa

Short Communication

Evaluation and application of gas chromatography - vacuum ultraviolet spectroscopy for drug- and explosive precursors and examination of non-negative matrix factorization for deconvolution

René Reiss [a], Beate Gruber [b], Sophie Klingbeil [a], Thomas Gröger [b], Sven Ehlert [a,*], Ralf Zimmermann [a,b]

[a] Joint Mass Spectrometry Centre, Chair of Analytical Chemistry, University of Rostock, Dr.-Lorenz-Weg 2, 18059 Rostock, Germany
[b] Joint Mass Spectrometry Centre, Comprehensive Molecular Analytics, Helmholtz Zentrum München, Ingolstädter Landstr. 1, 85764 Neuherberg, Germany

ARTICLE INFO

Article history:
Received 28 December 2018
Received in revised form 14 April 2019
Accepted 15 April 2019
Available online 17 April 2019

Keywords:
VUV
Drugs
Precursor
Deconvolution
Forensic chemistry
Isomeric separation

ABSTRACT

Since the introduction of a benchtop vacuum ultraviolet (VUV) absorption spectroscope with an increased wavelength range towards to the high energetic ultraviolet radiation, gas chromatography coupled to VUV has been proven a powerful tool in several fields of application such as petroleomics, permanent gas analytic, pesticide analytic and many more. In this study, the potential of GC-VUV for investigations was examined, focusing on drug- and explosive precursors as well as chemical warfare simulants. The ability of VUV absorption spectra to differentiate isomers is presented, among others for nitroaromatics. In addition, the limit of detection for target compounds was determined to 0.7 ng absolute on column. Furthermore, non-negative matrix factorization (NMF) was successfully implemented as alternative deconvolution approach and evaluated for the deconvolution of unknown substances. In comparison, the spectral library-based deconvolution was applied to a standard mixture and a simulated case study. The results reveal that the NMF is a useful additional tool for deconvolution because, unlike library-based deconvolution, it allows to investigate unknown substances as well.

1. Introduction

Drugs, drug precursors, and explosive precursors are prominent target compounds in forensic science. Due to their expanding amount and the wide variety of compound structures, strong analytical techniques and detection systems are required. Commonly, gas chromatography coupled to a flame ionisation detector (GC-FID) or gas chromatography coupled to mass spectrometry (GC–MS) are applied as analytical techniques for analysing volatile representatives of these substance classes [1–3]. While a FID is an almost universal and robust technique with straightforward quantification and a wide linear dynamic range, it lacks specific and identifiable analyte information. In case of chemical warfare agents, flame photometric detectors (FPD) are also utilized because of their specificity for sulphur- and phosphorous compounds [4]. Nevertheless, as with FID, identification of compounds is not possible. MS with electron ionisation provides universal analyte-specific information, but common drawbacks are the need for a more sophisticated quantification and more complex instrumentation. On the one hand, the investigation of complex samples like differentiation of isomeric compounds via GC tandem or high-resolution mass spectrometry ($GC–MS^n$, GC-HRMS) is possible [5]. On the other hand, drawbacks of MS are amplified for $GC–MS^n$ and GC-HRMS.

Vacuum ultraviolet (VUV) absorption spectroscopy overcomes the above mentioned drawbacks and combines the selectivity of a spectral detection system with the robustness of an absorption based spectroscopic system. While the early coupling of GC with a far ultraviolet (UV) detection dates back to 1987 [6], and is still in use [10], recent instrumentation improvements led to a growing interest in the use of VUV detectors [7–9]. The advantage of VUV is its quite universal detection behaviour, since nearly every chemical substance absorbs light at wavelengths below 185 nm, and therefore exhibits a higher sensitivity compared to UV as well as the generation of substance-specific absorption spectra. In addition, it benefits from a straightforward and robust quantification applying Beer-Lambert's Law as known from UV spectroscopy. So far, GC-VUV has been utilized for the investigation of new designer stimulants and cannabinoids [11,12], as well as for identification of thermal decomposition products of nitrate ester explosives [13], demonstrating its power regarding the detection of specific forensic target compounds. Other substance classes such as drug- and explosive precursors have not yet been investigated. In this study, GC-VUV was applied for the analysis of drug- and explosive precursors as well as chemical warfare agent simulants. Therefore, isomeric differentiation was investigated and the limit of detection was determined. Furthermore, its potential for forensic target compounds was evaluated using an artificially spiked gasoline matrix. For the mathematical separation of co-eluting chromatographic peaks, two different deconvolution approaches were utilized and compared, viz. spectral based deconvolution and non-negative matrix factorization (NMF).

* Corresponding author.
E-mail address: sven.ehlert@uni-rostock.de (S. Ehlert).

https://doi.org/10.1016/j.saa.2019.04.032
1386-1425/

2. Material and methods

2.1. Material and equipment

Safrole, phenylacetone, propofol, 4-hydroxy propofol and piperonyl methyl ketone were obtained from the German Federal Criminal Police Office (BKA, Wiesbaden, Germany). Nitromethane was bought from Carl Roth GmbH + Co. KG (Karlsruhe, Germany) and 2-nitrotoluene from Alfa Aesar (Karlsruhe, Germany). 2-/3-/4-Nitrophenol were obtained from Ferak Berlin (Berlin, Germany), 3,4-dinitrotoluene from Dr. Ehrenstofer GmbH (Augsburg, Germany) and 1-adamantylamine from ABCR GmbH & Co. KG, (Karlsruhe, Germany). Methyl salicylate, 2,4/2,6-dinitrotoluene, dimethyl methylphosphonate, trimethyl phosphate, triethyl phosphonate, tributyl phosphate and diisopropyl methylphosphonate were obtained from Sigma Aldrich Chemie GmbH (Steinheim, Germany). Premium grade gasoline (98 octane, DIN EN 228) was bought from TEAM Mineralöle GmbH (Süderbrarup, Germany). All analytes were dissolved in methanol from Carl Roth GmbH + Co. KG (Karlsruhe, Germany).

The VUV detector VGA-100 (VUV Analytics, Inc., Austin, USA) was coupled to an Agilent 7890A gas chromatograph (Agilent Technologies, Palo Alto, USA). The GC separation was achieved by a 30 m Rxi-1 ms column (0.32 mm ID, 4 μm df; RESTEK GmbH, Bad Homburg, Germany). The VUV detector parameters were chosen as follows: A wavelength range of 125–240 nm, an acquisition rate of 11 ms per spectrum before averaging, 20 micro-spectra averaged, nitrogen with a purity of 5.0 as makeup gas with a pressure of 10.3 kPa and a flow cell temperature of 275 °C. 1 μl analyte was injected in split mode, 1:10 for calibration and 1:200 for the samples. The injection port temperature was set at 200 °C, and a constant He carrier flow of 1.3 ml/min was applied with a purity of 5.0. The oven temperature program consisted of 35 °C start temperature held for 1 min, subsequently raised with a temperature ramp of 5 °C/min to 320 °C, and held for 1 min. For data processing and evaluation, VUV Model & Analyze (v5.05.194), VUV Spectra LLB (v5.05.194), and VGA 100 Viewer (v5.05.194), from VUV Analytics (Austin, USA) were exploited.

2.2. Deconvolution based on linear combination of spectra

The deconvolution can be based on characteristic compound-specific absorption cross sections. If the absolute cross sections for the applied wavelength range of the investigated substances are unknown, pre-recorded reference spectra can be used. The model spectrum with n analytes included can be calculated by Formula (1).

$$A = \sum_{i=1}^{n} f_i A_{i,ref} = \left(f_1 A_{1,ref} + f_2 A_{2,ref} + \ldots + f_n A_{n,ref}\right) \quad (1)$$

A is the calculated spectrum, f_i are the weighting factors, and $A_{i,\,ref}$ are the basis functions. For every analyte calculated, one term is used in this equation. By linear optimisation of the unknown weighting factors, while considering the base functions, a model spectrum is obtained that appears similarly to the measured one. As demonstrated in previous publications [14,15], this approach can be applied automatically to e.g. fatty acid methyl esters or polychlorinated biphenyls.

2.3. Application of non-negative matrix factorization for deconvolution of spectral information

NMF allows calculating NMF loadings and their contribution on the signal intensity at given datasets [16], e.g. the influence of a substance on a time depending overall absorption spectrum. NMF segments a [$m \times n$]-matrix M into a [$m \times k$]-matrix W and a [$k \times n$]-matrix H. Only the variable k and therefore the number of factors is predefined. In this case, k is defined as 3, because it is assumed that a co-eluting peak consists of 2 separate peaks and background noise. This results in W_1 and W_2 for the peaks and W_3 for the noise. By multiplying W and H the so called non-negative matrix factorization of M is obtained, as described in Formula (2). NMF itself is an iterative technique and needs an optimisation algorithm for these iterations. Therefore, an alternating least-squares algorithm was used and the iteration starts with random variables of W_0 and H_0 for W and H. The minimised function:

$$f\left(\mathrm{W}_{[m\times k]}, H_{[k\times n]}, k\right) = \frac{1}{2}\left\|M_{[m\times n]} - W_{[m\times k]}H_{[k\times n]}\right\|_F^2 \quad (2)$$

is verified by adding a boundary condition. Every result that does not fulfil this condition is rejected because these results would not be physically reasonable. This boundary condition states that every deconvoluted signal should only consist of a single chromatographic peak, because deconvolution should lead to a separated signal for each substance. Therefore, every result with two signals for a single substance is rejected. The utilized MATLAB® script can be found in the Supplementary material (Supplement A).

2.4. Examining NMF capabilities

For examining the capabilities of NMF, artificial convolutions were prepared. This was done by linear addition of known deconvoluted peaks. The resulting convoluted spectrum is based on the examined samples to enable good agreement for practical samples.

3. Results and discussion

3.1. Limit of detection and absorption spectra

The limits of detection (LOD) for a total of 19 substances were determined as given in Table 1. For this purpose, these substances were analysed in a single mixed standard. LOD determination was done by regression analysis according to DIN 32645 [17]. An integration interval from 125 nm to 240 nm was applied for all substances. The detection limits range from 1.4 to 2.4 ng for drug precursors that can be used for drug production, such as safrole or phenylacetone. Explosive precursors, such as 3,4-dinitrotoluene or nitromethane exhibit LODs from 0.7 to 4.2 ng. In addition, chemical warfare agent simulants such as trialkylphosphates revealed a LOD of 1.8 to 3.3 ng. For most of the mentioned substances, the LOD is higher compared to other substances published [7]. This can be explained due to differences in the applied integration range and other LOD determination standards. For example, Schug

Table 1
LOD for different explosive- and drug precursors as well as chemical warfare agent simulants.

Substance name	Limit of detection/ng on column
Nitromethane	4.2
Dimethyl methylphosphonate	1.8
Trimethyl phosphate	3.3
Triethyl phosphate	2.0
Diisopropyl methanephosphonate	1.9
Tributyl phosphate	2.4
Phenylacetone	2.4
2-Nitrotoluene	0.7
Methyl salicylate	1.5
1-Adamantylamine	1.6
Safrole	1.4
Propofol	1.6
4-Hydroxy propofol	2.1
2-Nitrophenol	0.7
3-Nitrophenol	1.9
2,4-Dinitrotoluene	1.7
2,6-Dinitrotoluene	0.8
3,4-Dinitrotoluene	0.8
Piperonyl methyl ketone	1.6

et al. [7] customized the applied integration range. While this yields the best limit of detection, it suffers from the need of manually setting these values. In contrast, in this work, a general method is applied by integration over the full wavelength range. Therefore, the obtained LOD differences are a good indication for the impact of such a difference in approach. In comparison to common detection techniques such as GC-FID, GC-VUV exhibit a ten times higher limit of detection utilizing a signal to noise ratio of S/N > 3 [18]. No correlations could be observed regarding the number of sigma bonds, hetero atoms or pi bonds. A lower LOD was obtained for the investigated analytes with an aromatic structure present. For further information, the relative process standard deviation can be found in the Supplementary material (Supplement B).

Absorption spectra of all investigated substances over the full wavelength range (125 nm to 240 nm) can be found in the Supplementary material (Supplement C). To the best of the authors' knowledge, most of these substances have not been investigated yet. The combination of known concentration and absorption at a particular wavelength will enable the calculation of extinction coefficients. Therefore, the used concentration for every attached spectrum is indicated in gram per litre. In addition, existing databases can be extended for identifying unknown compounds, similar to MS fragment spectral databases.

3.2. Isomer discrimination via spectral library comparison

One general advantage of the VGA-100 compared to MS is the ability to differentiate isomeric compounds based on their absorption spectra. Two examples of such an isomeric differentiation can be seen in Fig. 1. Part A) exhibits the behaviour for 2-/3-/4-nitrophenol with slight variations between the isomers. The main absorption band at 175 nm reveals a hypsochromic shift for an increasing distance between the phenol- and nitro functional groups. The second absorption band at higher wavelengths also shifts hypsochrom resulting in one broad absorption band for 4-nitrophenol. These differences allow for the differentiation between the isomers. Fig. 1B) demonstrates the isomeric differentiability for the more complex dinitrotoluene isomers. When isomeric discrimination is not sufficient and discrete isomer allocation is required, known absorption spectra of all investigated isomers are necessary. These spectra can be obtained by isomer database hits. Thereby, isomers can be allocated straightforward and fully automatic. If the analyte was not recorded and is not available in a database, isomer allocation is not possible. To overcome this limitation, in silico calculated spectra are under investigation. Few authors have presented calculations of VUV absorption spectra [11,19]. Compared to VUV absorption spectra, calculations of mass spectrometry fragment spectra are also under development, but lacking in predictability [20]. In theory, the calculation of VUV absorption spectra can be useful to gain information about stimulated electronic states and occurring absorption bands to identify target compounds. However, high amounts of calculation power and –time are required, as well as a solid knowledge about proper calculation methods. Therefore, these methods are hardly applicable for daily laboratory usage and more likely reserves for special cases only.

3.3. Homologous rows

Similar to the isomeric separations, VUV absorption spectroscopy results in distinct spectra of homologous alkyl phosphates and structurally related substances. In Fig. 1C), VUV absorption spectra of trimethyl-, triethyl-, and tributyl-phosphate as well as dimethyl methylphosphonate (DMMP) and diisopropyl methylphosphonate (DIMP) are shown. Maximum $\sigma \rightarrow \sigma^*$ absorption occurs in the low nm range. Utilizing the VGA-100, no absorption was detected from 180 nm to 240 nm. Differences in the relative absorption intensity at around 165 nm can be explained due to the structural disparities. Firstly, shorter alkyl chains yield a higher relative absorption at 165 nm. This can be observed for alkyl phosphates as well as for both phosphonates. Secondly, the relative absorption at 165 nm seems to be higher and the absorption bandwidth is narrower when all substituents are esters, compared to phosphonates with alkyl side chain.

3.4. Deconvolution and simulated realistic case

Co-eluting peaks are frequently encountered with chromatographic separations of complex mixtures. Therefore, either multiple measurements using different chromatographic approaches or deconvolution of the co-eluting peaks can be utilized. For VUV absorption spectroscopy, a supervised method that is based on a linear combination of spectra has been established [7]. It is assumed, that for a known retention time all co-eluting compounds are known and retention indices as well as spectra are deposited in a spectral library. The method is very fast and robust and will indicate if compounds are present, which are not found in a library. For this type of deconvolution, peak profiles are not necessary, however only known co-elutions are handled properly. Therefore, the need for pre-determined library is one of the biggest drawbacks of VUV deconvolution. To extend the abilities of VUV detectors and overcome the mentioned limitations, NMF is a promising technique to survey for overcoming these limitations. It does not require pre-determined retention indices and a spectral library, which allows deconvoluting unknown substances, as in non-targeted studies. For the investigation of two co-eluting substances, NMF works best if the background noise is determined as well. While NMF in general is a well-known mathematical technique and has been adopted to other chromatographic techniques, such as GC–MS and HPLC-MS [21,22], no investigations have been carried out before with respect to a successful application to VUV absorption spectroscopy. In this study, both deconvolution approaches were applied and compared using different co-eluting samples as well as a simulated case study (Fig. 2).

In Fig. 2A), the co-elution of cyclandelate and safrole is demonstrated. The spectral similarity based on the sum-squared residual of

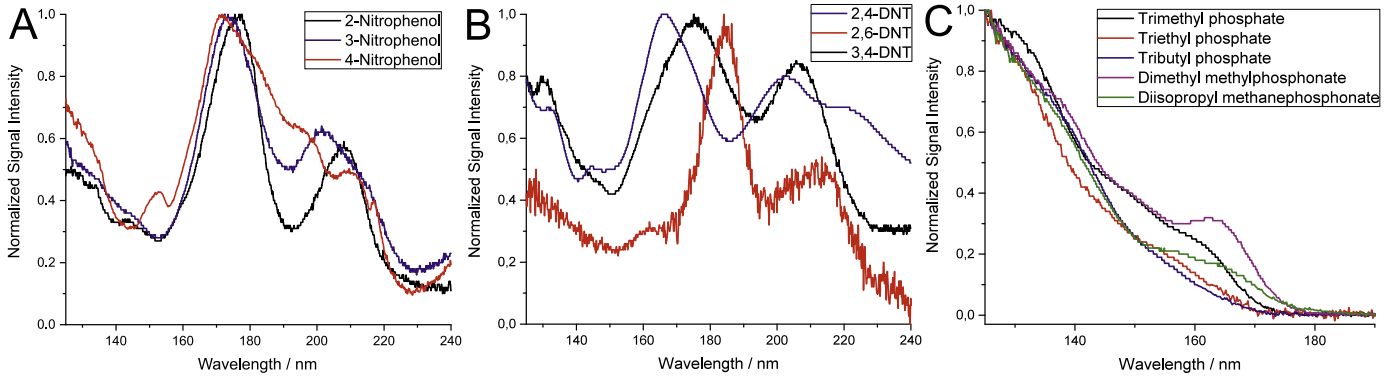

Fig. 1. A) Normalised absorption spectra of three nitrophenols. B) Normalised absorption spectra of three different dinitrotoluene isomers. C) Normalised absorption spectra of five chemical warfare agent simulants.

pairwise-compared spectra is 10.0. This value can be used to describe the similarity between two compared spectra. Further details and values for other compounds measured with VUV have been published previously [19,23]. Both deconvolution approaches exhibit good alignment with the investigated substances. When comparing spectral deconvolution with NMF, a slightly better agreement for cyclandelate was achieved for spectral deconvolution. For safrole a small peak overestimation was observed, compared to a slight peak underestimation for spectral deconvolution. For quantifying the match between measured and calculated spectra, the deviation between both areas was calculated. While spectral based deconvolution reveals an overall area error of 3.2%, NMF yielded a result with 1.2% error. Another example with a four times reduced signal intensity is presented for the deconvolution of 3-nitrophenol and 2,6-DNT (Fig. 2B). This comparison features a spectral similarity of 2.9. While the 3-NP signal is correctly deconvoluted for both methods, NMF exhibits noticeable noise for 3-NP. This noise can only be observed with NMF because of a different separation approach. While spectral deconvolution applies noise free spectra from a database, NMF subtracts the noise from the original spectra, resulting in noisy looking spectra. Nevertheless, both methods exhibit good alignment to the measured spectra, as well as good comparability with each other. Similar to the deconvolution of cyclandelate and safrole, the deviation between the areas of 3-NP and 2,6-DNT was determined. While spectral based deconvolution reveals an overall area error of 0.4%, NMF yielded a result with 5.0% error. Higher and more differentiated errors are in agreement with the noisier NMF spectra (Fig. 2B). While the signal intensity of B) is only one fourth of A), the overall error increases slightly, but remains in the dimension for both methods. Therefore, it could be assumed that the basic deconvolution error is at the same level for both methods and the measured deviations are random errors.

A more complex deconvolution example is given in Fig. 2C) by the detection of drug precursors in a gasoline matrix using GC-VUV, which is a known forensic scenario [24]. To simulate such a sample, gasoline was spiked with 1‰ safrole and phenylacetone, which corresponds to a sample with mostly gasoline but relevant residues of drug precursors. Safrole is a precursor for the 3,4-Methylenedioxymethamphetamine (MDMA) synthesis and phenylacetone is utilized for amphetamine and methamphetamine synthesis. The total-intensity GC-VUV chromatogram of the analysed sample exhibits that one of the target compounds co-elutes with the matrix. While safrole (at 43 min) is separated from the complex gasoline matrix, phenylacetone (at 38 min) co-elutes with 1,2-diethylbenzene. Quantification and identification of phenylacetone would therefore be challenging, especially because both peak maxima cannot be distinguished. To overcome this issue, a deconvolution of phenylacetone and 1,2-diethylbenzene is performed, at first via spectral deconvolution and secondly by NMF. Therefore, spectral information for both substances was added to the library. To verify the obtained results, the deviation between the calculated area of the hidden matrix and the measured area from pure gasoline is calculated.

For spectral deconvolution, the measured area of the non-spiked 1,2-diethylbenzene and the deconvoluted area of the spiked sample results in a deviation of about 7%. Given that the area of 1,2-diethylbenzene is small compared to the phenylacetone signal (about 4% area), it is highly probable that this deviation can be tolerated for many cases. This result reveals that spectra based deconvolution can be an alternative to time-consuming, additional measurements when co-elution occurs. This is especially useful for the analysis of complex samples and when full peak separation becomes challenging by one-dimensional gas chromatography. While NMF is capable to separate an approximately 1:1 separation, completely similar signals are known to be not deconvolutable by NMF [25]. While NMF is capable to separate an approximately 1:1 separation, the attempt of deconvoluting phenylacetone spiked gasoline reveals no useful information, because of the non-applicability of the boundary conditions, described in Section 2.4. In this case, both deconvoluted peaks reveal no separable maxima and therefore NMF delivers no physically reasonable results. Therefore, the need for separable maxima is a major drawback of the NFM method. However, this drawback can be overcome with spectral deconvolution or by changing the chromatographic setup slightly to generate coleuting peaks with two maxima. An additional drawback, compared to spectral deconvolution, is the need to know how many substances are convoluted in a co-eluting peak, prior to the deconvolution. A solution for only partly deconvoluted peaks could be to alternate the number of presumed compounds for NMF.

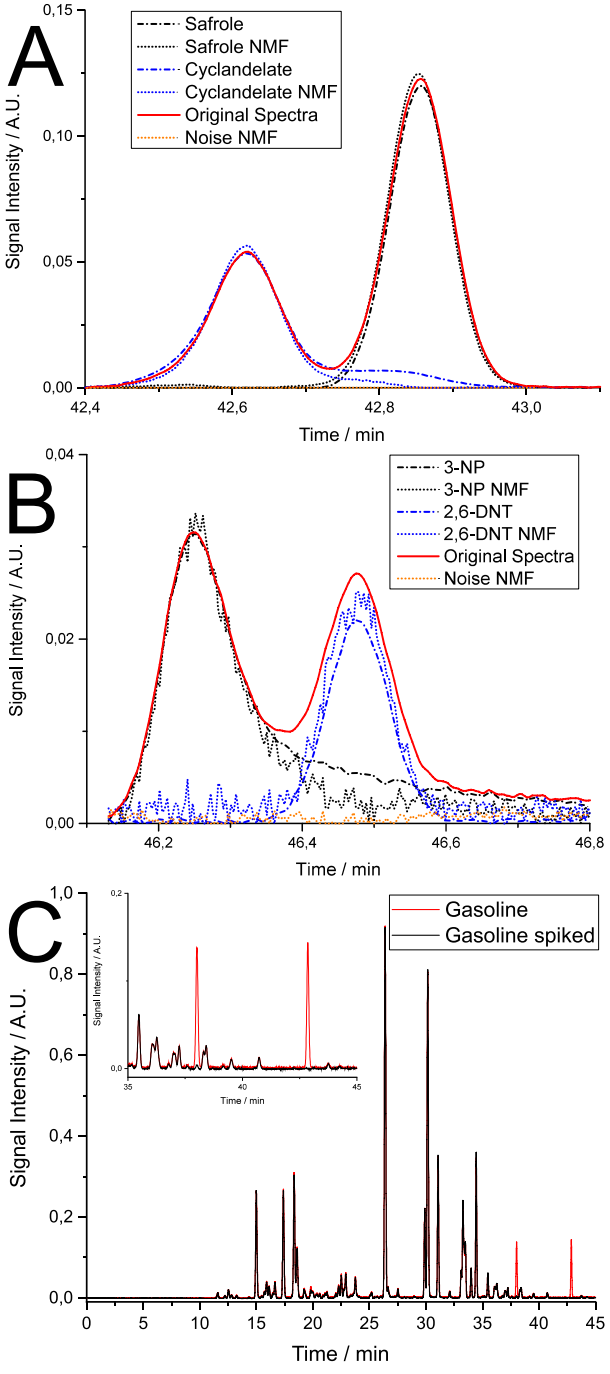

Fig. 2. A) Deconvolution of cyclandelate and safrole via spectral deconvolution (dotdashed line) and NMF (dotted line) from a deconvolution sample. B) Deconvolution of 3-nitrophenol and 2,6-DNT via spectral deconvolution (dotdashed line) and NMF (dotted line) from the same measurement as A). C) Comparison of the GC chromatograms of the spiked and non-spiked gasoline sample. The enlarged part exhibits the co-eluting peaks at 38 min.

Since this is the first report for the application of NMF for VUV deconvolution, supplementary tests were performed. Repeatability, allowed peak ratio and maximum peak overlap were determined. Furthermore, the obtained values were compared to spectral deconvolution. Spectral deconvolution is reported to separate mixed components with a ratio of up to 99:1 [19]. In comparison, calculations with NMF reveal a ratio of down to 10:1 with a maximum relative standard deviation of <10%. While the spectral deconvolution is capable of separating fully overlaying chromatographic peaks, NMF operates, for investigated cases, up to an overlap of 33% with a maximum relative standard deviation of <10%. More detailed results are given in Fig. 3. Therein, the systematic measurement of repeatability and compliance of NMF deconvolution for different deconvolution issues of two peaks is investigated. For this, the results for every investigated combination of the area ratio between peak 1 and peak 2 and the area overlap of peak 2 with peak 1 are expressed by a coloured pixel. The colour coding is arbitrary and should reflect levels of interest. These levels are green for relative deviations of up to 5%, yellow for relative deviations between 5 and 10% and orange for >10% relative deviation. The investigated deconvolutions range from an area ratio between peak 1 and peak 2 from one to ten with only slightly area overlap (Fig. 3A-I) to practically equal peaks with high area overlap (Fig. 3A-III). Fig. 3B illustrates the repeatability of every single investigated combination by measuring the maximum standard deviation based on the thousandfold calculation of the NMF. As a result, the relative maximum standard deviation for most peaks with an area overlap of up to 33% is <5%. In addition, the peak area ratio only has only little effect on the deviation, while a higher peak overlap above 33% results in increased deviations. This increase reaches its maximum at 10.9% with almost complete overlap and would allow separating nearly fully overlapping peaks for all peak ratios. For Fig. 3C, the deconvoluted peaks are summed up again and are compared afterwards with the original spectra. As a result, the relative difference of both areas was plotted. Fig. 3C reveals different maximum standard deviations, especially for a highly overlapping peak area. This is most likely due to the hard colour cut applied for better interpretability. For peaks with an area overlap of up to 33%, the error is <10% and with a maximum error of 13.8% all peaks can be separated. In general, these results indicate that NMF is able to separate all investigated combinations of peak ratios and peak overlaps and can reproduce the initial data with minor challenges.

4. Conclusion

In this study, the capability of GC-VUV is shown for drug- and explosive precursors as well as chemical warfare simulants. Measurements proved that VUV absorption spectroscopy is well suited for these compound classes. The possibility to distinguish different isomers (e.g. common nitroaromatics), regardless of the separation efficiency, is an advantage over other analyser techniques such as mass spectrometric detectors. In addition, the non-destructive characteristic of VUV absorption detection allows coupling to a subsequent detector. Furthermore, the capability to deconvolute co-eluted peaks in a chromatogram was shown using two approaches, which is less time-consuming and eliminates extensive method development. Necessary requirements to

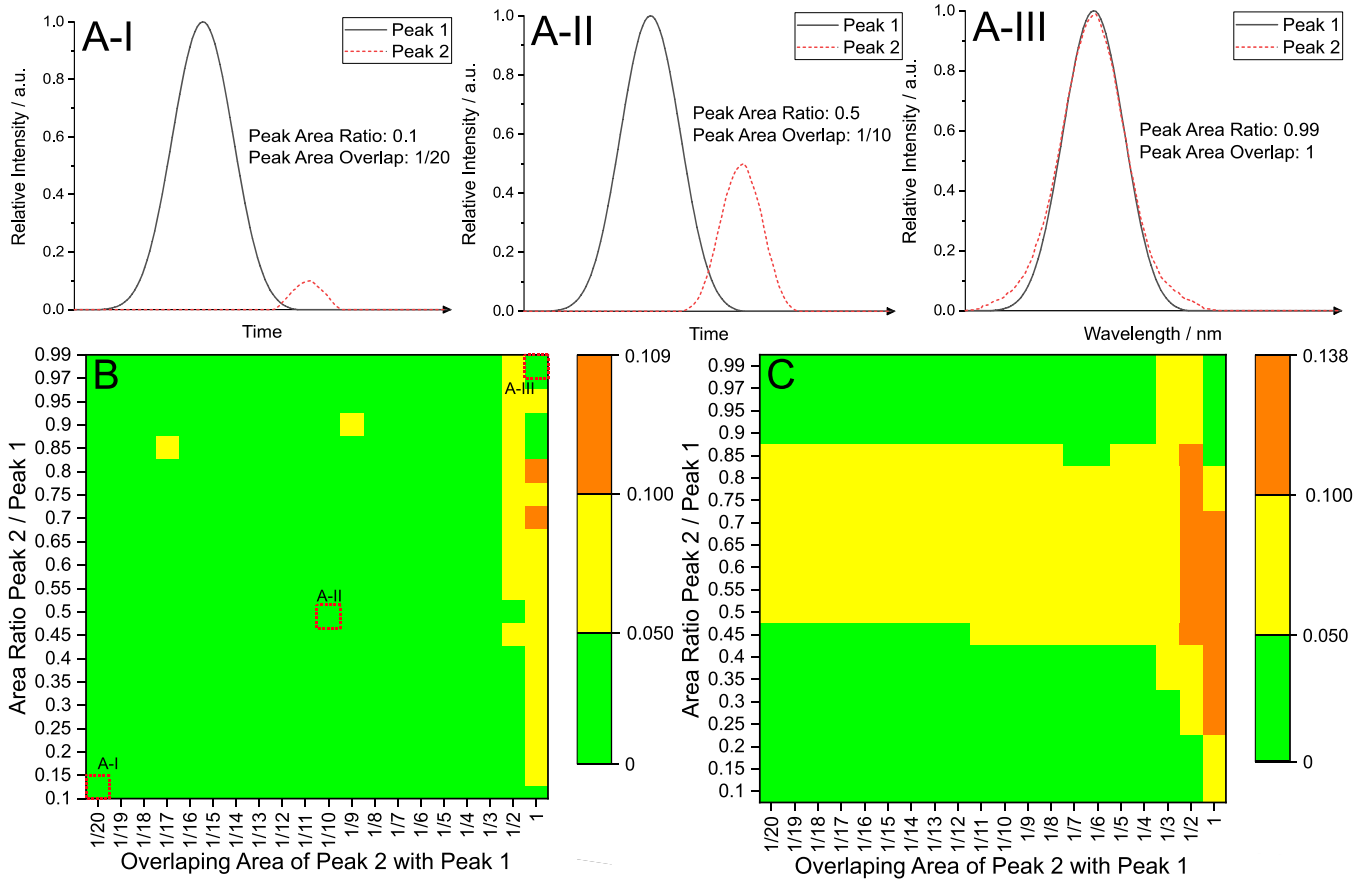

Fig. 3. Systematic measurement of reproducibility and compliance of NMF deconvolution for different deconvolution issues of two peaks. Therefore, the results are expressed by a coloured pixel for every investigated combination of the area ratio between peak 1 and peak 2 and area overlap of peak 2 with peak 1. The colour coding is arbitrary and should reflect relevant levels. These levels are green for relative deviations of up to 5%, yellow for relative deviations between 5 and 10% and orange for over 10% relative deviation. The measured deconvolutions range from an area ratio between peak 1 and peak 2 from one to ten with only slight overlap (panel A-I) to practically equal peaks with high area overlap (panel A-III). Panel B illustrates the reproducibility, by measuring the maximum standard deviation of 1000 measurements for every single investigated combination. Examples of the red marked pixels are drawn at panel A. For panel C, the deconvoluted peaks are summed up again and then compared with the original spectra and the resulting relative difference of both areas was plotted.

conduct spectral deconvolution are the availability of pure substance spectra. In contrast, NMF can be applied to discovery-based approaches when unknown compounds are studied. Therefore, both deconvolution techniques reveal a different scope depending on the availability of pure substance spectra. If pure substance spectra of target compounds are available, spectral deconvolution allows a more flexible application. For scenarios such as the measurement of new synthesised substances or non-target analytics, NMF will be the method of choice. This is especially useful in forensic science because of the ongoing development of new drugs and synthesis routes.

Supplementary data to this article can be found online at https://doi.org/10.1016/j.saa.2019.04.032.

Acknowledgements

This work was supported by the Federal Ministry of the Interior (BMI) and the Federal Office of Civil Protection and Disaster Assistance of Germany [grant number FP406 “SEMFreS”].

References

[1] N. Raikos, K. Christopoulou, G. Theodoridis, H. Tsoukali, D. Psaroulis, Determination of amphetamines in human urine by headspace solid-phase microextraction and gas chromatography, J. Chromatogr. B 789 (2003) 59–63, https://doi.org/10.1016/S1570-0232(03)00047-3.

[2] B. Fodor, I. Molnár-Perl, The role of derivatization techniques in the analysis of plant cannabinoids by gas chromatography mass spectrometry, TrAC Trends Anal. Chem. 95 (2017) 149–158, https://doi.org/10.1016/j.trac.2017.07.022.

[3] J.M. Perr, K.G. Furton, J.R. Almirall, Gas chromatography positive chemical ionization and tandem mass spectrometry for the analysis of organic high explosives, Talanta 67 (2005) 430–436, https://doi.org/10.1016/j.talanta.2005.01.035.

[4] Z. Witkiewicz, E. Sliwka, S. Neffe, Chromatographic analysis of chemical compounds related to the Chemical Weapons Convention, TrAC Trends Anal. Chem. 85 (2016) 21–33, https://doi.org/10.1016/j.trac.2016.05.006.

[5] K. Zaitsu, H. Miyagawa, Y. Sakamoto, S. Matsuta, K. Tsuboi, H. Nishioka, M. Katagi, T. Sato, M. Tatsuno, H. Tsuchihashi, K. Suzuki, A. Ishii, Mass spectrometric differentiation of the isomers of mono-methoxyethylamphetamines and mono-methoxydimethylamphetamines by GC–EI–MS–MS, Forensic Toxicol. 31 (2013) 292–300, https://doi.org/10.1007/s11419-013-0193-6.

[6] B.S. Middleditch, N.-J. Sung, A. Zlatkis, G. Settembre, Trace analysis of volatile polar organics by direct aqueous injection gas chromatography, Chromatographia 23 (1987) 273–278, https://doi.org/10.1007/BF02311779.

[7] K.A. Schug, I. Sawicki, D.D. Carlton, H. Fan, H.M. McNair, J.P. Nimmo, P. Kroll, J. Smuts, P. Walsh, D. Harrison, Vacuum ultraviolet detector for gas chromatography, Anal. Chem. 86 (2014) 8329–8335, https://doi.org/10.1021/ac5018343.

[8] I.G.M. Anthony, M.R. Brantley, C.A. Gaw, A.R. Floyd, T. Solouki, Vacuum ultraviolet spectroscopy and mass spectrometry: a tandem detection approach for improved identification of gas chromatography-eluting compounds, Anal. Chem. 90 (2018) 4878–4885, https://doi.org/10.1021/acs.analchem.8b00531.

[9] I.G.M. Anthony, M.R. Brantley, A.R. Floyd, C.A. Gaw, T. Solouki, Improving accuracy and confidence of chemical identification by gas chromatography/vacuum ultraviolet spectroscopy-mass spectrometry: parallel gas chromatography, vacuum ultraviolet, and mass spectrometry library searches, Anal. Chem. 90 (2018) 12307–12313, https://doi.org/10.1021/acs.analchem.8b04028.

[10] J. Andrasko, L. Lagesson-Andrasko, J. Dahlén, B.-H. Jonsson, Analysis of explosives by GC-UV, J. Forensic Sci. 62 (2017) 1022–1027, https://doi.org/10.1111/1556-4029.13364.

[11] L. Skultety, P. Frycak, C. Qiu, J. Smuts, L. Shear-Laude, K. Lemr, J.X. Mao, P. Kroll, K.A. Schug, A. Szewczak, C. Vaught, I. Lurie, V. Havlicek, Resolution of isomeric new designer stimulants using gas chromatography - vacuum ultraviolet spectroscopy and theoretical computations, Anal. Chim. Acta 971 (2017) 55–67, https://doi.org/10.1016/j.aca.2017.03.023.

[12] A. Leghissa, J. Smuts, C. Qiu, Z.L. Hildenbrand, K.A. Schug, Detection of cannabinoids and cannabinoid metabolites using gas chromatography with vacuum ultraviolet spectroscopy, Sep. Sci. Plus 1 (2018) 37–42, https://doi.org/10.1002/sscp.201700005.

[13] C.A. Cruse, J.V. Goodpaster, Generating highly specific spectra and identifying thermal decomposition products via Gas Chromatography/Vacuum Ultraviolet Spectroscopy (GC/VUV): application to nitrate ester explosives, Talanta 195 (2019) 580–586, https://doi.org/10.1016/j.talanta.2018.11.060.

[14] H. Fan, J. Smuts, L. Bai, P. Walsh, D.W. Armstrong, K.A. Schug, Gas chromatography-vacuum ultraviolet spectroscopy for analysis of fatty acid methyl esters, Food Chem. 194 (2016) 265–271, https://doi.org/10.1016/j.foodchem.2015.08.004.

[15] C. Qiu, J. Cochran, J. Smuts, P. Walsh, K.A. Schug, Gas chromatography-vacuum ultraviolet detection for classification and speciation of polychlorinated biphenyls in industrial mixtures, J. Chromatogr. A 1490 (2017) 191–200, https://doi.org/10.1016/j.chroma.2017.02.031.

[16] M.W. Berry, M. Browne, A.N. Langville, V.P. Pauca, R.J. Plemmons, Algorithms and applications for approximate nonnegative matrix factorization, Comput. Stat. Data Anal. 52 (2007) 155–173, https://doi.org/10.1016/j.csda.2006.11.006.

[17] Deutsches Institut für Normung, DIN 32645: Chemical Analysis - Decision Limit, Detection Limit and Determination Limit Under Repeatability Conditions - Terms, Methods, Evaluation, 2008th ed. Beuth, Berlin, 2008 71.040.01.

[18] E. Matisová, S. Škrabáková, Applicability of a novel carbon sorbent for the preconcentration of volatile chlorinated hydrocarbons, Anal. Chim. Acta 309 (1995) 181–188, https://doi.org/10.1016/0003-2670(95)00089-I.

[19] J. Schenk, J.X. Mao, J. Smuts, P. Walsh, P. Kroll, K.A. Schug, Analysis and deconvolution of dimethylnaphthalene isomers using gas chromatography vacuum ultraviolet spectroscopy and theoretical computations, Anal. Chim. Acta 945 (2016) 1–8, https://doi.org/10.1016/j.aca.2016.09.021.

[20] A. Schwarzenberg, J.-C. Tabet, R.B. Cole, X. Machuron-Mandard, H. Dossmann, New insights into dissociation of deprotonated 2,4-dinitrotoluene by combined high-resolution mass spectrometry and density functional theory calculations, Rapid Commun. Mass Spectrom. 29 (2015) 29–34, https://doi.org/10.1002/rcm.7076.

[21] T. Ieda, S. Hashimoto, T. Isobe, T. Kunisue, S. Tanabe, Evaluation of a data-processing method for target and non-target screening using comprehensive two-dimensional gas chromatography coupled with high-resolution time-of-flight mass spectrometry for environmental samples, Talanta 194 (2019) 461–468, https://doi.org/10.1016/j.talanta.2018.10.050.

[22] J. Rapin, A. Souloumiac, J. Bobin, A. Larue, C. Junot, M. Ouethrani, J.-L. Starck, Application of non-negative matrix factorization to LC/MS data, Signal Process. 123 (2016) 75–83, https://doi.org/10.1016/j.sigpro.2015.12.014.

[23] C. Weston, J. Smuts, J.X. Mao, K.A. Schug, Investigation of gas phase absorption spectral similarity for stable-isotopically labeled compounds in the 125–240 nm wavelength range, Talanta 177 (2018) 41–46, https://doi.org/10.1016/j.talanta.2017.09.033.

[24] Europol, Largest ever European haul of amphetamine precursor BMK seized, https://www.europol.europa.eu/newsroom/news/largest-ever-european-haul-of-amphetamine-precursor-bmk-seized 2015, Accessed date: 8 June 2018.

[25] E.J. Karjalainen, U.P. Karjalainen, Component reconstruction in the primary space of spectra and concentrations. Alternating regression and related direct methods, Anal. Chim. Acta 250 (1991) 169–179, https://doi.org/10.1016/0003-2670(91)85070-9.

9.3.2 Publication 2

Ambient Pressure Laser Desorption—Chemical Ionization Mass Spectrometry for Fast and Reliable Detection of Explosives, Drugs, and Their Precursors

Published by

René Reiss, Sven Ehlert, Jan Heide, Michael Pütz, Thomas Forster and Ralf Zimmermann

Applied Sciences, Year 2018, Volume 8, Issue 6, 933

DOI: 10.3390/app8060933

applied sciences

MDPI

Article

Ambient Pressure Laser Desorption—Chemical Ionization Mass Spectrometry for Fast and Reliable Detection of Explosives, Drugs, and Their Precursors

René Reiss [1], Sven Ehlert [1], Jan Heide [1], Michael Pütz [2], Thomas Forster [2] and Ralf Zimmermann [1,3,*]

1 Joint Mass Spectrometry Centre, Chair of Analytical Chemistry, University of Rostock, Dr.-Lorenz-Weg 2, 18059 Rostock, Germany; rene.reiss@uni-rostock.de (R.R.); sven.ehlert@uni-rostock.de (S.E.); jan.heide@uni-rostock.de (J.H.)
2 Bundeskriminalamt-Federal Criminal Police Office (BKA), Forensic Science Institute, Äppelallee 45, 65203 Wiesbaden, Germany; Michael.Puetz@bka.bund.de (M.P.); Thomas.Forster@bka.bund.de (T.F.)
3 Joint Mass Spectrometry Centre, Comprehensive Molecular Analytics, Helmholtz Zentrum München, Ingolstädter Landstr. 1, 85764 Neuherberg, Germany
* Correspondence: ralf.zimmermann@helmholtz-muenchen.de; Tel.: +49-381-498-6460

Received: 6 May 2018; Accepted: 2 June 2018; Published: 5 June 2018

Featured Application: Direct detection of safety relevant, low volatile substances on surfaces, ranging from tableted drugs to suspicious remnants on surfaces like bags, luggage, or even containers.

Abstract: Fast and reliable information is crucial for first responders to draw correct conclusions at crime scenes. An ambient pressure laser desorption (APLD) mass spectrometer is introduced for this scenario, which enables detecting substances on surfaces without sample pretreatment. It is especially useful for substances with low vapor pressure and thermolabile ones. The APLD allows for the separation of desorption and ionization into two steps and, therefore, both can be optimized separately. Within this work, an improved version of the developed system is shown that achieves limits of detection (LOD) down to 500 pg while remaining fast and flexible. Furthermore, realistic scenarios are applied to prove the usability of this system in real-world issues. For this purpose, post-blast residues of a bomb from the Second World War were analyzed, and the presence of PETN was proven without sample pretreatment. In addition, the analyzable substance range could be expanded by various drugs and drug precursors. Thus, the presented instrumentation can be utilized for an increased number of forensically important compound classes without changing the setup. Drug precursors revealed a LOD ranging from 6 to 100 ng. Drugs such as cocaine hydrochloride, heroin, (3,4-methylendioxy-methamphetamine) hydrochloride (MDMA) hydrochloride, and others exhibit a LOD between 10 to 200 ng.

Keywords: APLD; drugs; explosives; post blast residue detection; mass spectrometry; chemical ionization; on-line measurement; forensic chemistry; mapping

1. Introduction

In real-world scenarios, the fast and selective detection of security-relevant substances can be crucial to ensure the most appropriate decision is taken as a foundation for further tactical procedures and minimization of risk for first responders and the civil population. In addition to other approaches like ion mobility spectrometry, mass spectrometry (MS) has been proven as a powerful and versatile technique to detect such substances. There are some MS techniques that should be mentioned, especially when focusing on explosives. In particular, gas chromatography coupled to

mass spectrometry (GC-MS) has to be mentioned as a lab based technique and is used for more than 40 years to detect explosives and is a still improving field [1–6]. Besides an increase of reliability due to chromatographic separation, some mass spectrometers allow selective ion fragmentation of potential target substance to prove identification. This so-called tandem mass spectrometry function increases significantly the probability of a correct positive detection result and enables a lower false alarm rate, e.g., at luggage checks on airports. Ion trap (IT) mass spectrometers equipped with different ionization techniques are commonly deployed for such tandem mass spectrometric experiments. Depending on the analytical target, most IT-MS can be equipped with different ionization techniques like electron ionization (EI), chemical ionization (CI) [7], or single photon ionization (SPI) [8]. Surface analyzing techniques allow for the observation of different potentially interesting targets in forensic science like luggage, letters, or clothes without time-consuming sample pretreatment. Direct analyses in real time (DART) [9,10], DART-Raman combination [11], desorption electrospray ionization (DESI) [12,13], solvent assisted desorption/ionization mass spectrometry (DI-MS) [14], or a variety of laser desorption/ionization (LDI) [15] systems are common techniques. Two of the most famous setups of these LDI systems are called matrix-assisted laser desorption/ionization (MALDI) [16,17] and surface-assisted laser desorption/ionization (SALDI) [10,18]. Omitting a special matrix and directly using the surface where a sample is located leads to the so called direct LDI approach. If interesting spots on bulky objects like containers, bulky luggage, or cars should be analyzed, highly mobile systems are preferable that can operate with a flexible sampling. Therefore, a separation of desorption and ionization processes can be beneficial because it allows a targeted optimization of the specific components to acquire enhanced results. One effective opportunity to realize the sampling is direct laser desorption (LD) that does not require additional media other than electricity. It is commonly used as the desorption step for various applications such as investigation of biological tissues [19–21], aerosols [22], pesticides [23], drugs [24], and explosives [25,26]. Drugs and explosives are relevant classes in forensic science. Explosives exhibit two characteristics that complicate their detection with common approaches but improves their applicability for LD: a very low vapor pressure, e.g., RDX (hexahydro-1,3,5-trinitro-1,3,5-triazine) has 4.4×10^{-9} mPa or HNS (hexanitrostilbene) with 6.2×10^{-18} mPa [27], and many of them are thermolabile. Some drugs also have a very low vapor pressure such as cocaine hydrochloride with 1.9×10^{-3} mPa or heroin hydrochloride with 1.2×10^{-3} mPa [28] and can be detected with this system even if they are not prone to a fast thermal degradation like explosives. By using a pulsed LD, instead of a continuous wave approach [29], thermal stress is lowered and leads to less fragmentation and better detection limits for explosives. Furthermore, a pulsed LD induces a shockwave-like ablation of the sample material from the surface and thus vapor pressure of the analyte is less crucial [29]. Some well-known and established vacuum ionization techniques that can be combined with LD are EI or CI. CI, for example, uses a reactant gas for a softer ionization [7]. Hence, spectra generated by CI mostly have fewer fragments and the quasi-molecular ion signal is more intense, which leads to easier interpretable spectra.

Recently, we suggested ambient pressure laser desorption (APLD) [30] in combination with CI [31] for different explosives and showed the advantages of this straightforward and field-deployable system. In particular, this design is considered as a benefit for on-site applications, because only electricity is required (and methane as reactant gas if CI is used). To enable the detection of even small amounts of analyte, it was attempted to improve the limit of detection. Therefore, improvements on the transfer system and the desorption unit are done in this work to further enhance the detection characteristics for different explosives and drug precursors. In addition, there are many other substances that are of potential interest in the forensic field and that could also benefit from the APLD. Because of this, we would like to show that the APLD is not limited to explosives but also allows for the measuring of drugs and drug precursors at a comparable level to other measurement techniques. This greatly enhances the versatility of this technique because it enables it to cover different forensically-relevant compound classes with a single system. A practical example could be the rapid search of containers for smuggled synthetic drug precursors in container ports.

2. Materials and Methods

Explosives, drugs, and drug precursors investigated in this study were obtained from the German Federal Criminal Police Office (BKA, Wiesbaden, Germany). Explosives were acquired as methanolic solutions with a concentration of 1 g/L and drug precursors as well as ketamine as pure substances. Explosives were trinitrotoluene, 1,3-dinitrobenzene, 2,4-dinitrotoluene, 2,6-dinitrotoluene, 2,4,6-trinitrophenylmethyl-nitramine, picric acid, 3,4-dinitrotoluene, triacetonetriperoxide, and ammonia nitrate. Drug precursors/drugs of abuse were ketamine hydrochloride, safrole, amantadine, and phenylacetone. Some 5F-Cumyl-PINACA, a cannabimimetic new psychoactive substance, coated on herbal blend and sold as "Rollin' High" was also received from the BKA. Potassium chlorate was obtained from Sigma Aldrich Chemie GmbH (Steinheim, Germany) and potassium perchlorate anhydrous was bought at Thermo Fisher GmbH (Kandel, Germany). Used solvents were dichloromethane and methanol from Carl Roth GmbH + Co. KG (Karlsruhe, Germany). Methane 4.5 as CI reactant gas and helium 5.0 were bought from Linde AG (Berlin, Germany). A schematic overview of the system and its parts can be seen in Figure 1. This figure describes all relevant parts of the system and is explained in detail at the end of this chapter. A Minilite neodymium-doped yttrium aluminum garnet (Nd:YAG) laser from Continuum Inc. (San Jose, CA, USA) was used for desorption in the second harmonic wavelength (λ = 532 nm). Mass spectra and software were acquired utilizing a Varian Inc. (Walnut Creek, CA, USA) ion trap 240-MS and Varian MS Workstation 6.9.1. The MS parameter for CI were a mass rage of 50 to 400 m/z, 1.7 Hz acquisition rate, 3 µs cans averaged, 3 mL/min helium cooling gas flow, and full scan for all measurements. For EI measurements, an acquisition rate of 0.8 Hz and an emission current of 25 µA were chosen. Other MS parameters were similar to CI. Calibration was done for EI and CI with pure perfluorotributylamine, as required by the instrument. Lens energy and tuning was carried out automatically by MS software. Laser light was transferred from the laser to the ambient pressure desorption head with a 1250 µm Optran UV laser fiber from CeramOptec GmbH (Bonn, Germany). The ambient pressure desorption head was self-built and made out of brass and polytetrafluoroethylene for thermal separation. A stainless steel capillary with 100 µm inner diameter was used as the transfer-line and was bought at IDEX Health & Science LLC (Oak Habor, WA, USA). Sample deposition on the sampling surface was done by a microliter syringe from Hamilton Bonaduz AG (Bonaduz, Switzerland). For automated and easy surface analysis, a self-build two-axis linear driving system (X-Y table) was combined with stepper motors and the MCC-2 stepper motor controller from Phytron GmbH (Gröbenzell, Germany). The sample desorption surface was a steel sheet made of V2A steel.

For sampling, 1 µL aliquots were spotted directly onto the steel target; spots were dried under ambient conditions, and the residue carrying surface was placed on the X-Y table. The sample spots were as small as possible, with a maximum diameter of 1 mm. Subsequently, the sample surface was scanned automatically with the APLD system until the residue was detected. Therefore, an area of 5 × 5 mm was scanned to ensure the substance was hit. Each spot was desorbed with a single laser pulse every millimeter distance at a repetition rate of 10 Hz. After all data was collected, the surface was cleaned with methanol and could be reused. The desorption head did not require further cleaning after a measurement. The APLD system was heated to 200 °C. For explosives and explosive precursors, negative detection mode was chosen. All other compounds were analyzed with positive detection mode. Due to the fact that ambient samples with high air intake were measured, CI with external ionization was realized. External ionization means that ions are formed outside the trap in a specific ionization region inside the mass spectrometer. Although, internal ionization would lead to better limits of detection (LOD), the mass resolution and mass accuracy would strongly decrease simultaneously due to higher amounts of air. External ionization is a compromise between sensitivity and mass resolution for direct sampling of target compounds in an environmental gas matrix.

pulse with a pulse energy of about 3–5 mJ was guided via a laser fiber to the sampling surface. The laser fiber was mounted at the desorption head with approximately three millimeters distance to the surface. The pulsed laser light ablated the analyte from the surface, and, subsequently, the ablated material was transferred through a capillary into the IT-MS. Desorption head and transfer capillary were heated to 200 °C to prevent unintended surface adsorption of analytes. Methane as reactant gas was used for chemical ionization, generating primarily protonated quasi molecular ions.

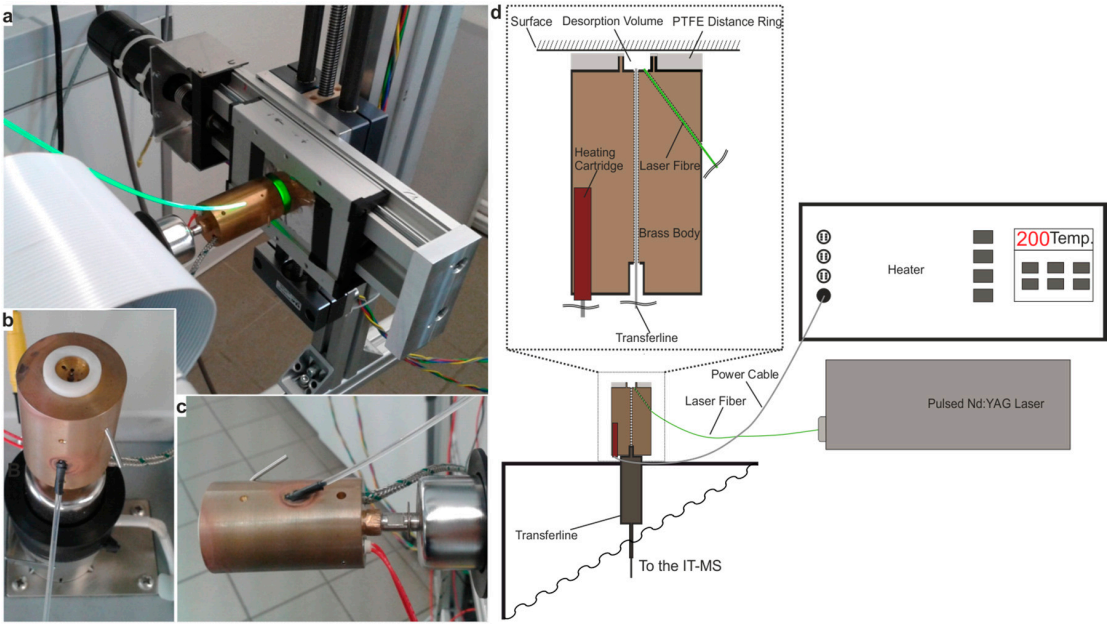

Figure 1. (**a**) Laser desorption sampling for mass spectrometric analysis from a stainless steel surface with a self-built X-Y table; (**b**) Deployed ambient pressure laser desorption (APLD) head with front view on desorption volume and polytetrafluoroethylene (PTFE) ring; (**c**) APLD head side view with attached laser fiber, heating cartridge, and thermocouple; (**d**) Schematic drawing of the APLD chemical ionization-mass spectrometer (APLD-CI-MS). The heating cartridge inside of the brass body ensures a complete heating of the sampling head. A laser fiber transfers pulsed laser light, produced by the Nd:YAG laser, to the surface. The ablated analyte is subsequently transferred into the transferline and afterwards into the IT-MS. There, it can be ionized by electron ionization (EI) or chemical ionization (CI) and then analyzed.

3. Results and Discussion

Real-world samples were held in front of the APLD, and the laser was activated. All settings were the same as for standard laboratory measurements. No cleaning was necessary after executed measurements.

3.1. Improved Detection Limits through Design Optimization

We recently demonstrated in a previous work [31] an ambient pressure laser desorption system for the sensitive and flexible mass spectrometric detection of explosives. The detection limits were in a suitable range for forensic application as presented in this work. Nevertheless, an improved detection limit can enhance the reliability of the analytical method. In the original setup, a non-heated front end laser desorption head in PEEK was applied.

The ambient pressure laser desorption, shown in Figure 1, operates by direct desorption of samples from surfaces with short laser pulses. At first, an approximately 5 ns wide Nd:YAG laser pulse with a pulse energy of about 3–5 mJ was guided via a laser fiber to the sampling surface. The laser fiber was mounted at the desorption head with approximately three millimeters distance to the surface. The pulsed laser light ablated the analyte from the surface, and, subsequently, the ablated material was transferred through a capillary into the IT-MS. Desorption head and transfer capillary were heated to 200 °C to prevent unintended surface adsorption of analytes. Methane as reactant gas was used for chemical ionization, generating primarily protonated quasi molecular ions.

3. Results and Discussion

3.1. Improved Detection Limits through Design Optimization

We recently demonstrated in a previous work [31] an ambient pressure laser desorption system for the sensitive and flexible mass spectrometric detection of explosives. The detection limits were in a suitable range for forensic application as presented in this work. Nevertheless, an improved detection

limit can enhance the reliability of the analytical method. In the original setup, a non-heated front end made out of polyether ether ketone (PEEK) was utilized.

In this study, several modifications to the existing system were performed. These modifications are the exchange of the type of material, establishing a heatable system, shortening the transferline, and increasing the laser fiber diameter. All these changes are discussed in the following section.

In this study, several modifications to the existing system were performed. These modifications are the exchange of the type of material, establishing a heatable system, shortening the transferline, and increasing the laser fiber diameter. All these changes are discussed in the following section.

3.1.1. Sampling Head Design Optimization

3.1.1. Sampling Head Design Optimization

The sampling head, crucial for a fast and sensitive detection, was modified first. The novel design, utilizing a heated brass body, was aimed to further improve the sampling. Within this modification, the brass area exposed to the analyte is minimized. Theoretically, imaginable catalytic surface processes can be neglected due to the fact that the analytes pass only a small brass surface area on their way into the transferline and only very few applications of brass for catalytic surface processes can be found [32]. Because of the minimized adsorption processes at the inside of this desorption head, a faster analyte transfer into the IT-MS is enabled. This in turn should give more narrow signals and better limits of detection. Heating of the investigated sample surface is prevented by mounting of a thin spacer of polytetrafluoroethylene (PTFE) at the top of the sampling head (Figure 1b). The influence of the transferline was investigated by varying the length and the diameter of the transferline while keeping the temperature and parameters constant. The diameter was adjusted to ensure a nearly similar sample flow into the MS. As exemplarily visualized in Figure 2 for the investigation of tetryl, the version with the shortened transferline revealed an approximately four-times improved signal width. This effect is caused by the higher temperature and a shorter transferline. On that account, a minimum of ad- and de-sorption within the transferline was achieved and thus more narrow peaks should be obtained.

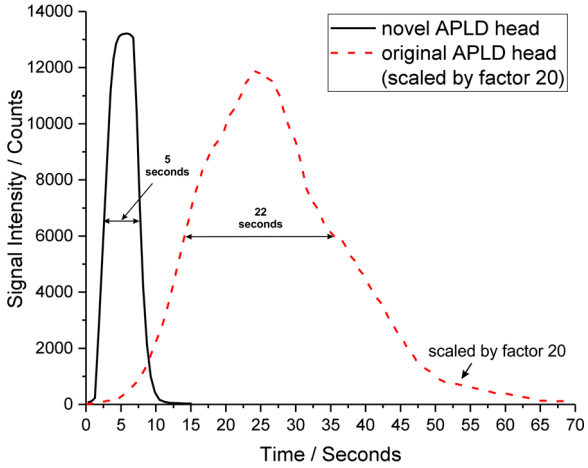

Figure 2. Compared smoothed desorption from spots with about 1.5 µg Tetryl. Measured at negative CI mode and fragment *m*/*z* 241. Novel system with short transferline and heated APLD head (solid line). Original measurement system with long transferline (dashed line). Compared is the full width at half maximum.

3.1.2. Optimization of Desorption Area

A further step that was implemented is the ability to use bigger laser fiber diameters at the same desorption volume inside the APLD head. By increasing the diameter of the laser fiber it is possible to transfer more laser light to the surface and simultaneously keeping the energy density constant. The diameter used before was about 0.6 mm, while the new fiber has a 1.25 mm diameter and thus increased the desorption area by four times while retaining the same divergence angle of the laser fiber. Laser fluence of both systems ranged between 0.2 to 0.4 J/cm^2. This lead to a higher analyte concentration within the gaseous phase above the sample spot.

3.1.3. Optimization Results

As can be seen in Figure 2, the full width at half maximum (FWHM) could be significantly decreased to about 5 s compared to 22 s with the original measurement system, reported previously

3.1.3. Optimization Results

As can be seen in Figure 2, the full width at half maximum (FWHM) could be significantly decreased to about 5 s compared to 22 s with the original measurement system, reported previously [31]. Starting point was the rise of the detector signal. At both measurements, the data acquisition was not triggered by laser shots and absolute delay was not regarded due to the lack of influence to the LOD. The transferline length differed from 1.5 m for the original system to 0.25 m for the novel one. As a result, the [illegible] contributed to the peak shape and subsequently to the system response time. A higher signal shape [illegible] was obtained that in addition should contribute to a lower [illegible] allows a flexible [illegible] analysis (reaching [illegible] to choose. On the one [illegible] can be obtained. On the other [illegible] transferline.

These [illegible] results are shown [illegible] and peroxide explosives [illegible] signals and were determined with the same procedure (described in the materials and methods section) at the same mass [illegible] by one order of magnitude [illegible] In addition, for other [illegible] amounts could be lowered significantly; for TNT down into the picogram range.

Table 2. Comparison of original and novel APLD systems by use of limit of detection (LOD) for different investigated explosives. All mentioned substances were used for the novel APLD system. The fragments are marked with [illegible] signals. All substances were measured in negative detection mode.

Substance Measured	LOD Original System	LOD Novel System	Structure
TNT (trinitrotoluene)	3 ng	500 pg	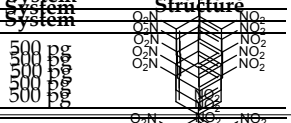
1,3-Dinitrobenzene	6 ng	1.5 ng	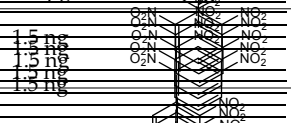
2,4-DNT (Dinitrotoluene)	3 ng	1.5 ng	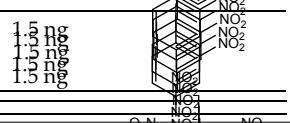
2,6-DNT	6 ng	2 ng	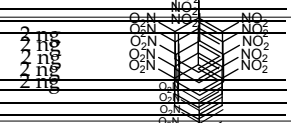
Tetryl (2,4,6-trinitrophenylmethylnitramine) *, *m/z* 241	30 ng	2 ng	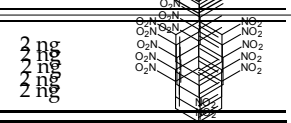

3.2. Target Compound Enhancement

In addition, to gain a more comprehensive impression about this system, other common explosives [illegible] (acetone peroxide) with a detection limit of about 800 ng. This can be explained due to the high

these explosives have a similar limit of detection of about 3 ng to 80 ng. The only exception is TATP (acetone peroxide) with a detection limit of about 800 ng. This can be explained due to the high thermal instability of this peroxide explosive making TATP difficult to detect for many different analyzing techniques. TATP's quite high vapor pressure limits the lowest amount of substance that can be prepared for a measurement, because the time before TATP evaporates completely decreases with the decreasing amount of substance used. Furthermore, potassium perchlorate and potassium chlorate were investigated but could not be detected within the investigated range of up to 2000 ng.

Drug precursors were additionally chosen because they are regarded as important target compounds in forensic science as some are already regulated or may give evidence for illegal drug synthesis. The APLD allows someone to scan the outer surfaces of liquid containers for drug precursor substances, which could indicate drug synthesis in a clandestine laboratory. Beside drug precursors, drugs of abuse were investigated to enhance the system capability. Therefore, ketamine and amantadine were considered as model substances for drugs of abuse [33,34]. In this work, ketamine represents possible sedatives and amantadine possible stimulants. Table 2 summarizes the limits of detection for these different substance classes. It has been shown that the capability of detecting drug precursors as well as drugs of abuse ranges from about 10 to 100 ng total substance amount compared to 0.5 to 800 ng for explosives. Therefore, the APLD system is also capable of detecting these compound classes and can be helpful for fast and straightforward collection of information and clues. To perform a substantial experiment to test the probability of detection, new substance deposition methods are needed. The applied "droplet method" is limited for such kinds of experiments because it cannot be assured that the spot density is high enough to mimic an evenly covered test surface.

Beside drugs precursors and drugs of abuse, also common illegal drugs like cocaine or heroin were investigated. All of these measured drugs are illicit and are, therefore, common target compounds in the forensic field. As a result of these measurements, the LOD could be determined to be in the same range as the other compound classes. Most substances could be detected at less than 20 ng absolute amount at the tested surface. While the LOD of real samples may differ substantially due to several effects, it should be interpreted as the lower operation range and a performance indicator. For real world samples, the LOD is less relevant because a yes or no answer is sufficient in most cases.

3.3. Real Sample Measurements

3.3.1. Shrapnel of Defused Bomb

Besides standard substances, samples from real-world scenarios were investigated to exploit the practical capabilities for forensic analysis. For this purpose, post-blast residues of a defused Second World War bomb are investigated. This bomb was defused by controlled explosion carried out by the Berlin Police. After the explosion, shrapnel were gathered up by hand, sent to our laboratory and stored in a cardboard box at room temperature inside the laboratory. This scenario is a good example of a real world scenario where only little information about the exploded bomb is available. No further information about the bomb is available because it was defused as part of a batch of old bombs.

Figure 3 shows the results of the investigation of one of the pictured shrapnel with the APLD system. In sum, four different shrapnel pieces were investigated and 2 to 4 locations per shrapnel measured. It turned out that all spectra exhibit a clear signal at m/z 227, which can be correlated to the molecular ion signal M^- of TNT. The presence of TNT can be assumed by the observed signals in the lower mass spectrum including the molecular ion signal of TNT at m/z 227, as well as two significant signals of respective fragments. As a comparison, the embedded mass spectrum shows an additional measurement of a 10 ng TNT standard sample measured under the same conditions. As can be observed in the mass spectrum, strong indications of TNT attached to the bomb shrapnel were found. In addition, fragmentation seems to be caused by the substrate. Therefore, results confirm that the APLD measurement system is not only suitable for laboratory measurements but also for answering realistic forensic questions. The APLD delivers valuable information about the used explosive.

Moreover, even longer periods between the collection of samples and the actual investigation seem to be acceptable.

Table 2. Limit of detection for different individually determined drug precursors, drugs, drugs of abuse, and some additional explosives measured with the novel APLD system. It is mutually assumed that the amount of substance is to be seen as a total amount and the sample spot is considered as totally desorbed at the measurement as described in the materials and methods section. Substances that have been detected as fragments are marked with an asterisk and with their *m/z* fragment value. All explosives were detected as molecular ion signals and all other substances as protonated molecular ions. All explosives were measured in negative detection mode, all other substances in positive detection mode.

Substances Measured at Novel Systems	LOD	Structure
Explosives		
PA (picric acid)	15 ng	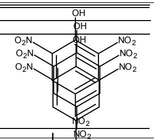
3,4-DNT	3 ng	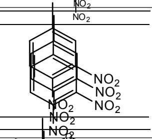
TATP (triacetonetriperoxide)	800 ng	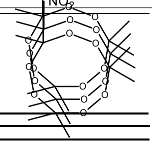
AN (ammonia nitrate) *, *m/z* 63	78 ng	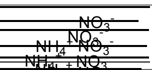
Drug precursors		
Safrole	100 ng	
Phenylacetone	50 ng	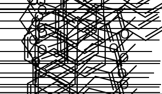
Drugs/drugs of abuse		
Amphetamine	20 ng	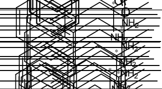
Methamphetamine	10 ng	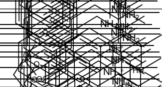
MDMA (3,4-methylendioxy-methamphetamine) hydrochloride	20 ng	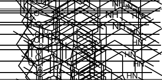
Heroin	200 ng	
Cocaine hydrochloride	17 ng	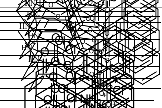
Ketamine hydrochloride	6 ng	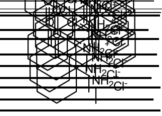

Appl. Sci. **2018**, *8*, x FOR PEER REVIEW 9 of 15

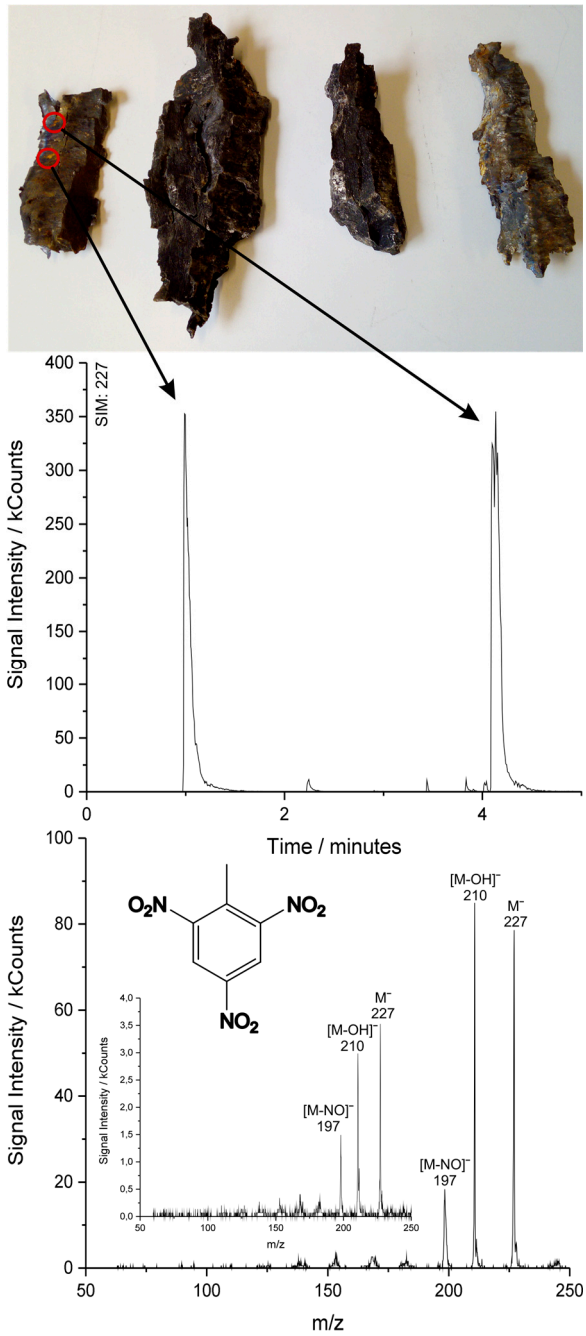

Figure 3. Desorption in negative CI mode of TNT from the surface of shrapnel recovered from a defused bomb of the Second World War. All shrapnel in the upper image show clear signals of TNT when investigated. A part of one of those single ion traces can be seen in the mass profile where the TNT signal at *m/z* 227 is plotted. The full size mass spectrum shows the first peak at about 1 min. The panel in the lower left shows the spectrum of a 10 ng TNT standard sample, measured under the same conditions. The signals look similar for every detected TNT trace and shrapnel.

Figure 3. Desorption in negative CI mode of TNT from the surface of shrapnel recovered from a defused bomb of the Second World War. All shrapnel in the upper image show clear signals of TNT when investigated. A part of one of those single ion traces can be seen in the mass profile where the TNT signal at *m/z* 227 is plotted. The full size mass spectrum shows the first peak at about 1 min. The panel in the lower left shows the spectrum of a 10 ng TNT standard sample, measured under the same conditions. The signals look similar for every detected TNT trace and shrapnel.

3.3.2. New Psychoactive Substance on Herbal Mixture

3.3.2. New Psychoactive Substance on Herbal Mixture

Another practical application is illustrated in Figure 4. It shows the ability to detect synthetic cannabinoid species directly on herbal mixtures. These herbal blends are commonly coated with so-called new psychoactive substances (NPS). The investigated compound belongs to these NPS and is a cannabimimetic aminoalkyl indazole with a carboxamide-linked cumyl moiety (5F-Cumyl-PINACA). For better comparability and reliable substance identification, through fragment identification, EI, was applied as the ionization technique.

Another practical application is illustrated in Figure 4. It shows the ability to detect synthetic cannabinoid species directly on herbal mixtures. These herbal blends are commonly coated with so-called new psychoactive substances (NPS). The investigated compound belongs to these NPS and is a cannabimimetic aminoalkyl indazole with a carboxamide-linked cumyl moiety (5F-Cumyl-PINACA).

5F-Cumyl-PINACA as an active substance at *m/z* 367 by comparing the molecular ion signal as well as the fragment pattern [35]. For direct measurement of the herbal mixture, a S/N ratio of 50.9 was calculated for the base peak at *m/z* 352 and a S/N ratio of 3.7 for the molecular ion signal at *m/z* 367. For the respective measurement of the emptied bag, the S/N ratio for the base peak at *m/z* 352 was 45.6 and for the molecular ion signal at *m/z* 367 the S/N ratio was 3.1. Even an emptied bag, in which the mixture was sold, showed a clear presence of 5F-Cumyl-PINACA. Therefore, a fast decision can be made whether the target substance is illicit or not simply by measuring suspect or confiscated objects. A reasonable scenario could be the rapid identification of designer drugs and related products found in conspicuous parcels in postal distribution centers.

45.6 and for the molecular ion signal at *m/z* 367 the S/N ratio was 3.1. Even an emptied bag, in which the mixture was sold, showed a clear presence of 5F-Cumyl-PINACA. Therefore, a fast decision can be made whether the target substance is illicit or not simply by measuring suspect or confiscated objects. A reasonable scenario could be the rapid identification of designer drugs and related products found in conspicuous parcels in postal distribution centers.

For better comparability and reliable substance identification, through fragment identification, EI was applied as the ionization technique.

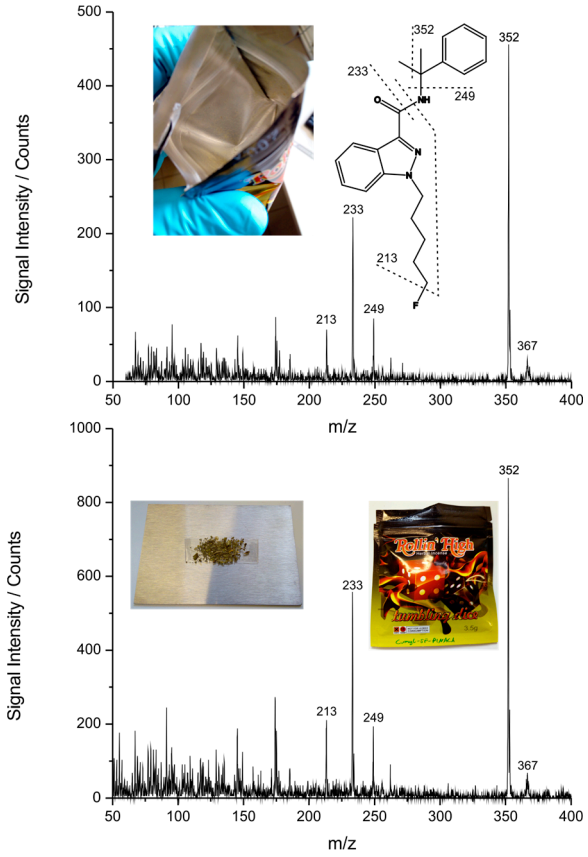

Figure 4. APLD EI-mass spectra of the herbal blend material. Direct laser desorption exhibits intense signals at higher *m/z*, tentatively assigned to 5F-Cumyl-PINACA from an herbal blend sold as "Rollin' High". This new psychoactive substance could be detected directly from herbal blend as well as residues sticking on the bag. The upper part shows a mass spectrum achieved by desorbing the inner side of the bag and the lower one a direct measurement of the herbal blend. A similar spectrum compared to the inside of the empty bag is revealed.

Figure 4. APLD EI-mass spectra of the herbal blend material. Direct laser desorption exhibits intense signals at higher *m/z*, tentatively assigned to 5F-Cumyl-PINACA from an herbal blend sold as "Rollin' High". This new psychoactive substance could be detected directly from herbal blend as well as residues sticking on the bag. The upper part shows a mass spectrum achieved by desorbing the inner side of the bag and the lower one a direct measurement of the herbal blend. A similar spectrum compared to the inside of the empty bag is revealed.

3.4. Additional Capabilities of the APLD Approach

Strong EI fragmentation signal at low *m/z* are typical when investigating complex natural samples. The LODs and the measurement speed of the APLD system allows not only for the measurement of samples on surfaces at trace levels, but it also enables an automated measurement of surfaces without sample pretreatment. For this purpose, a computer controlled X-Y table was mounted in front of the APLD head. In consequence, the automated mapping of flat surfaces can be performed, which reveals APLD spectra with sub-millimeter lateral resolution. Analysis of non-flat surfaces could be difficult due to delocalization of target compounds by touching the PTFE ring. The actual system performance is illustrated in Figure 5. This figure shows the possibility to detect the spatial distribution of an artificially prepared substance trace on a surface. An imaginable scenario in context of a preliminary investigation that benefits from APLD capabilities could be the analysis of

Direct measurement of the investigated herbal mixture revealed the usage of 5F-Cumyl-PINACA as an active substance at *m/z* 367 by comparing the molecular ion signal as well as the fragment pattern [35]. For direct measurement of the herbal mixture, a S/N ratio of 50.9 was calculated for the base peak at *m/z* 352 and a S/N ratio of 3.7 for the molecular ion signal at *m/z* 367. For the respective measurement of the emptied bag, the S/N ratio for the base peak at *m/z* 352 was 45.6 and for the molecular ion signal at *m/z* 367 the S/N ratio was 3.1. Even an emptied bag, in which the mixture was sold, showed a clear presence of 5F-Cumyl-PINACA. Therefore, a fast decision can be made whether the target substance is illicit or not simply by measuring suspect or confiscated objects. A reasonable scenario could be the rapid identification of designer drugs and related products found in conspicuous parcels in postal distribution centers.

3.4. Additional Capabilities of the APLD Approach

The LODs and the measurement speed of the APLD system allows not only for the measurement of samples on surfaces at trace levels, but it also enables an automated measurement of surfaces without sample pretreatment. For this purpose, a computer controlled X-Y table was mounted in

front of the APLD head. In consequence, the automated mapping of flat surfaces can be performed, which reveals APLD spectra with sub-millimeter lateral resolution. Analysis of non-flat surfaces could be difficult due to delocalization of target compounds by touching the PTFE ring. The actual system performance is illustrated in Figure 5. This figure shows the possibility to detect the spatial distribution of an artificially prepared substance trace on a surface. An imaginable scenario in context of a preliminary investigation that benefits from APLD capabilities could be the analysis of fingerprint residues from plastic explosives. In this case, the identification can be challenging due to the strong presence of matrix signals in the plastic explosive.

Appl. Sci. **2018**, *8*, x FOR PEER REVIEW 11 of 15

fingerprint residues from plastic explosives. In this case, the identification can be challenging due to the strong presence of matrix signals in the plastic explosive.

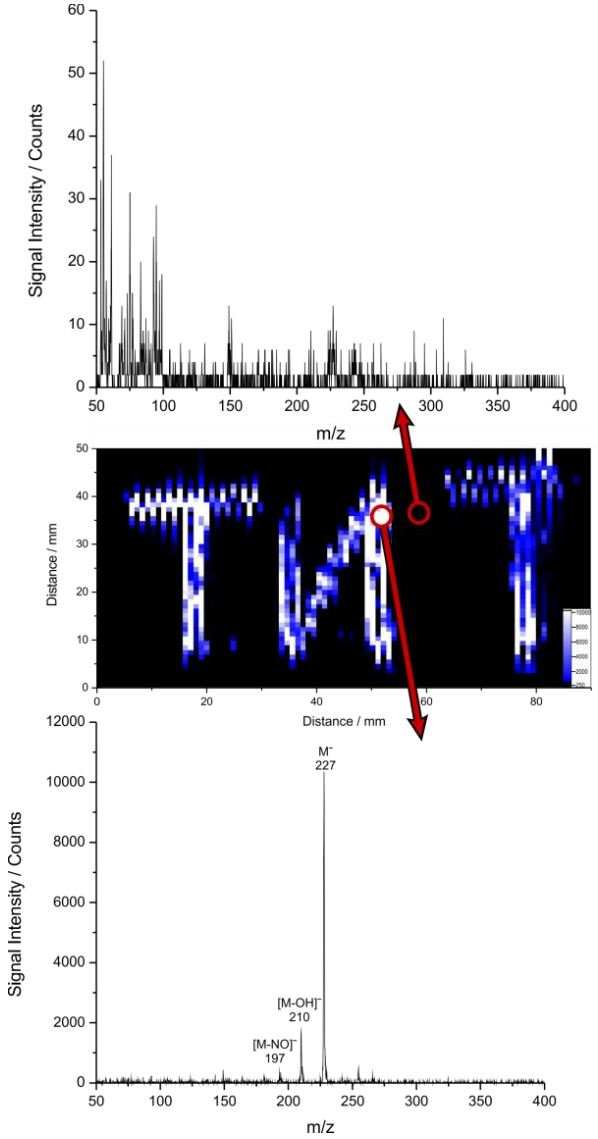

Figure 5. APLD mapping capabilities shown at a TNT example generated with CI negative detection mode. Two typical mass spectra can be seen above. If the position of the X-Y table and the signal intensity is combined at any point of the surface the image on the top right can be achieved. This image shows a prepared stainless steel surface that was labeled with the word TNT. This label was produced with 1 mg/L TNT solution and a µL syringe. The total amount of substance applied for this image was about 20 µg. The color changes from black (no TNT detected) to white (high amounts of TNT detected). Therefore, the upper spectrum indicates a "black" area and the lower spectrum reveals the basis for a "white area". For mapping purposes a LabVIEW TM script was created, which can be found in the Supplementary Material.

Figure 5. APLD mapping capabilities shown at a TNT example generated with CI negative detection mode. Two typical mass spectra can be seen above. If the position of the X-Y table and the signal intensity is combined at any point of the surface the image on the top right can be achieved. This image shows a prepared stainless steel surface that was labeled with the word TNT. This label was produced with 1 mg/L TNT solution and a µL syringe. The total amount of substance applied for this image was about 20 µg. The color changes from black (no TNT detected) to white (high amounts of TNT detected). Therefore, the upper spectrum indicates a "black" area and the lower spectrum reveals the basis for a "white area". For mapping purposes a LabVIEW TM script was created, which can be found in the Supplementary Material.

Comparing APLD to other analytical techniques that are available to detect directly trace levels of security relevant substances like explosives, drugs, or drug precursors leads to similar results regarding the LODs, ranging mostly in the low nanogram scale. Table 3 summaries compared analytical techniques and achieved LODs. In detail, the APLD allows similar LODs compared to Raman spectroscopy [36], ion mobility spectrometry [37], and thermal desorption (TD) MS [38,39]. Compared to APLD, desorption spray ionization (DESI) achieves better LODs for explosives [40]

Comparing APLD to other analytical techniques that are available to detect directly trace levels of security relevant substances like explosives, drugs, or drug precursors leads to similar results regarding the LODs, ranging mostly in the low nanogram scale. Table 3 summaries compared analytical techniques and achieved LODs. In detail, the APLD allows similar LODs compared to Raman spectroscopy [36], ion mobility spectrometry [37], and thermal desorption (TD) MS [38,39]. Compared to APLD, desorption spray ionization (DESI) achieves better LODs for explosives [40] with the disadvantage of a more complex setup and the need of a liquid solvent supply. The LOD for TNT with DESI is about 10 fg. The achieved LODs for amphetamine using DESI is about 14 ng compared to 20 ng using APLD [41]. The low-temperature plasma (LTP) probe [42] methodology behaves similarly to DESI by also achieving a better limit of detection for explosives, but still with the need of a more complex setup due to the additional gas supply. For tetryl, the LOD of this technique was 0.25 ng. DART-TD-MS [43] is mostly comparable to APLD related to explosives and drugs. While the LOD for (3,4-methylendioxy-methamphetamine) hydrochloride (MDMA) is slightly better than that for DART with 2 ng compared to 10 ng, respectively, both systems can detect 2 ng tetryl. Raman spectroscopy in combination with an advanced swab system achieve a LOD of about 5 ng of 2,4-DNT, whereas APLD can measure down to 1.5 ng. Moreover, Raman detection limits for cocaine-hydrochloride [44] can be found at about 1 µg whereas APLD achieves a LOD of 17 ng. According to the author, this high LOD is due to the low analyte cross section and affects all Raman measurements [36]. Ion mobility spectrometry is capable of detecting 350 pg total amount of TNT and 5 ng of cocaine. TD MS allows for the detection of 5 ng of TNT while APLD can detect 500 pg. For cocaine [45], a LOD of 388 ng and 2 ng for MDMA [38] is reported.

Table 3. Comparison of LOD of different analytical techniques to APLD for explosives and drugs. DART-TD-MS = Direct analyses in real time-thermal desorption-mass spectrometry.

Compared Analytical Technique	Measured Substance	LOD Ref. Technique/ng	LOD APLD/ng
Raman spectroscopy	2,4-DNT	5	1.5
	Cocaine HCl	1000	17
Ion mobility spectrometry	TNT	0.35	0.5
	Cocaine HCl	5	5
Thermal desorption MS	TNT	5	0.5
	Cocaine HCl	388	17
	MDMA	2	10
Desorption spray ionization	TNT	10 fg	0.5
	Amphetamine	14	20
Low-temperature plasma probe	Tetryl	0.25	2
DART-TD-MS	Tetryl	2	2
	MDMA	2	10

4. Conclusions

Within this study, we successfully showed the performance of an improved APLD setup. Various parameters, such as temperature of sampling, desorption area, or desorption head material were modified, while retaining easy handling and flexibility of the system. The novel system showed improved LODs, which are significantly below the original APLD approach and mostly comparable to other atmospheric pressure ionization methods or spectroscopic techniques. The LOD, at laboratory measurements, was 0.5 ng for trinitrotoluene, 17 ng for cocaine hydrochloride, and 6 ng for ketamine, to mention only some of the tested materials.

In particular, the investigation of real-world scenarios exhibited the capabilities of the flexible laser desorption sampling, the soft chemical ionization, and fast ion-trap mass spectrometric detection.

This allows detection of TNT on bomb shell residues and residues of a new psychoactive substance on the inside of its package.

Furthermore, the system was extended by a unit for the automatized investigation of surfaces by mapping individual pixels. Consequently, the manual laser desorption sampling is no longer required for such surfaces, which improves systematic mapping capabilities.

In summary, APLD with an improved sampling does not require pretreatment of the surface and rapidly exploits a chemical profile. Therefore, it gives indices for conclusions of first responders or at onsite screening operations. By choosing an appropriate transferline length, better LODs or more flexibility can be achieved, depending on the scenario.

For further investigations, cross-sensitivities as well as high throughput behavior would be interesting. In addition, an attempt could be made to use the mapping capability at ambient conditions to scan thin layer chromatography plates, for example, to separate isomeric compounds that are difficult for exclusively MS-based approaches. The use of a more mobile and flexible MS could be beneficial for highly mobile application scenarios if the inherent restrictions in system performance are acceptable. Therefore, APLD in combination with a portable ion trap [46] is promising.

Supplementary Materials: The following are available online at http://www.mdpi.com/2076-3417/8/6/933/s1. LabVIEW script for generated heat map, used in Figure 5.

Author Contributions: J.H. and R.R. conceived and designed the experiments; J.H. and R.R. performed the experiments; R.R. analyzed the data; M.P. and T.F. contributed reagents, samples, measurement tools, and expert knowledge for those; R.R. wrote the paper; S.E. and R.Z. contributed significantly to the discussion and revision.

Acknowledgments: This investigation was performed within the SEMFreS project funded by the Federal Ministry of the Interior (BMI) and the Federal Office of Civil Protection and Disaster Assistance, FP406 "SEMFreS". We want to especially thank the German Federal Criminal Police Office (BKA) for providing the samples and the opportunity of a measurement campaign with real samples in Wiesbaden.

Conflicts of Interest: The authors declare no conflict of interest. The founding sponsors had no role in the design of the study; in the collection, analyses, or interpretation of data; in the writing of the manuscript, and in the decision to publish the results.

References

1. Boumsellek, S.; Alajajian, H.; Chutjian, A. Negative-Ion formation in the explosives RDX, PETN, and TNT by using the reversal electron attachment detection technique. *J. Am. Soc. Mass Spectrom.* **1992**, *3*, 243–247. [CrossRef]
2. Gielsdorf, W. Identifizierung einiger Sprengstoffe mit Hilfe spezieller GC/MS-Techniken, insbesondere der PPNICI-Methode. *Fresenius Z. Anal. Chem.* **1981**, *308*, 123–128. [CrossRef]
3. Gillis, R.G. Chemical ionisation mass spectra of explosives. *Org. Mass Spectrom.* **1974**, *9*, 359–364. [CrossRef]
4. Pate, C.T.; Mach, M.H. Analysis of explosives using chemical ionization mass spectroscopy. *Int. J. Mass Spectrom. Ion Phys.* **1978**, *26*, 267–277. [CrossRef]
5. Wu, Y.-H.; Lin, K.-L.; Chen, S.-C.; Chang, Y.-Z. Integration of GC/EI-MS and GC/NCI-MS for simultaneous quantitative determination of opiates, amphetamines, MDMA, ketamine, and metabolites in human hair. *J. Chromatogr. B Anal. Technol. Biomed. Life Sci.* **2008**, *870*, 192–202. [CrossRef] [PubMed]
6. Yinon, J.; McClellan, J.E.; Yost, R.A.; Lifshitz, C. Electrospray ionization tandem mass spectrometry collision-induced dissociation study of explosives in an ion trap mass spectrometer. *Rapid Commun. Mass Spectrom.* **1997**, *11*, 1961–1970. [CrossRef]
7. March, R.E. An Introduction to Quadrupole Ion Trap Mass Spectrometry. *J. Mass Spectrom.* **1997**, *32*, 351–369. [CrossRef]
8. Schramm, E.; Sklorz, M.; Zimmermann, R.H. Verfahren und Vorrichtung für den Nachweis von Organischen Spurenbestandteilen auf Oberflächen. Patent No. DE102007045361, 22 September 2007.
9. Nilles, J.M.; Connell, T.R.; Stokes, S.T.; Dupont Durst, H. Explosives Detection Using Direct Analysis in Real Time (DART) Mass Spectrometry. *Propellants Explos. Pyrotech.* **2010**, *35*, 446–451. [CrossRef]
10. Rowell, F.; Seviour, J.; Lim, A.Y.; Elumbaring-Salazar, C.G.; Loke, J.; Ma, J. Detection of nitro-organic and peroxide explosives in latent fingermarks by DART- and SALDI-TOF-mass spectrometry. *Forensic Sci. Int.* **2012**, *221*, 84–91. [CrossRef] [PubMed]

11. Bridoux, M.C.; Schwarzenberg, A.; Schramm, S.; Cole, R.B. Combined use of direct analysis in real-time/Orbitrap mass spectrometry and micro-Raman spectroscopy for the comprehensive characterization of real explosive samples. *Anal. Bioanal. Chem.* **2016**, *408*, 5677–5687. [CrossRef] [PubMed]
12. Chen, C.-H.; Lin, Z.; Garimella, S.; Zheng, L.; Shi, R.; Cooks, R.G.; Ouyang, Z. Development of a mass spectrometry sampling probe for chemical analysis in surgical and endoscopic procedures. *Anal. Chem.* **2013**, *85*, 11843–11850. [CrossRef] [PubMed]
13. Justes, D.R.; Talaty, N.; Cotte-Rodriguez, I.; Cooks, R.G. Detection of explosives on skin using ambient ionization mass spectrometry. *Chem. Commun.* **2007**, 2142–2144. [CrossRef] [PubMed]
14. Mirabelli, M.F.; Coviello, G.; Volmer, D.A. Determining fatty acids by desorption/ionization mass spectrometry using thin-layer chromatography substrates. *Anal. Bioanal. Chem.* **2015**, *407*, 4513–4522. [CrossRef] [PubMed]
15. Matthews, B.; Walker, G.S.; Kobus, H.; Pigou, P.; Bird, C.; Smith, G. The analysis of dyes in ball point pen inks on single paper fibres using laser desorption ionisation time of flight mass spectrometry (LDI-TOFMS). *Forensic Sci. Int.* **2011**, *209*, e26–e30. [CrossRef] [PubMed]
16. Karas, M.; Bachmann, D.; Hillenkamp, F. Influence of the Wavelength in High-Irradiance Ultraviolet Laser Desorption Mass Spectrometry of Organic Molecules. *Anal. Chem.* **1985**, *57*, 2935–2939. [CrossRef]
17. Zhang, M.; Shi, Z.; Bai, Y.; Gao, Y.; Hu, R.; Zhao, F. Using molecular recognition of beta-cyclodextrin to determine molecular weights of low-molecular-weight explosives by MALDI-TOF mass spectrometry. *J. Am. Soc. Mass Spectrom.* **2006**, *17*, 189–193. [CrossRef] [PubMed]
18. Silina, Y.E.; Koch, M.; Volmer, D.A. The role of physical and chemical properties of Pd nanostructured materials immobilized on inorganic carriers on ion formation in atmospheric pressure laser desorption/ionization mass spectrometry. *J. Mass Spectrom.* **2014**, *49*, 468–480. [CrossRef] [PubMed]
19. Compton, L.R.; Reschke, B.; Friend, J.; Powell, M.; Vertes, A. Remote laser ablation electrospray ionization mass spectrometry for non-proximate analysis of biological tissues. *Rapid Commun. Mass Spectrom.* **2015**, *29*, 67–73. [CrossRef] [PubMed]
20. Lorenz, M.; Ovchinnikova, O.S.; Kertesz, V.; Van Berkel, G.J. Laser microdissection and atmospheric pressure chemical ionization mass spectrometry coupled for multimodal imaging. *Rapid Commun. Mass Spectrom.* **2013**, *27*, 1429–1436. [CrossRef] [PubMed]
21. Roy-Lachapelle, A.; Solliec, M.; Sinotte, M.; Deblois, C.; Sauvé, S. High resolution/accurate mass (HRMS) detection of anatoxin-a in lake water using LDTD-APCI coupled to a Q-Exactive mass spectrometer. *Talanta* **2015**, *132*, 836–844. [CrossRef] [PubMed]
22. Morrical, B.D.; Fergenson, D.P.; Prather, K.A. Coupling two-step laser desorption/ionization with aerosol time-of-flight mass spectrometry for the analysis of individual organic particles. *J. Am. Soc. Mass Spectrom.* **1998**, *9*, 1068–1073. [CrossRef]
23. Weickhardt, C.; Kaiser, N.; Borsdorf, H. Ion mobility spectrometry of laser desorbed pesticides from fruit surfaces. *Int. J. Ion Mobil. Spectrom.* **2012**, *15*, 55–62. [CrossRef]
24. Bermúdez, C.; Cabezas, C.; Mata, S.; Berdakin, M.; Tejedor, J.M.; Alonso, J.L. Analysis of illicit drugs by direct ablation of solid samples. *Eur. J. Mass Spectrom.* **2015**, *21*, 775–781. [CrossRef] [PubMed]
25. Morgan, J.S.; Bryden, W.A.; Miragliotta, J.A.; Aamodt, L.C. Improved Detection of Explosive Residues by Laser Thermal Desorption. *Johns Hopkins APL Tech. Digest* **1999**, *20*, 389–395.
26. Sabo, M.; Malásková, M.; Matejčík, Š. Laser desorption with corona discharge ion mobility spectrometry for direct surface detection of explosives. *Analyst* **2014**, *139*, 5112–5117. [CrossRef] [PubMed]
27. Östmark, H.; Wallin, S.; Ang, H.G. Vapor Pressure of Explosives: A Critical Review. *Propellants Explos. Pyrotech.* **2012**, *37*, 12–23. [CrossRef]
28. Dindal, A.B.; Jenkins, R.A.; Buchanan, M.V.; Bayne, C.K. Determination of cocaine and heroin vapor pressures using commercial and illicit samples. *Analyst* **2000**, *125*, 1393–1396. [CrossRef] [PubMed]
29. Li, L.; Lubman, D.M. Pulsed laser desorption method for volatilizing thermally labile molecules for supersonic jet spectroscopy. *Rev. Sci. Instrum.* **1988**, *59*, 557. [CrossRef]
30. Ehlert, S.; Walte, A.; Zimmermann, R. Ambient pressure laser desorption and laser-induced acoustic desorption ion mobility spectrometry detection of explosives. *Anal. Chem.* **2013**, *85*, 11047–11053. [CrossRef] [PubMed]

31. Ehlert, S.; Hölzer, J.; Rittgen, J.; Pütz, M.; Schulte-Ladbeck, R.; Zimmermann, R. Rapid on-site detection of explosives on surfaces by ambient pressure laser desorption and direct inlet single photon ionization or chemical ionization mass spectrometry. *Anal. Bioanal. Chem.* **2013**, *405*, 6979–6993. [CrossRef] [PubMed]
32. Lamb, A.; Tollefson, E.L. Catalytic reduction of nitric oxide in low concentration high velocity gas streams. *Can. J. Chem. Eng.* **1973**, *51*, 191–200. [CrossRef]
33. Ford, L.T.; Berg, J.D. 1-Adamantylamine a simple urine marker for screening for third generation adamantyl-type synthetic cannabinoids by ultra-performance liquid chromatography tandem mass spectrometry. *Ann. Clin. Biochem.* **2016**, *53*, 640–646. [CrossRef] [PubMed]
34. So, P.-K.; Ng, T.-T.; Wang, H.; Hu, B.; Yao, Z.-P. Rapid detection and quantitation of ketamine and norketamine in urine and oral fluid by wooden-tip electrospray ionization mass spectrometry. *Analyst* **2013**, *138*, 2239–2243. [CrossRef] [PubMed]
35. Asada, A.; Doi, T.; Tagami, T.; Takeda, A.; Satsuki, Y.; Kawaguchi, M.; Nakamura, A.; Sawabe, Y. Cannabimimetic activities of cumyl carboxamide-type synthetic cannabinoids. *Forensic Toxicol.* **2017**, *31*, 44. [CrossRef]
36. Gong, Z.; Du, H.; Cheng, F.; Wang, C.; Wang, C.; Fan, M. Fabrication of SERS swab for direct detection of trace explosives in fingerprints. *ACS Appl. Mater. Interfaces* **2014**, *6*, 21931–21937. [CrossRef] [PubMed]
37. Sabo, M.; Malásková, M.; Matejčík, Š. Ion mobility spectrometry–mass spectrometry studies of ion processes in air at atmospheric pressure and their application to thermal desorption of 2,4,6-trinitrotoluene. *Plasma Sources Sci. Technol.* **2014**, *23*, 15025. [CrossRef]
38. Forbes, T.P.; Staymates, M.; Sisco, E. Broad spectrum infrared thermal desorption of wipe-based explosive and narcotic samples for trace mass spectrometric detection. *Analyst* **2017**, *142*, 3002–3010. [CrossRef] [PubMed]
39. Zhao, Q.; Liu, J.; Wang, B.; Zhang, X.; Huang, G.; Xu, W. Rapid screening of explosives in ambient environment by aerodynamic assisted thermo desorption mass spectrometry. *J. Mass Spectrom.* **2017**, *52*, 1–6. [CrossRef] [PubMed]
40. Green, F.M.; Salter, T.L.; Stokes, P.; Gilmore, I.S.; O'Connor, G. Ambient mass spectrometry: Advances and applications in forensics. *Surf. Interface Anal.* **2010**, *42*, 347–357. [CrossRef]
41. Stojanovska, N.; Kelly, T.; Tahtouh, M.; Beavis, A.; Fu, S. Analysis of amphetamine-type substances and piperazine analogues using desorption electrospray ionisation mass spectrometry. *Rapid Commun. Mass Spectrom.* **2014**, *28*, 731–740. [CrossRef] [PubMed]
42. Garcia-Reyes, J.F.; Harper, J.D.; Salazar, G.A.; Charipar, N.A.; Ouyang, Z.; Cooks, R.G. Detection of explosives and related compounds by low-temperature plasma ambient ionization mass spectrometry. *Anal. Chem.* **2011**, *83*, 1084–1092. [CrossRef] [PubMed]
43. Sisco, E.; Forbes, T.P.; Staymates, M.E.; Gillen, G. Rapid Analysis of Trace Drugs and Metabolites Using a Thermal Desorption DART-MS Configuration. *Anal. Methods: Adv. Methods Appl.* **2016**, *8*, 6494–6499. [CrossRef] [PubMed]
44. Sägmüller, B.; Schwarze, B.; Brehm, G.; Trachta, G.; Schneider, S. Identification of illicit drugs by a combination of liquid chromatography and surface-enhanced Raman scattering spectroscopy. *J. Mol. Struct.* **2003**, *661–662*, 279–290. [CrossRef]
45. Demoranville, L.T.; Brewer, T.M. Ambient pressure thermal desorption ionization mass spectrometry for the analysis of substances of forensic interest. *Analyst* **2013**, *138*, 5332–5337. [CrossRef] [PubMed]
46. Gao, L.; Song, Q.; Patterson, G.E.; Cooks, R.G.; Ouyang, Z. Handheld rectilinear ion trap mass spectrometer. *Anal. Chem.* **2006**, *78*, 5994–6002. [CrossRef] [PubMed]

9.3.3 Publication 3

Comparison of three analytical methods for the on-site analysis of traces at clandestine drug laboratories

Published by

René Reiss, Frank Hauser, Sven Ehlert, Michael Pütz and Ralf Zimmermann

Science & Justice
Submitted

Comparison of three analytical methods for the on-site analysis of traces at clandestine drug laboratories

René Reiss (1)[+], Frank Hauser (2)[+], Sven Ehlert (1)*, Michael Pütz (2) and Ralf Zimmermann (1,3)

[+]: Co-first authorship

1 Joint Mass Spectrometry Centre, Chair of Analytical Chemistry, University of Rostock, Dr.-Lorenz-Weg 2, 18059 Rostock, Germany

2 Bundeskriminalamt-Federal Criminal Police Office (BKA), Forensic Science Institute, Äppelallee 45, 65203 Wiesbaden, Germany

3 Joint Mass Spectrometry Centre, Comprehensive Molecular Analytics, Helmholtz Zentrum München, Ingolstädter Landstr. 1, 85764 Neuherberg, Germany

* Correspondence: sven.ehlert@uni-rostock.de; Tel.: +49-381-498-6532

Declarations of interest: none

Highlights:

- All techniques obtained good results for within their limitations
- Obtainable information varies strongly for investigates samples
- Detection of MDMA and amphetamine from real samples with all techniques possible

1. Abstract

Amphetamine-type stimulants are the most prevalent drug class in Europe after cannabis and cocaine. Seizure data reveal that the production of amphetamine mainly takes place at large-scale clandestine laboratories. While fast and reliable analytical results are crucial for first responders to make adequate decisions, these can be difficult to establish, especially at large-scale clandestine laboratories. To overcome this issue, multiple techniques at different levels of complexity are available. These techniques require different skill levels and training, ranging from a short introduction to several weeks of training for highly sophisticated systems. Beside the level of complexity their information value differs as well. Within this publication, a comparison between three techniques that can be applied for on-site analysis is performed. These techniques range from ones with a simple yes or no response to sophisticated ones that allows to receive complex information about a sample. The three evaluated techniques are immunoassay drug tests representing easy to handle and fast to explain systems, ion mobility spectrometry as state of the art equipment that needs training and experience prior to use and ambient pressure laser desorption with the need for a highly skilled operator as possible future technique that is currently under development. Beside the measurement of validation parameters, real case samples are investigated to obtain practically relevant information about the capabilities and limitations of these techniques for on-site operations. These real case samples include surface samples of different spots at a former clandestine 3,4-methylenedioxy-N-methamphetamine (MDMA) laboratory and synthesis waste from an amphetamine-contaminated glassware. Results demonstrate that in general all techniques deliver valid results, but the bandwidth of information widely varies between the investigated techniques.

Keywords:
amphetamine; MDMA; precursor; method comparison; on-site; clandestine laboratory

2. Introduction

Drugs like amphetamine, methamphetamine or 3,4-methylenedioxy-N-methamphetamine (MDMA) are known as amphetamine-type stimulants (ATS) [1]. Based on reported seizures, they are the most prevalent drugs after cannabis and cocaine in Europe [2]. Especially amphetamines and MDMA are predominantly found in northern and eastern Europe [2]. While most of the amphetamine production takes place in Belgium, the Netherlands and Poland, methamphetamine is mainly produced in the Czech Republic [2]. For MDMA, the main production takes place in the Netherlands and Belgium [2]. The most common synthesis route for the illicit production of amphetamine is the Leuckart method [3]. The preferred production method of methamphetamine is the Nagai route and the production via Birch reduction [3]. While the usage of the Leuckart method for MDMA is known, most frequently the reductive amination with methylamine, hydrogen and platinum dioxide catalyst is utilized [3]. Amphetamine is usually produced from the precursor phenylacetone (BMK or benzyl methyl ketone) [3]. In the case of methamphetamine, ephedrine and pseudoephedrine is a common choice [3]. For MDMA, piperonyl methyl ketone (PMK) is chosen frequently [3]. In order to circumvent the transport of scheduled precursor chemicals like BMK, producers started to utilize non-scheduled pre-precursors [2]. This is done, because most pre-precursors are not “scheduled” monitored. As the first step, a pre-precursor is converted to the needed precursor that is afterwards applied to produce the drug itself. In recent years, one of the most relevant pre-precursors turned out to be alpha-phenylacetoacetonitrile (APAAN) [4]. APAAN is converted into BMK which is then utilised to produce amphetamine. These pre-precursors extend the possible compounds that can be found at clandestine laboratories. Therefore, interpretation of results is aggravated. This in turn, can imply the need for powerful analytical techniques in order to keep pace. In general, the investigation of clandestine laboratories is highly complex, since every laboratory has a unique setup. Examples of these differences can be different equipment to synthesise drugs, purities of chemicals and solvents, carefulness of the producers, size and complexity of the laboratory itself and many more. Especially for amphetamine, large-scale productions are frequently observed which is supported by seizure data of amphetamine freebase in multiple countries, that originates from the Netherlands [4]. Due to this large-scale laboratory size, on-site assessment at clandestine laboratories becomes more difficult as the number of samples and their complexity, based on the diverse nature of the target compounds, increase as well. This applies particularly to inactive laboratories that are no longer in use and evidence of a former usage must be proven by taking samples from multiple surfaces. Another reason why trace analysis can be important, is to get quick information about worktops at laboratory storage sites if they are contaminated. This can be a necessary step of self-protection prior to crime scene investigations if highly potent and in non-visible amounts fully active drugs could be present. Some well-known techniques suitable for on-site analysis, are immunoassay drug tests (IDT) [5], tabletop nuclear magnetic resonance (NMR) spectroscopy [6], raman spectroscopy [7], infrared (IR) spectroscopy [8], ion mobility spectrometry (IMS) [9] and mass spectrometry (MS) [10]. While IR, NMR and raman spectroscopy are able to analyse known and unknown target compounds, their need for visible amounts of the target compound makes them unsuitable for trace analysis. Therefore, these techniques are not considered for the current evaluation and subsequent IDT, IMS and ambient pressure laser desorption hyphenated mass spectrometry (APLD-MS) are investigated. In addition, these techniques can be seen as representatives for other techniques of a similar complexity in each case. IDTs are fast to use, lightweight and straightforward. They are a well-established method and frequently used at laboratories, driver controls and can even be used by

unskilled persons at workplaces [5]. Furthermore, they enable a fast, easy to use and affordable analysis for specific target compounds. In addition, the result interpretation is straightforward. Possible drawbacks are, that mainly sum-parameters results are measured and a linear increase in cost and time if multiple samples should be analysed. IMS with thermal desorption represents portable state-of-the-art tools for surface analysis. It is an approved technique, which is applied for a long time, benefits from fast analysis time and is capable of detecting even traces of a target compound. Most relevant drawbacks are a low resolution, which leads to relative high false alert rates and easy overload which leads to time intensive cleaning [11]. Current research for on-site equipment is done in the field of direct desorption MS [9]. Within this field, the coupling of a desorption unit and an MS creates a system that combines benefits from both techniques. While a direct desorption allows for fast sample throughput, the MS enables the investigation of complex samples. For this coupling, multiple techniques are under investigation. In addition, some of these systems also allow to directly investigate suspicious surfaces. This further speeds up sample throughput and allow for spatially resolved surface investigations. The possibility to investigate only small areas of a given surface and bypass sampling swabs, also allows impression/mark preserving analysis to allow further investigations later on. This work focuses on the coupling of MS with laser desorption at ambient pressure, because no auxiliary media, such as gases or liquids, are needed and former research indicates the usefulness of this technique for such applications [removed due to journal double-blind policy] [12–14]. In addition, APLD-MS as the third technique for on-site detection, is seen as an example of a possible future technique that could be implemented for routine analysis and demonstrated promising results at this field of application. While all three techniques were examined for these target compounds, literature lacks of direct comparisons of on-site samples and practical evaluation over different technology levels. Therefore the aim of this publication is to compare IDT, IMS and APLD-MS for trace analysis of amphetamine, methamphetamine and MDMA, intermediates, such as N-formylamphetamine (NFA) that are carried over to the main product [3] and drug precursors in clandestine laboratories. The limits of detection (LODs) were determined, real case scenario samples from former drug synthesis and seized clandestine laboratories are investigated. These samples demonstrate target analytes on complex matrices, resulting from on-site sampling. These real case scenarios aim to support the comparability of the investigated techniques on-site.

3. Materials and methods

3.1. Chemicals

The following substances were obtained from the German Federal Criminal Police Office (BKA, Wiesbaden, Germany): 2-phenylacetoacetonitrile, amphetamine sulphate, ephedrine hydrochloride, amphetamine base, NFA, PMK, methamphetamine, MDMA hydrochloride and amphetamine synthesis wastes. BMK was purchased from Sigma-Aldrich (St Louis, USA). Caffeine was bought from Alfa Aesar (Karlsruhe, Germany). All analytes were dissolved in methanol from Carl Roth GmbH + Co. KG (Karlsruhe, Germany). Methane 4.5 as chemical ionisation (CI) reactant gas for MS and helium 5.0 were bought from Linde AG (Berlin, Germany).

3.2. Sampling swabs

Sampling swabs are used for all measurements except for the LOD determination with drug test kits. For all other measurements Teflon sampling swabs from Smiths Detection Inc. (Wiesbaden, Germany) were used as sample tool.

3.3. Drug test kits

The applied drug test kits are called “Drugwipe 2” from Securetec Detektions-Systeme AG (Brunnthal, Germany). Tests were conducted according to the producer’s instruction. LODs were determined by placing 1 µl of analyte at the sampling surface of the test kit. For practical samples, the test kit was wiped over the surface according to the producer’s instruction. Results were interpreted optically under day light.

3.4. IMS

The IMS measurements were conducted with an Ionscan 500 DT version 3.05.031, build by Smiths Detection Inc. (Wiesbaden, Germany). Version of the operation system is 6.0. Applied parameters are a drift tube flow of 300 ml/min, a desorber temperature of 245 °C, a positive drift tube voltage of 1577 V and ambient pressure of 1020 hPa. Sampling was done in positive mode, according to the recommendation of the manufacturer. Therefore, the sampling swab was inserted in the IMS and the measurement was started via software. This was done for LOD determination and practical sample measurement. For all samples, the cleanliness of the IMS was tested prior to a measurement with a clean sample swab. If contaminations from previous measurements were detected, the device was cleaned and tested again.

3.5. APLD-MS

A 445 nm laser diode NDB7875 from Nichia (Tokushima, Japan) was applied for desorption with a surface power input of 0.98 W. The laser was operated in continuous wave (CW) mode. Mass spectra were acquired utilizing a Varian Inc. (Walnut Creek, USA) ion trap 240-MS. Laser light is transferred from the laser to the ambient pressure desorption head with a 1250 µm Optran UV laser fibre from CeramOptec GmbH (Bonn, Germany). The ambient pressure desorption head was self-build and made out of brass and polytetrafluoroethylene for thermal separation. A detailed schematic of the APLD and its parts is available in a previous publication [removed due to journal double-blind policy] [12].

The procedure to analyse a sample, was to place a sample in front of the APLD and activate the laser while the MS is active. The APLD system was heated to 200°C with a flow rate of 3 ml/min helium. All compounds were analysed with positive polarity mode. Methane as reactant gas is used for chemical ionization generating primarily protonated quasi molecular ions. For practical sample measurement, settings are the same as for LOD measurements.

3.6. Determination of limits of detection + sampling of real case samples

For LOD determination, one microliter of a diluted analyte solution was dropped on a sampling swab surface to prepare a sample. The pure substance was diluted with methanol to the needed concentration. After the solvent evaporated, the residue carrying surface was analysed.

For the real case samples, sampling swabs were wiped three times over the suspicious surface with a sampling length of about 0.1 m each. Sampling swabs were prepared for every technique and stored afterwards, sealed in reusable plastic bags, inside a refrigerator until analysis.

4. Results and Discussion

4.1. Method comparison

One major parameter for a comparison is the possibility to detect target compounds. For the investigated target compounds there is a clear trend for the three investigated methods. Drug test kits are only capable of detecting compounds that they are specifically made for. In this case, amphetamine, methamphetamine and MDMA. Comparted to IDTs, IMS systems are more flexible and allow to detect a broader range of analytes. The ability to ionise target compounds is the main limitation for IMS systems, valid for e.g. BMK. In this study, all target compounds had been detected successfully with APLD-MS. Like IMS, MS is limited to analytes that can be ionised. Due to the utilized chemical ionization method, this technique is capable to analyse a wide variety of substances. This leads to the observation, that the APLD-MS can detect the highest number of compounds.

The parameter selectivity is of interest as well as it influences the possible field of application. While drug test kits are made to investigate if a number of target compounds are present, no information can be gathered on what specific substance triggered a positive signal. In addition, every new target compound that should be investigated needs a new test kit. In theory, IMS is capable to distinguish different possible substances. Practically, the low resolution of most IMS makes it difficult to distinguish between similar compounds and for the same reason, the presence of multiple substances can be an issue, too. In contrast to drug test kits, IMS libraries can be updated to detect new target compounds. The most selective system in this study, even for multiple substances present, is the APLD-MS. It allows to identify target compounds and even unknown substances can be presumed, based on the mass spectra.

Another major parameter is the complexity of the analytical technique and its user requirements. Drug test kits are very compact, cheap, easy to handle and require only knowledge about possible cross reactions and contraindications. IMS in comparison, needs significant set-up time previous to a measurement, is considerably larger, orders of magnitude more expensive in acquisition and needs trained personal for operation. In addition, many IMS utilize a Ni^{63}-source and thus may require radiation protection trained personal. As many on-site measurements were done for target compounds that can be found in a system-integrated library, result interpretation is done by the device and hence no addition training is needed for the operator. APLD-MS needs a well-trained operator, electricity and pressurised gases. Its set-up time is higher compared to IMS and the operator’s knowledge needs to be the highest of all three methods. The operators training is

needed for performing measurements as well as interpreting obtained results. Therefore, APLD-MS is the most sophisticated system that was investigated.

Beside the above discussed set-up time, duration per measurement, as another parameter, is especially relevant for larger operations and time critical activities. According to the conducted experiments, the highest sample throughput is achievable for IMS. It took about eight seconds to perform one measurement. APLD-MS needed about 30-60 seconds to obtain results. The longest time was necessary for the drug test kit. About three minutes passed before the enzymatic reaction was concluded. Depending on the sample number and available staff, parallel testing could decrease this time to a certain extend and change the necessary total time. These results imply, that the sample amount was adequate and no overload occurred. This overload is imaginable for real samples with unknown concentration, especially at on-site measurements. This additional cleaning affects only IMS and APLD-MS because drug test kits are only used once. In addition, the possibility of IDTs to analyse two or more drugs at once should be mentioned as well.

4.1.1. Limits of detection

Table 1: Total LOD of all investigated substances for all investigated methods. Two bars mean no LOD determinable.

Substance name	LOD enzymatic test kits / ng	LOD IMS / ng	LOD APLD-MS / ng
Amphetamine base	2	2	20
Amphetamine sulphate	2	2	10
MDMA HCl	2	5	21
Methamphetamine	2	1	11
APAAN	--	5	10
Ephedrine HCl	--	1	6
NFA	--	9	9
BMK	--	--	11
PMK	--	--	6

Drug test kits

The investigated drug test kits are designed to detect amphetamine, methamphetamine and MDMA. Therefore these test kits are a suitable example to examine the chosen target compounds. The information gathered from a measurement is that one of the investigated substances is present or not. No statement is made what specific target compound is found if a positive result is obtained. To gain further information about the capabilities of these test kits, the LOD was determined for amphetamine, methamphetamine and MDMA separately. The results of Table 1 reveal that clear visible indication is possible down to 2 ng total target compound. In some cases, lower substance amounts down to 1 ng resulted in positive

signals as well, but were discarded due to the inconsistency of the results. In addition, all three substances yielded the same LOD. This is interesting because in most cases at on-site analysis this test only informs about a sum parameter. The knowledge that all investigated compounds can be detected at a similar amount eases the practical use for first responders. Cross reactions were tested with all listed drug precursors and caffeine. No false positive results were obtained up to the investigated limit of one thousand times the LOD (2000 ng) per substance.

IMS

The chosen IMS is mobile and needs only electricity for operation. Therefore, it is suitable for on-site analysis of suspicious surfaces. To achieve practically relevant LODs, Table 1 shows the lowest total amount of substance that was necessary to trigger an alert. The alert itself was trigger for signal to noise ratios of S/N ≥ 10. This procedure was chosen, because most first responders are no analytical chemists and cannot interpret raw plasmagram data. LODs in the low nanogram range were obtained for all drugs and most drug precursors. Only BMK and PMK gave no response at all. For amphetamine it was investigated if the salt form, and therefore physical properties like vapour pressure, has an influence on the LOD. As Table 1 reveals, no such behaviour was observed. Therefore, the salt form seems to have negligible influence for the detectability by IMS.

APLD-MS

The MS does not have a specific trigger or detection alert for detected compounds, because it is a normal laboratory device. Therefore, the LODs are defined by a signal to noise ratio S/N of three. To obtain comparable results, the signal intensity was not extrapolated to a S/N of three, instead the LOD represents the lowest total amount of substance that was actually measured. The APLD was capable of detecting all investigated target compounds and the achieved LODs for all substances are in the same order of magnitude, ranging from 6 ng for PMK to 21 ng for MDMA HCl.

Besides APLD, there are other direct sampling techniques that benefit from a combination with MS such as direct analysis in real time (DART) [15], desorption spray ionization (DESI) [16], dielectric barrier discharge ionization (DBDI) [17], easy ambient sonic spray ionization (EASI) [18], infrared thermal desorption (TDIR) [10] and low-temperature plasma probe (LTP) [19]. Because of this, a comparison for the most prominent techniques is given in Table 2. These techniques are also under ongoing development and while all have their own strengths and weaknesses, all chosen techniques could be used to investigate the same samples. A noticeable difference of the compared techniques to APLD is the utilization of ambient pressure ionisation, compared to vacuum ionisation for APLD, resulting in potentially lower LODs and increased possible matrix effects. All of these techniques are compared for the total amount of detectable substance. However, comparison should be done with caution because the method to determine the LOD is not consistent for the mentioned techniques. Some, like APLD define the lowest actual detectable amount as LOD, others utilize a signal to noise ratio of S/N ≥ 3 for the LOD and some prefer regression analysis to calculate the LOD. None the less, with given caution a comparison still delivers useful information. When comparing DART and TDIR, both exhibit LODs that are comparable to APLD. DESI, DBDI and LTP allow ten to one thousand times better LODs and EASI reveal about one hundred times inferior LODs compared to APLD. Beside the LOD, system complexity is an important consideration for on-site investigations. For most techniques, complexity is contrary to the

observed LODs. APLD and TDIR only require a power source. LTP, DBDI and DART need further gas supply and the requirements for DESI, as well as EASI, are a power source, solvent and gas supply. Therefore, the most suitable technique depends, inter alia, from the investigated scenario and the therein needed LOD.

Table 2: Comparison of LOD of different analytical techniques to APLD for examined target compounds

Compared analytical technique	Measured substance	LOD ref. technique / ng	LOD APLD / ng
DART [15]	Amphetamine	1	10
	MDMA	0.75	21
DESI [16]	Amphetamine	0.14	10
	Methamphetamine	0.14	11
DBDI [17]	Amphetamine	0.01	10
EASI [18]	Amphetamine	3000	10
TDIR [10]	Methamphetamine	2	11
	MDMA	2	21
LTP [19]	MDMA	0.065	21

If, in summary, the LOD is compared between all investigated techniques, no major variations are observed. While drug test kits reveal the best overall LODs with 2 ng for all substances, IMS results are slightly higher and deviate between 1 ng for methamphetamine and 9 ng for NFA. In the utilized setup, APLD-MS obtained 2 ng to 21 ng and therefore about two to ten times higher LODs, compared to drug test kits.

4.1.2. Key parameters

To break down this comparison, the three analytical methods were compared based on eight key parameters. These parameters were the cost per measurement, acquisition cost, ease of use, ease of interpretation, possibility to implement new compounds, adaptability to sample shapes and types, measurement time and need for maintenance. Every technique was given a rating, corresponding to the capability in comparison with the other two techniques. These parameters intend to cover the major points that need to be considered for the application of these techniques in praxis. The possible values are minus for negative or worse, zero for neutral or in between and plus for positive or better, in contrast to the other techniques. Figure 1 illustrates this comparison in a graphical way. It displays the different focus areas of the three techniques and is in agreement with the other data presented. It exhibits that each technique has its strengths and weaknesses and that there is not a single technique that is suitable for all applications. The big advantage of the IDTs is their simple setup which makes them easy to use and also leads to low acquisition cost for a single kit. However, they are very limited in the compounds that they can detect and the cost per measurement is higher compared to the other two techniques. The IMS is in general a good all-rounder that has a big advantage in the measurement time and also the cost per measurement. The APLD-MS provides the most detailed report on a sample since it allows to identify and distinguish

substances based on their mass spectra profile. In addition, it detects the widest array of compounds. However, it is also the most expensive piece of equipment and requires extensive training. Future developments might reduce these limitations and allow for a wider application of this technique.

If only few samples should be analysed for amphetamine, methamphetamine or MDMA, IDTs could be the method of choice. In case that routine measurements are needed and the target compounds are limited to known compounds of a drug production, the use of IMS could be the method of choice. Assuming that complex samples need to be investigated, APLD-MS or another ambient MS technique can demonstrate its strengths.

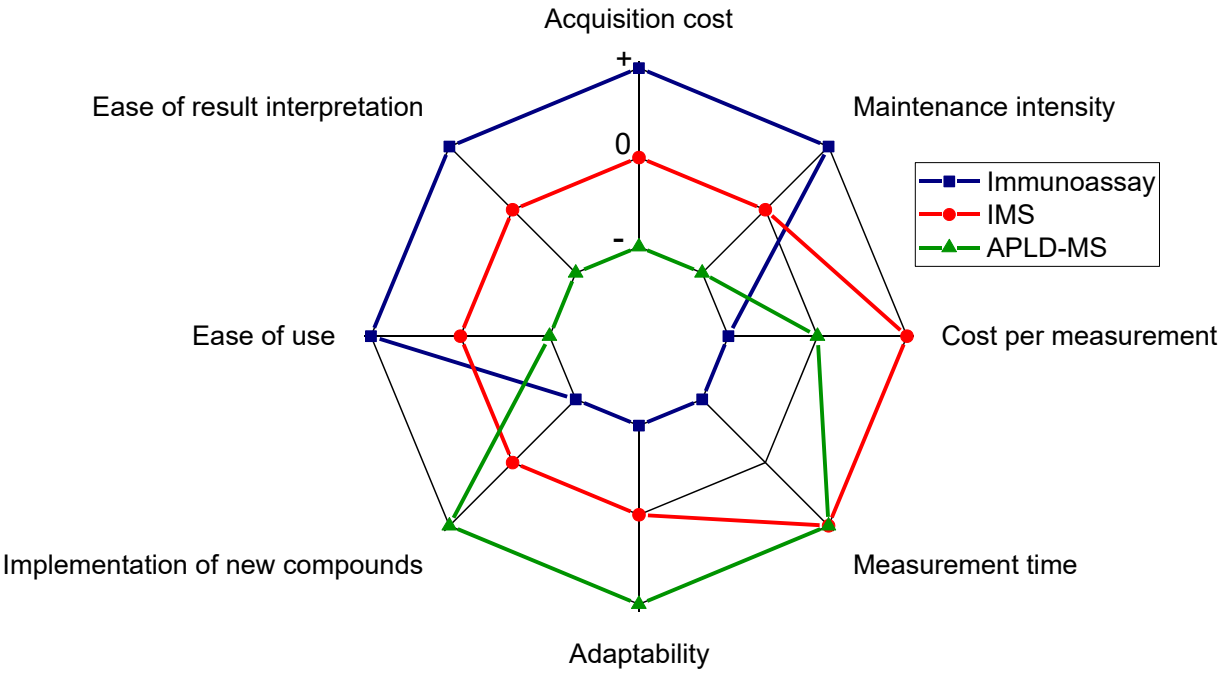

Figure 1: Visualisation of key parameters for the comparison of all three methods. Plus means positive or better, zero means neutral or in between and minus means negative or worse, in comparison to the other techniques.

4.2. Analysis of real samples

4.2.1. Samples from a former MDMA lab

To gain information about the capabilities of the tested techniques under real conditions, practical measurements were performed at a former clandestine MDMA laboratory. The clandestine laboratory and parts of the utilized equipment can be seen in Figure 2. Three different samples were acquired and analysed. Beside two spots from an actively used Büchner funnel and drying cabinet, one sample was obtained from the wall behind the equipment. This sample is particularly interesting because the laboratory was equipped with professional equipment allowing a less MDMA contaminating work flow during production, compared to amateur productions. At Figure 2 A), all sample spots, in the clandestine laboratory, are marked with red rectangles. Visual results of the IDT are drawn at Figure 2 B). While the drying cabinet and the Büchner funnel exhibit similar colour intensities, a lower colour intensity and therefore, lower concentration of MDMA was found for the wall

sample. Detection results of MDMA for IMS are plotted in Figure 2 C). Therein, the peak at around 9.8 ms is related to MDMA and exhibit similar concentrations for the wall sample and the drying cabinet. A higher concentration of MDMA was found for the Büchner funnel. This discrepancies can be explained due local variations in concentration at the surface of the drying cabinet and funnel. These variations are most likely based on the use of multiple sample swabs, applied at areas close together, which were necessary for the applied test procedure. At Figure 2 D), the positive CI mass spectra of the investigated surfaces are plotted. The measured concentration are in good agreement with the IDT results. The highest concentration of MDMA was found for the Büchner funnel, followed by the drying cabinet. The lowest concentration observed correlates to the wall sample.

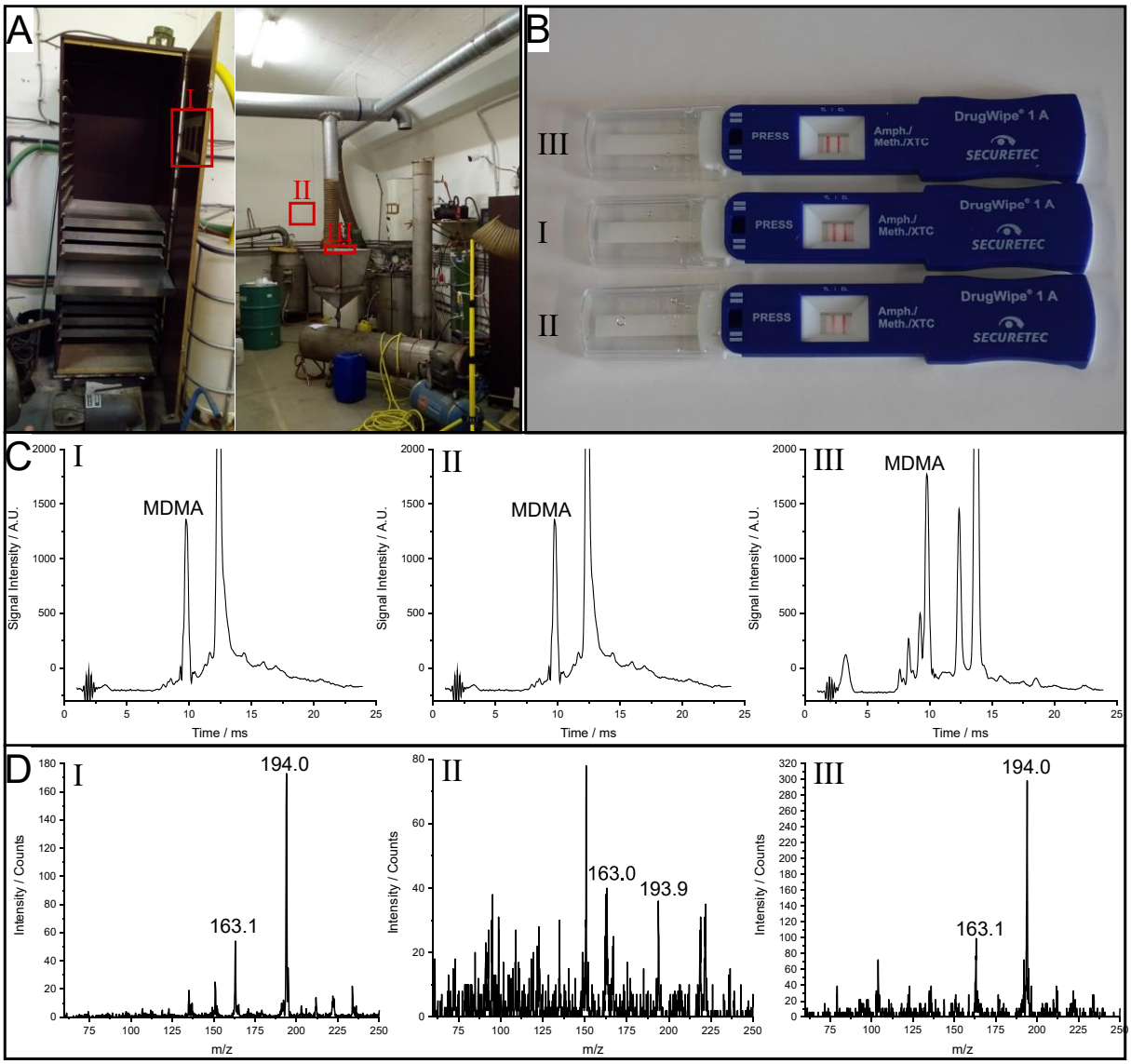

Figure 2: A) Sampling spots at a former clandestine MDMA laboratory in Germany. Sampled areas are (left to right): drying cabinet, wall and Büchner funnel, all marked with red rectangles. B) Positive IDTs of the sample areas indicated at A). Results are (from up to down): Büchner funnel, drying cabinet and wall. C) IMS measurements of the three sampling sports. The signal at around 9.8 ms is related to MDMA. IMS plasmagrams are in the following order (left to right): drying cabinet, wall and Büchner funnel. D) Positive CI mass spectra of the three sampling spots. The signal of 194 m/z is related to the molecular ion

peak [M+H] and 163 m/z corresponds to [M-HN-CH3]. Spectra are in the following order (left to right): drying cabinet, wall and Büchner funnel.

Table 3 summaries the results for the investigation of sample swabs from all three areas for the three investigated techniques. The measured concentration differs for IMS and APLD-MS. For IMS, the Büchner funnel yielded the highest signal intensities and similar intensities for the wall and the drying cabinet. APLD-MS measured the highest signal intensities for the drying cabinet, followed by the Büchner funnel and the lowest signals for the wall sample. Observed signal differences could be based on sampling variations, such as pressure applied to the sample swab or sampled area, MDMA surface concentration inhomogeneity or differences in sample transfer efficiency between pad and investigated surface. While the concentration of MDMA differs between the sample spots, positive detection was possible for all samples with all investigated methods. Therefore the LOD of all techniques seems to be sufficient for this practical scenario.

Table 3: Sampling swabs applied at different spots of a clandestine MDMA laboratory. All sampling swabs are examined for MDMA. Plus means positive detection.

Sample	Test Kit	IMS	APLD-MS
Drying cabinet	+	+	+
Büchner funnel	+	+	+
Wall	+	+	+

4.2.2. Amphetamine samples from contaminated glassware

Further practical measurement experience was gained, by analysing residues on equipment of an amphetamine synthesis. For this investigation the Leuckart method for synthesising amphetamine was chosen. This was done by a four step reaction [20–22]. First step was the conversion of APAAN into BMK with concentrated sulphuric acid and water. The generated, BMK containing, organic phase was afterwards mixed with formamide and formic acid, without purification (Leuckart step 1). The thereby generated, NFA containing, organic phase was once more utilized without further purification, and mixed with concentrated hydrochloric acid and neutralised after the reaction was finished (Leuckart step 2). Last step was the precipitation of amphetamine sulphate with the aid of sulphuric acid. In addition to both Leuckart step residues and accrued aqueous waste was investigated. For all three samples, the pre-precursor APAAN, the precursor BMK, the intermediate NFA and the product amphetamine were investigated. Table 4 summarises all observed results. For the first Leuckart step, only NFA was detected positively with IMS and APLD-MS. The other substances gave no signal, either due to low abundancy or because the technique is not suitable to analyse them. For the second Leuckart step, all three techniques were able to detect amphetamine. Additional traces of NFA were only detected with APLD-MS. Analysis of the aqueous waste resulted in positive detection of amphetamine for all three techniques. In comparison to this, BMK was found with APLD-MS only. While synthesis waste can be commonly found at clandestine laboratories, the executed measurements indicate that they

can be difficult to analyse on-site. The observed difficulties could be related to the complexity of the mixtures and the concentration differences of the analytes. Overall, IDTs were able to correctly detect amphetamine regarding to the laboratory analysis results. IMS was able to detect amphetamine and in addition, NFA at Leuckart step one. Most analytes were detected with APLD-MS, the observed analytes are amphetamine, NFA, and BMK. Therefore, these practical measurements indicate similar findings as the practical samples from chapter 4.2.1. Within the limitations of a technique, all techniques deliver useful information for the presence of target compounds. In addition, the more complex and sophisticated a setup is, the more information can be obtained.

Table 4: Sampling swabs applied at different glassware of an amphetamine. Two bars mean technically not detectable, plus means positive detection and minus means negative detection. All samples were measured once, due to limited samples.

Sample	**Test Kit**	**IMS**	**APLD-MS**
Aqueous waste Leuckart step 1			
APAAN	--	-	-
BMK	--	--	-
NFA	--	+	+
Amphetamine	-	-	-
Aqueous waste Leuckart step 2			
APAAN	--	-	-
BMK	--	--	-
NFA	--	+	+
Amphetamine	+	+	+
Aqueous waste Steam distillation			
APAAN	--	-	-
BMK	--	--	+
NFA	--	-	-
Amphetamine	+	+	+

5. Conclusion

For the investigation of target compound traces at clandestine laboratories, IDT, IMS and APLD-MS were compared. These three techniques represent different approaches for the on-site analysis of target compounds. IDTs are inexpensive and can be handled properly after a short briefing. The major drawback is the limitation to specific target compounds. IMS is capable of analysing multiple target compounds and more cost effective if many samples should be analysed. Drawbacks are the higher device acquisition costs and the need for a trained operator. Ambient MS is capable of analysing a wide variety of target compounds, even simultaneously. To achieve these benefits, high expenses and a highly trained operator are necessary. For the technique comparison, real samples were collected from contaminated surfaces of a clandestine MDMA and amphetamine-contaminated glassware. All techniques were able to detect MDMA on different collected sampling swabs, collected across the clandestine laboratory. Furthermore, the LOD is similar for all three techniques and ranges in the low nanogram range for most target compounds. Samples from contaminated glassware are analysed for the presence of amphetamine itself, the intermediate NFA and the precursors APAAN and BMK. While, like for MDMA, all techniques were able to detect amphetamine, only IMS and APLD-MS were able to detect the intermediate and only APLD achieved to detect BMK as a drug precursor.

In conclusion, all techniques obtained good results for within their limitations. Therefore, the preferred technique depends on the analytical capabilities needed for a certain issue. More analytical flexibility and explanatory power is correlated to higher sophisticated techniques. And the choice, which technique to choose, should be based on the needed complexity of analytical results on-site.

6. Acknowledgements

This work was supported by the Federal Ministry of the Interior (BMI) and the Federal Office of Civil Protection and Disaster Assistance of Germany [grant number FP406 “SEMFreS”].

References

[1] United Nations Office on Drugs and Crime, World Drug Report 2018, United Nations, Vienna, 2018.

[2] European Monitoring Centre for Drugs and Drug Addiction and Europol, European Drug Report 2018. Trends and Developments, Publications Office of the European Union, Luxembourg, 2018.

[3] United Nations Office on Drugs and Crime, RECOMMENDED METHODS FOR THE IDENTIFICATION AND ANALYSIS OF AMPHETAMINE, METHAMPHETAMINE AND THEIR RING-SUBSTITUTED ANALOGUES IN SEIZED MATERIALS, United Nations, Vienna, 2006.

[4] European Monitoring Centre for Drugs and Drug Addiction and Europol, EU Drug Markets Report 2016. In-depth Analysis, Publications Office of the European Union, Luxembourg, 2016.

[5] N. de Giovanni, N. Fucci, The Current Status of Sweat Testing For Drugs of Abuse: A Review, Current Medicinal Chemistry 20 (2013) 545–561. https://doi.org/10.2174/092986713804910139.

[6] Y. Zhong, K. Huang, Q. Luo, S. Yao, X. Liu, N. Yang, C. Lin, X. Luo, The Application of a Desktop NMR Spectrometer in Drug Analysis, International journal of analytical chemistry 2018 (2018) 3104569. https://doi.org/10.1155/2018/3104569.

[7] E. Gerace, F. Seganti, C. Luciano, T. Lombardo, D. Di Corcia, H. Teifel, M. Vincenti, A. Salomone, On-site identification of psychoactive drugs by portable Raman spectroscopy during drug-checking service in electronic music events, Drug and alcohol review 38 (2019) 50–56. https://doi.org/10.1111/dar.12887.

[8] K. Tsujikawa, T. Yamamuro, K. Kuwayama, T. Kanamori, Y.T. Iwata, K. Miyamoto, F. Kasuya, H. Inoue, Development of a Library Search-Based Screening System for 3,4-Methylenedioxymethamphetamine in Ecstasy Tablets Using a Portable Near-Infrared Spectrometer, Journal of forensic sciences 61 (2016) 1208–1214. https://doi.org/10.1111/1556-4029.13122.

[9] E. Sisco, J. Verkouteren, J. Staymates, J. Lawrence, Rapid detection of fentanyl, fentanyl analogues, and opioids for on-site or laboratory based drug seizure screening using thermal desorption DART-MS and ion mobility spectrometry, Forensic chemistry 4 (2017) 108–115. https://doi.org/10.1016/j.forc.2017.04.001.

[10] T.P. Forbes, M. Staymates, E. Sisco, Broad spectrum infrared thermal desorption of wipe-based explosive and narcotic samples for trace mass spectrometric detection, The Analyst 142 (2017) 3002–3010. https://doi.org/10.1039/c7an00721c.

[11] Y. Seto, M. Kanamori-Kataoka, K. Tsuge, I. Ohsawa, K. Matsushita, H. Sekiguchi, T. Itoi, K. Iura, Y. Sano, S. Yamashiro, Sensing technology for chemical-warfare agents and its evaluation using authentic agents, Sensors and Actuators B: Chemical 108 (2005) 193–197. https://doi.org/10.1016/j.snb.2004.12.084.

[12] R. Reiss, S. Ehlert, J. Heide, M. Pütz, T. Forster, R. Zimmermann, Ambient Pressure Laser Desorption—Chemical Ionization Mass Spectrometry for Fast and Reliable Detection of Explosives, Drugs, and Their Precursors, Applied Sciences 8 (2018) 933. https://doi.org/10.3390/app8060933.

[13] S. Ehlert, J. Hölzer, J. Rittgen, M. Pütz, R. Schulte-Ladbeck, R. Zimmermann, Rapid on-site detection of explosives on surfaces by ambient pressure laser desorption and direct inlet single photon ionization or chemical ionization mass spectrometry, Analytical and bioanalytical chemistry 405 (2013) 6979–6993. https://doi.org/10.1007/s00216-013-6839-8.

[14] S. Ehlert, A. Walte, R. Zimmermann, Ambient pressure laser desorption and laser-induced acoustic desorption ion mobility spectrometry detection of explosives, Analytical chemistry 85 (2013) 11047–11053. https://doi.org/10.1021/ac402704c.
[15] E. Sisco, T.P. Forbes, M.E. Staymates, G. Gillen, Rapid Analysis of Trace Drugs and Metabolites Using a Thermal Desorption DART-MS Configuration, Analytical methods : advancing methods and applications 8 (2016) 6494–6499. https://doi.org/10.1039/C6AY01851C.
[16] N. Stojanovska, T. Kelly, M. Tahtouh, A. Beavis, S. Fu, Analysis of amphetamine-type substances and piperazine analogues using desorption electrospray ionisation mass spectrometry, Rapid communications in mass spectrometry : RCM 28 (2014) 731–740. https://doi.org/10.1002/rcm.6832.
[17] K. Hiraoka, S. Ninomiya, L.C. Chen, T. Iwama, M.K. Mandal, H. Suzuki, O. Ariyada, H. Furuya, K. Takekawa, Development of double cylindrical dielectric barrier discharge ion source, The Analyst 136 (2011) 1210–1215. https://doi.org/10.1039/c0an00621a.
[18] B.D. Sabino, M.L. Sodré, E.A. Alves, H.F. Rozenbaum, F.O.M. Alonso, D.N. Correa, M.N. Eberlin, W. Romão, Analysis of street Ecstasy tablets by thin layer chromatography coupled to easy ambient sonic-spray ionization mass spectrometry, Brazilian Journal of Analytical Chemistry 1 (2011) 222–227.
[19] J.K. Dalgleish, M. Wleklinski, J.T. Shelley, C.C. Mulligan, Z. Ouyang, R. Graham Cooks, Arrays of low-temperature plasma probes for ambient ionization mass spectrometry, Rapid communications in mass spectrometry : RCM 27 (2013) 135–142. https://doi.org/10.1002/rcm.6435.
[20] J.D. Power, M.G. Barry, K.R. Scott, P.V. Kavanagh, An unusual presentation of a customs importation seizure containing amphetamine, possibly synthesized by the APAAN-P2P-Leuckart route, Forensic science international 234 (2014) e10-3. https://doi.org/10.1016/j.forsciint.2013.10.003.
[21] F.S. CROSSLEY, M.L. MOORE, STUDIES ON THE LEUCKART REACTION, J. Org. Chem. 09 (1944) 529–536. https://doi.org/10.1021/jo01188a006.
[22] F.M. Hauser, T. Rößler, J.W. Hulshof, D. Weigel, R. Zimmermann, M. Pütz, Identification of specific markers for amphetamine synthesised from the pre-precursor APAAN following the Leuckart route and retrospective search for APAAN markers in profiling databases from Germany and the Netherlands, Drug testing and analysis 10 (2018) 671–680. https://doi.org/10.1002/dta.2296.